

IDENTYFIKACJA MODÓW obserwowanych pulsacji (część 2)

**(na podstawie przeglądownego referatu
A.A.P. i J. Daszyńskiej-Daszkiewicz
dla konferencji w Hiszpanii:
„Impact of new instrumentation & new insights
in stellar pulsations”, Granada, 5-9 September 2011)**

(prezentacja oraz tekst dla Proceedings)

Two approaches to mode identification from photometry:

- 1) Comparing theoretical and observational values of the amplitude ratios and phase differences (f from theory)
- 2) Making use of the amplitudes and phases themselves (f is determined from observations together with ℓ)

both methods need input from model atmospheres !

If we ignore rotation,
the amplitude ratios and phase differences
are independent of the inclination angle, i ,
and the azimuthal order, m .

Complex amplitude of monochromatic flux variations

$$A_\lambda(i) = \varepsilon Y_\ell^m(i, 0) b_\ell^\lambda (D_{1,\ell}^\lambda + D_{2,\ell} + D_{3,\ell}^\lambda)$$

$$D_{1,\ell}^\lambda = \frac{1}{4} f \frac{\partial \log(\mathcal{F}_\lambda |b_\ell^\lambda|)}{\partial \log T_{\text{eff}}}$$

temperature
term

$$D_{2,\ell} = (2 + \ell)(1 - \ell)$$

geometrical
term

$$D_{3,\ell}^\lambda = - \left(2 + \frac{3\omega^2}{4\pi G \langle \rho \rangle} \right) \frac{\partial \log(\mathcal{F}_\lambda |b_\ell^\lambda|)}{\partial \log g_{\text{eff}}^0}$$

pressure
term

$$b_\ell^\lambda = \int_0^1 h_\lambda^0(\mu) \mu P_\ell(\mu) d\mu$$

disc averaging
factor

f - the ratio of the bolometric flux variation to the radial displacement at the photosphere level

$$\frac{\delta \mathcal{F}_{\text{bol}}}{\mathcal{F}_{\text{bol}}} = \text{Re}\{\varepsilon f Y_{\ell}^m e^{-i\omega t}\},$$

A SYSTEM OF EQUATIONS

$$\mathcal{D}_\ell^\lambda(\tilde{\varepsilon}f) + \mathcal{E}_\ell^\lambda \tilde{\varepsilon} = A^\lambda,$$

$$\tilde{\varepsilon} = \varepsilon Y_\ell^m(i, 0),$$

$$\mathcal{D}_\ell^\lambda = \frac{1}{4} b_\ell^\lambda \frac{\partial \log(\mathcal{F}_\lambda |b_\ell^\lambda|)}{\partial \log T_{\text{eff}}},$$

$$\mathcal{E}_\ell^\lambda = b_\ell^\lambda \left[(2 + \ell)(1 - \ell) - \left(\frac{\omega^2 R^3}{GM} + 2 \right) \frac{\partial \log(\mathcal{F}_\lambda |b_\ell^\lambda|)}{\partial \log g} \right].$$

METHOD

Two complex unknown quantities

$$(\tilde{\epsilon} f), \tilde{\epsilon}.$$

For a given degree, ℓ , the system is solved by the least-square method to find the minimum of χ^2 .

ADDING THE RADIAL VELOCITY

$$i\omega R \left(u_\ell^\lambda + \frac{GM}{R^3\omega^2} v_\ell^\lambda \right) \tilde{\varepsilon} = V_{rad}(i)$$

$$u_\ell = \int_0^1 h\mu^2 P_\ell(\mu) d\mu,$$
$$v_\ell = \ell \int_0^1 h(P_{\ell-1} - \mu P_\ell)\mu d\mu,$$

Examples: δ SCUTI STARS

β Cas, FG Vir, 44 Tau, HD144277

- Daszyńska-Daszkiewicz, Dziembowski & Pamyatnykh, 2003, A&A 407, 999
Daszynska-Daszkiewicz, Dziembowski, Pamyatnykh et al., 2005, A&A 438, 653
Lenz, Pamyatnykh, Breger & Antoci, 2008, A&A 478, 855
Lenz, Pamyatnykh, Zdravkov & Breger, 2010, A&A 509, A90
Zwintz, Lenz, Breger, Pamyatnykh et al., 2011, A&A, 533, id. A133

44 Tauri

15 frequencies (degree l is identified for 10 of them),

Sp F2 IV-V,

$m_V = 5.399$,

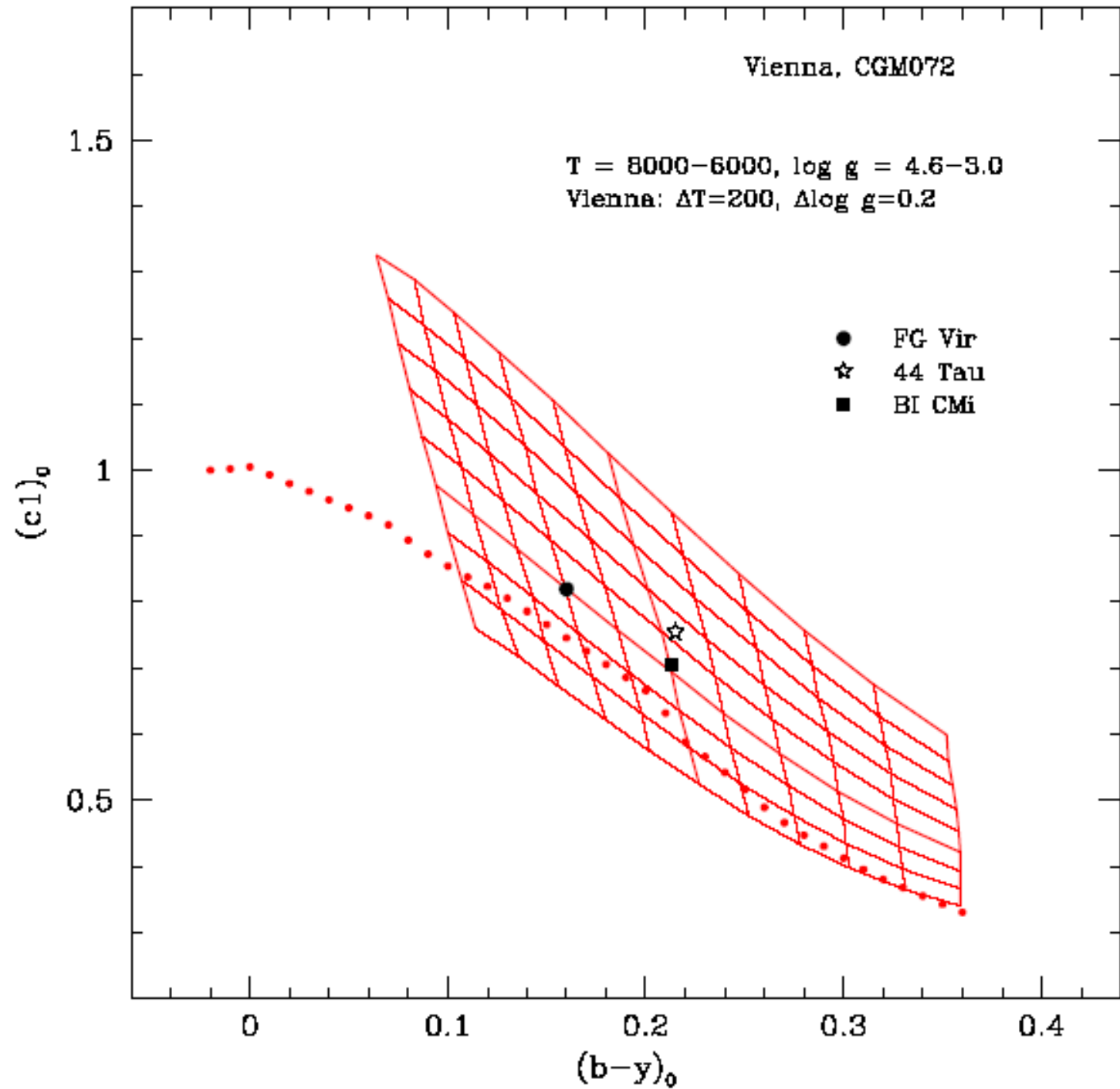
$p = 16.72 \pm 0.93$ mas,

$V_{\text{rot}} = 3 \pm 2$ km/s,

$[m/H] = \text{approx } 0.0$,

$T_{\text{eff}} = 6900 \pm 100$ K,

$\log g = 3.6 \pm 0.1$

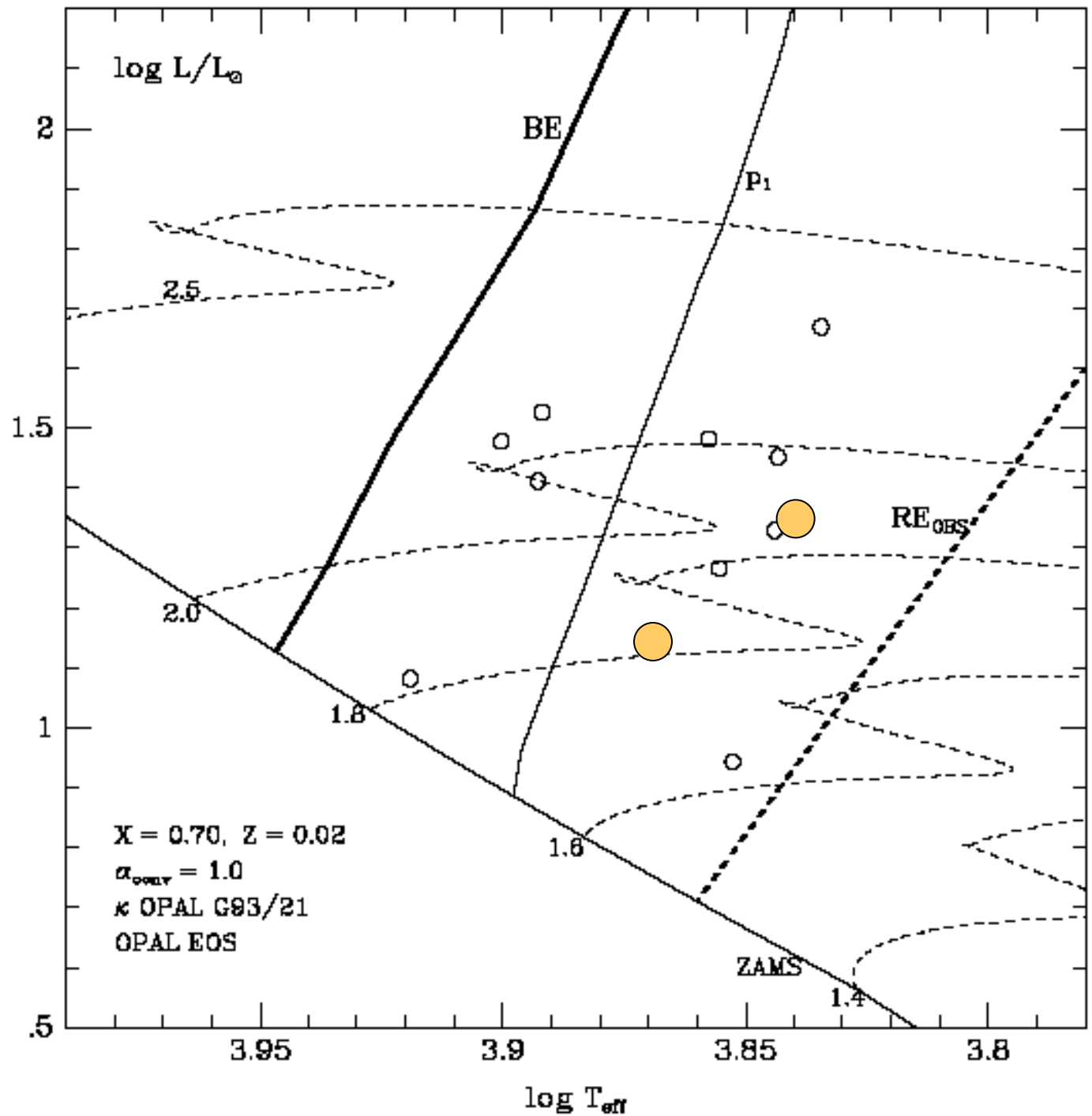


FG Vir (MS)

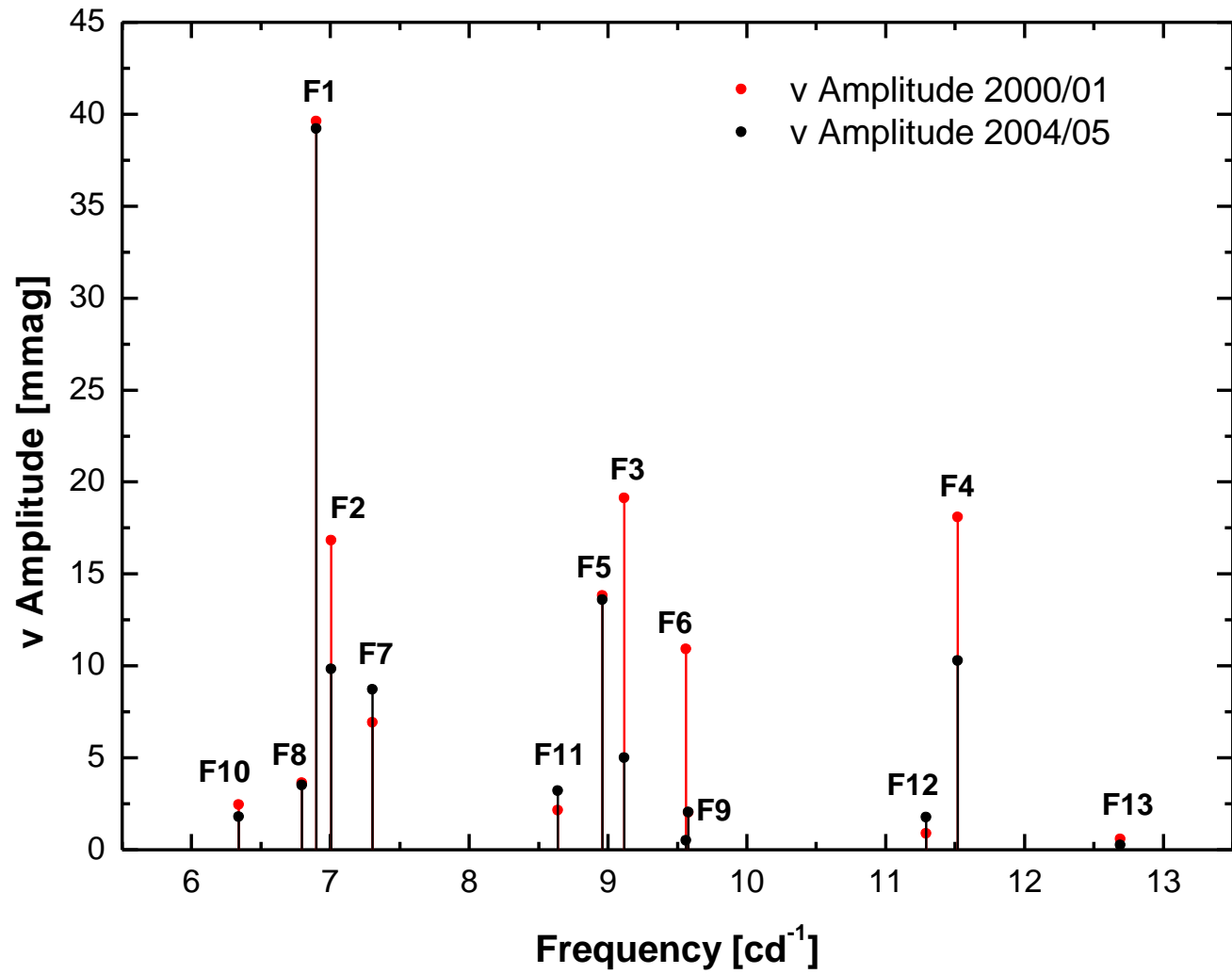
and

44 Tau
(post-MS)

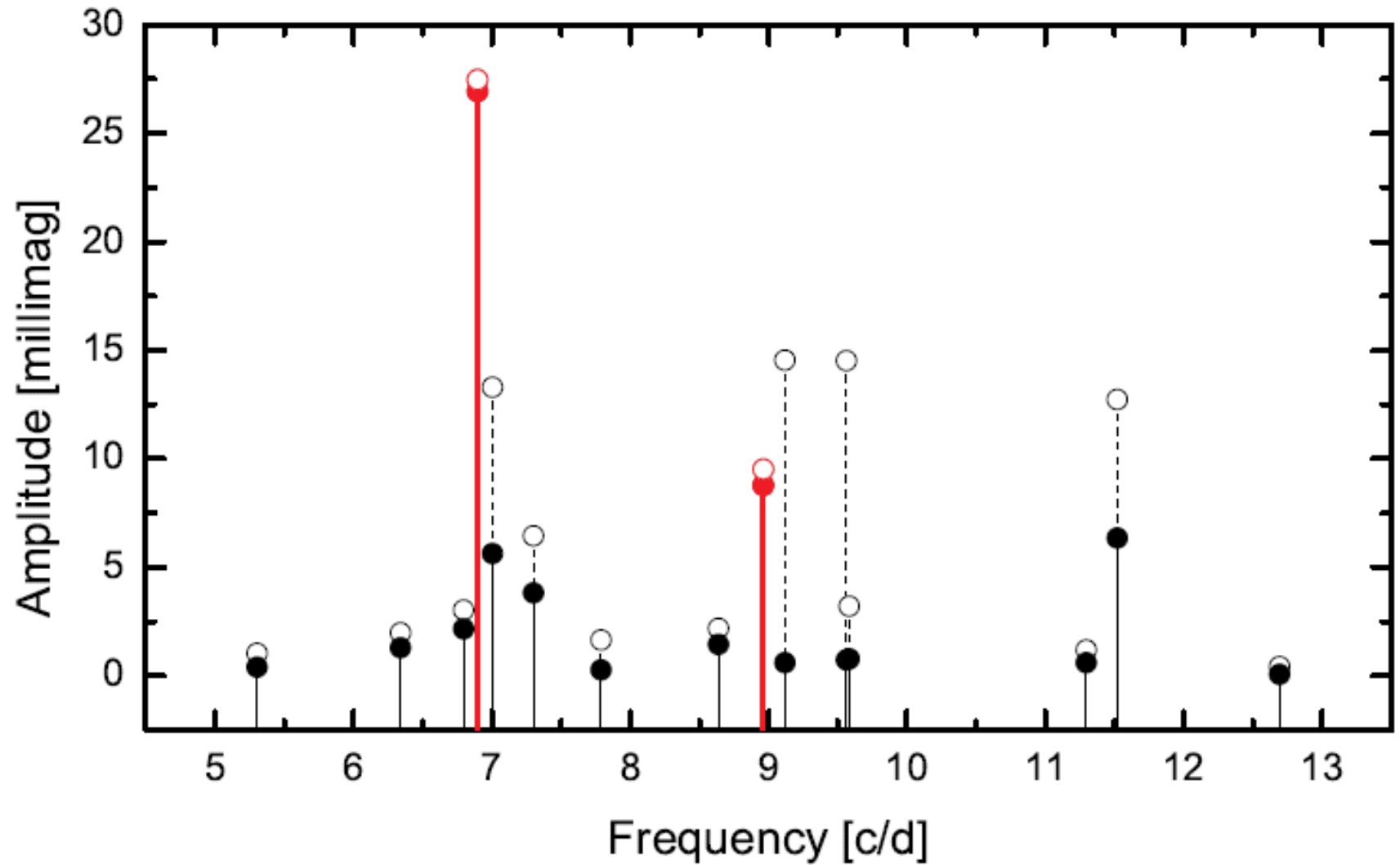
in the δ Scuti
instability domain



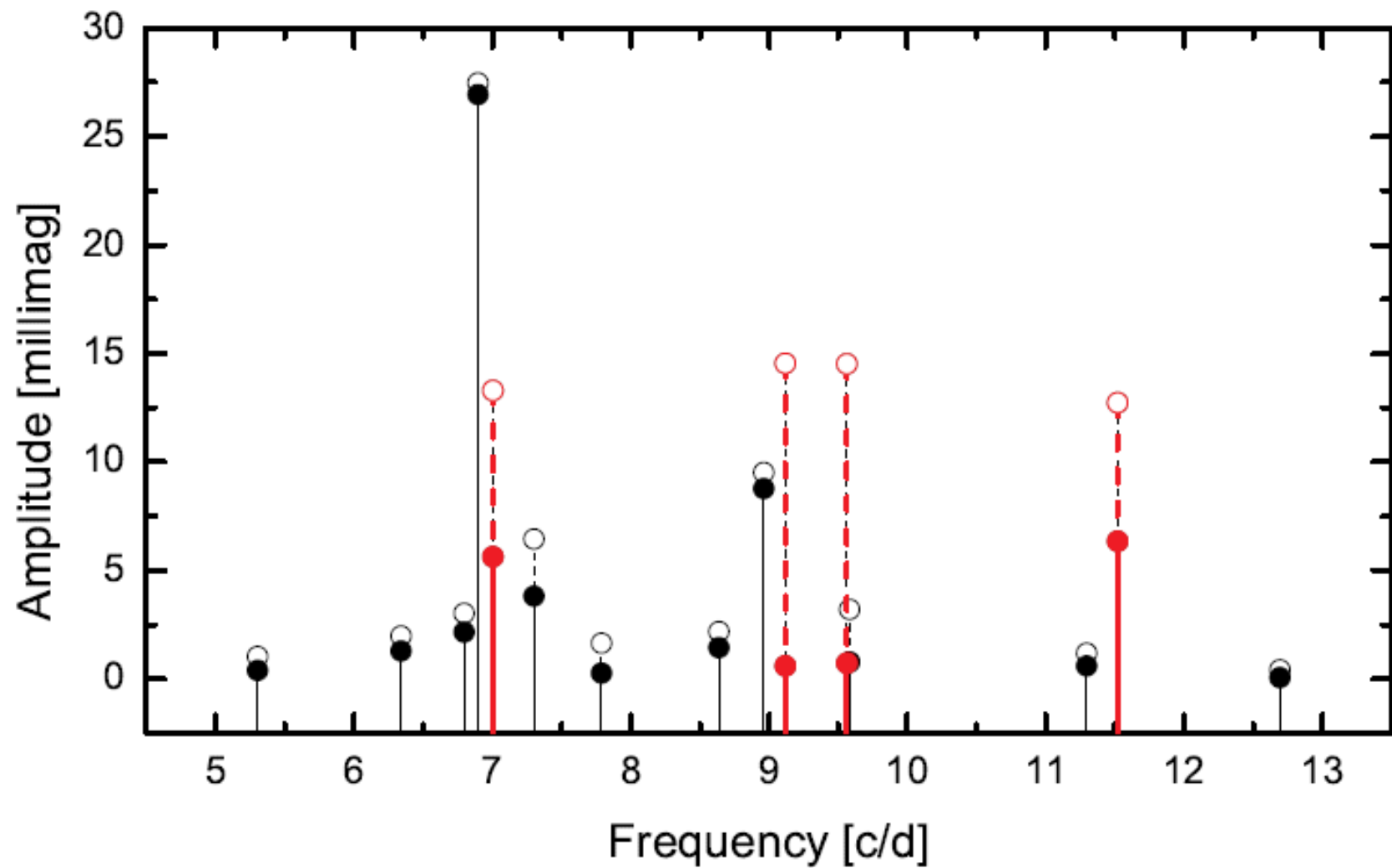
44 Tau



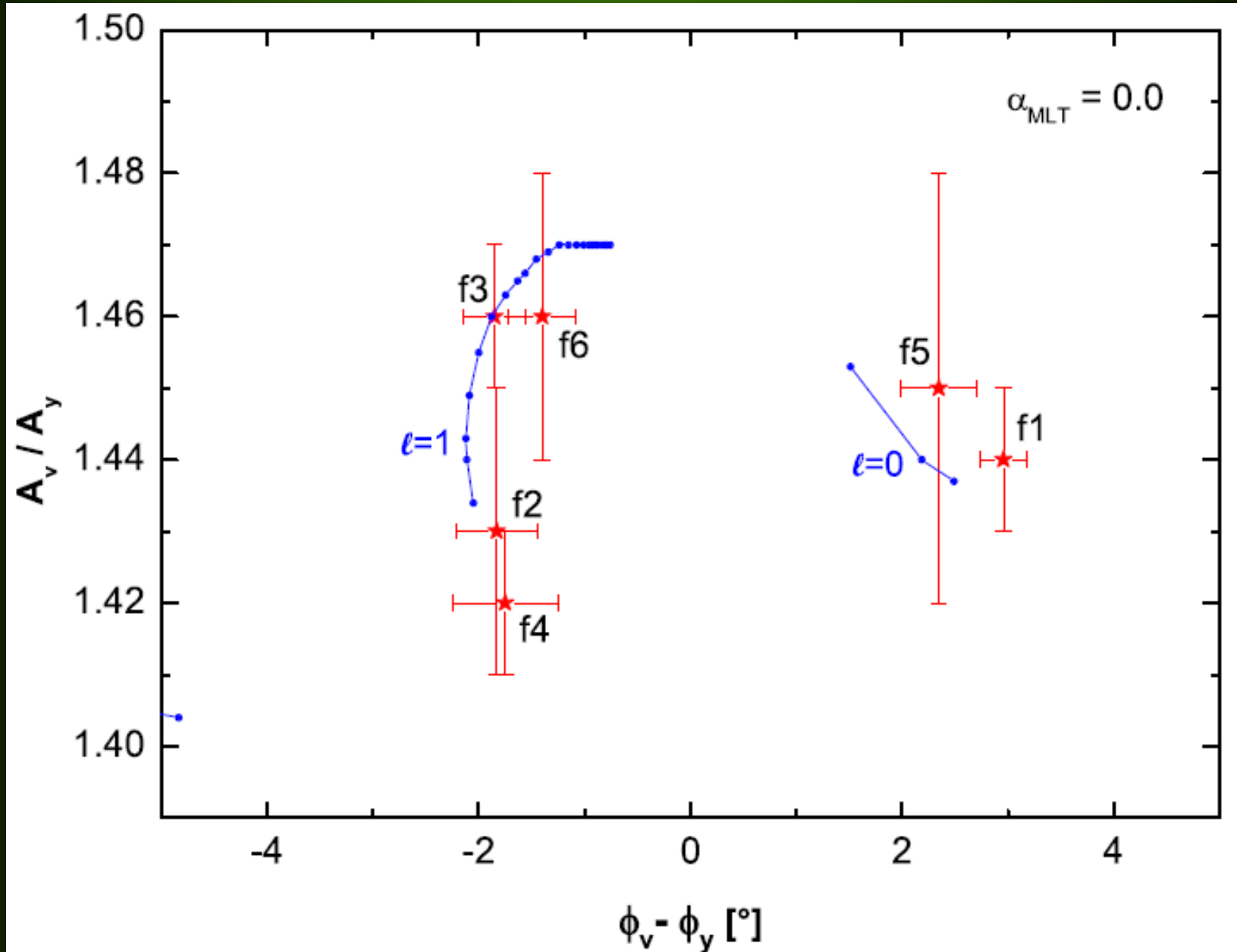
44 Tau, photometry, radial



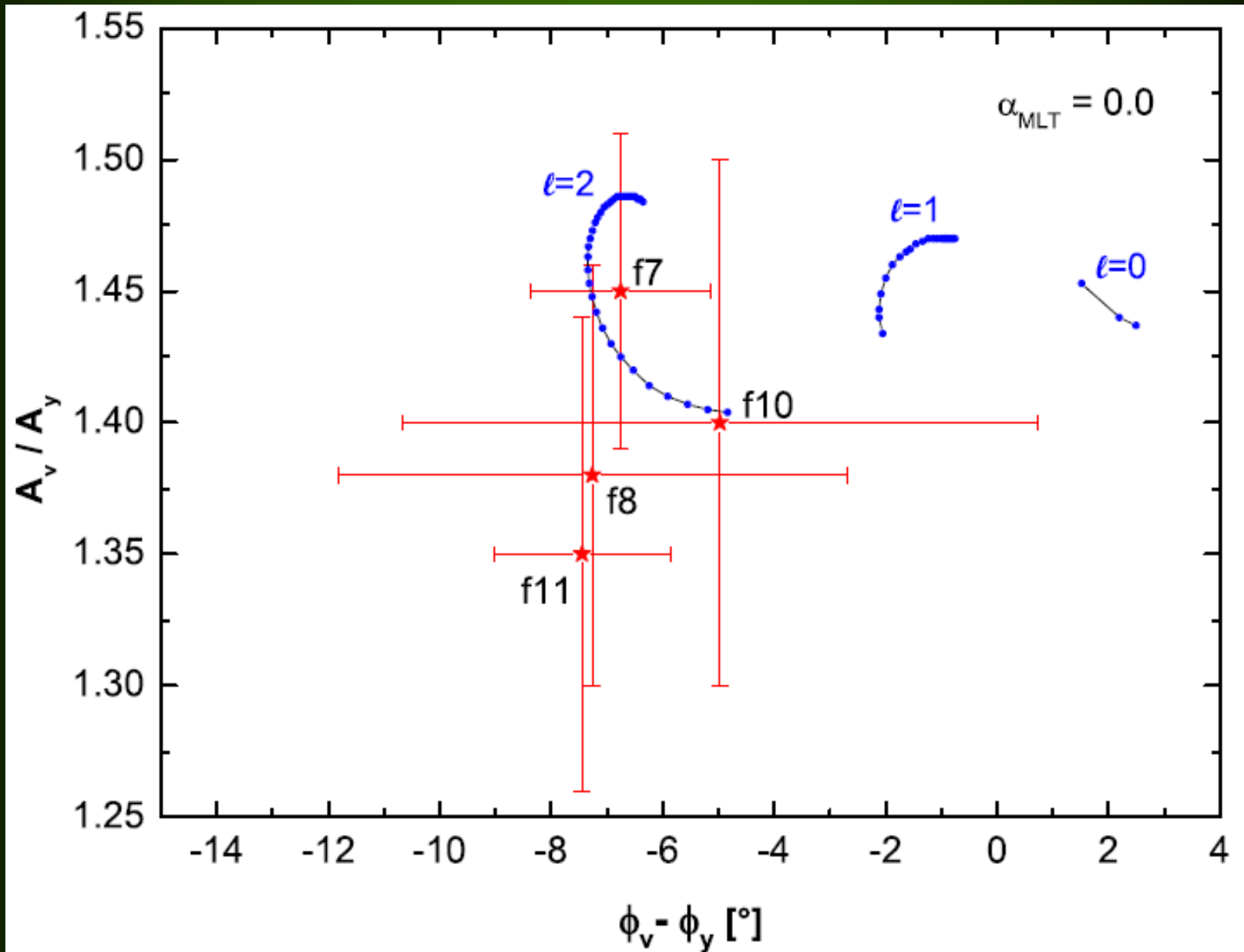
44 Tau, photometry, dipole



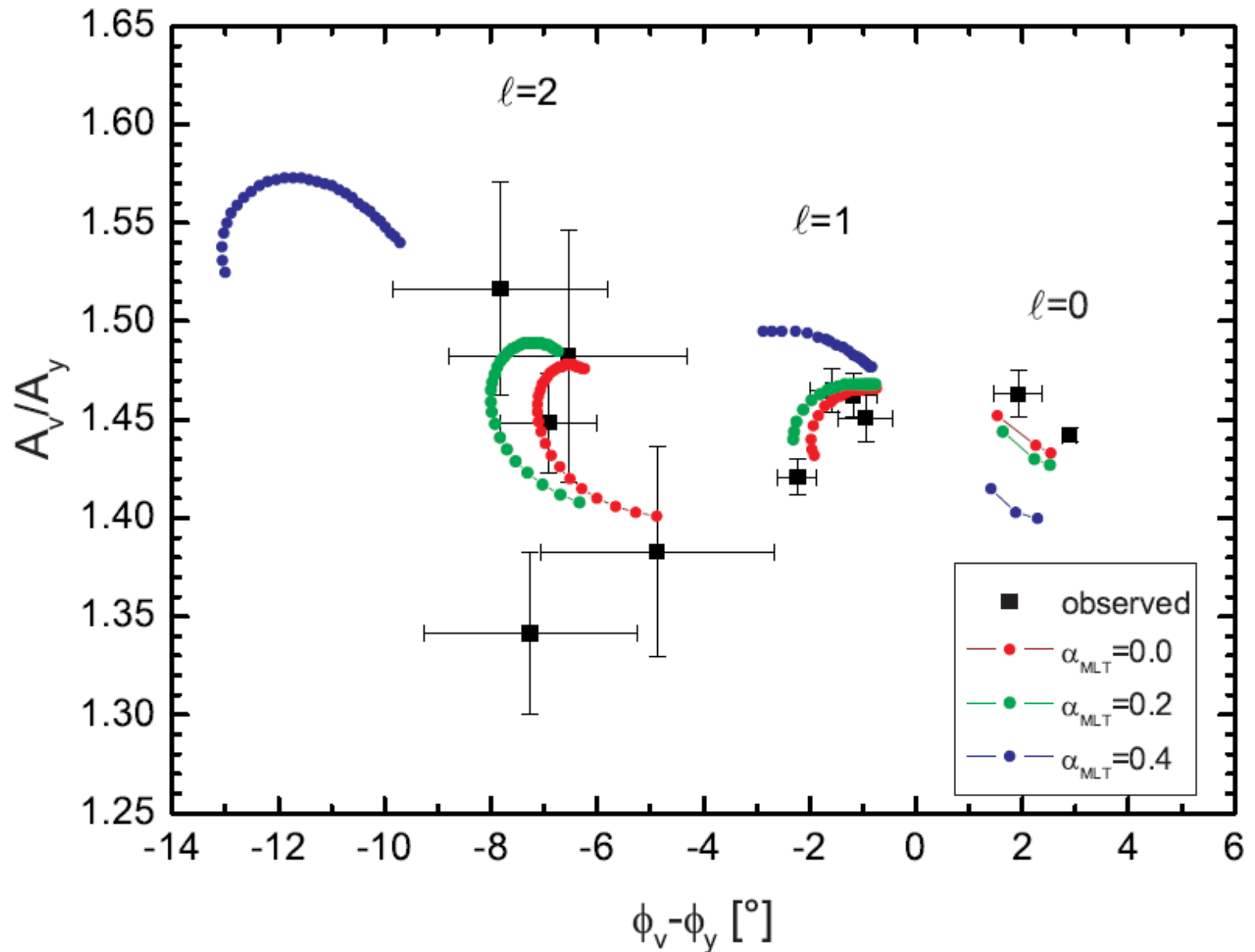
44 Tau, mode identification



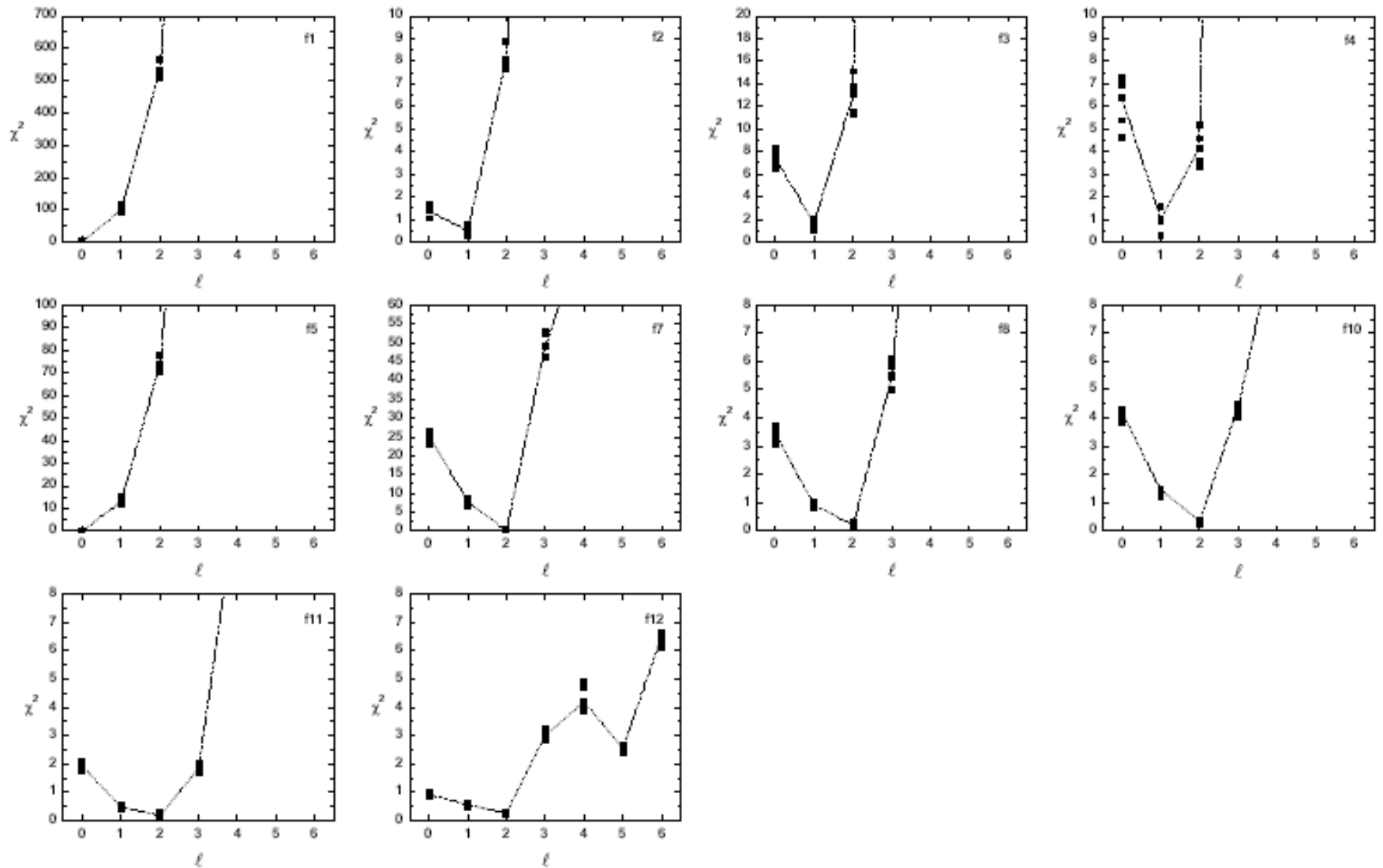
44 Tau, mode identification



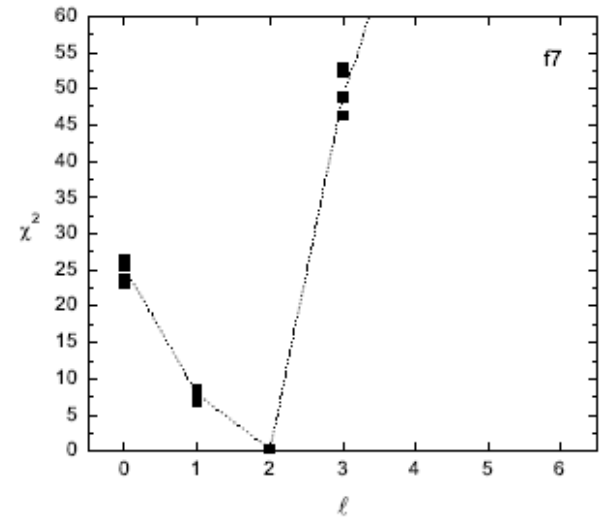
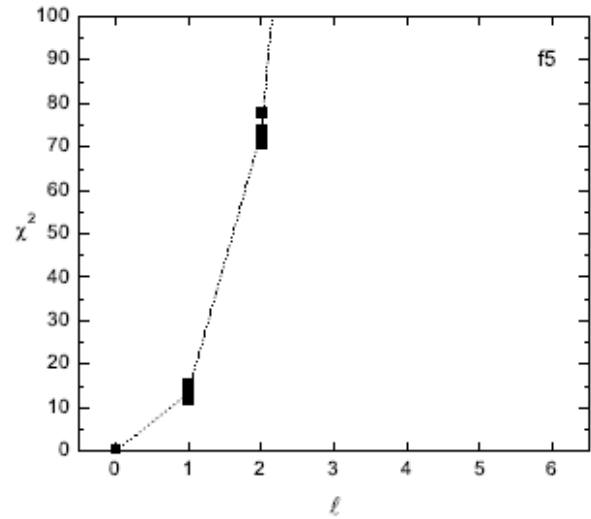
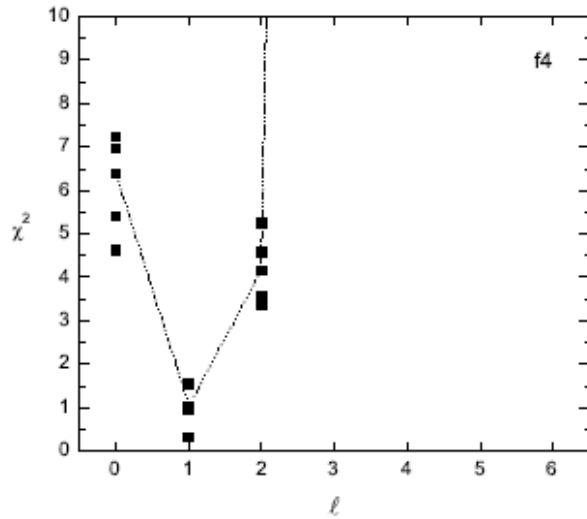
44 Tau, mode identification



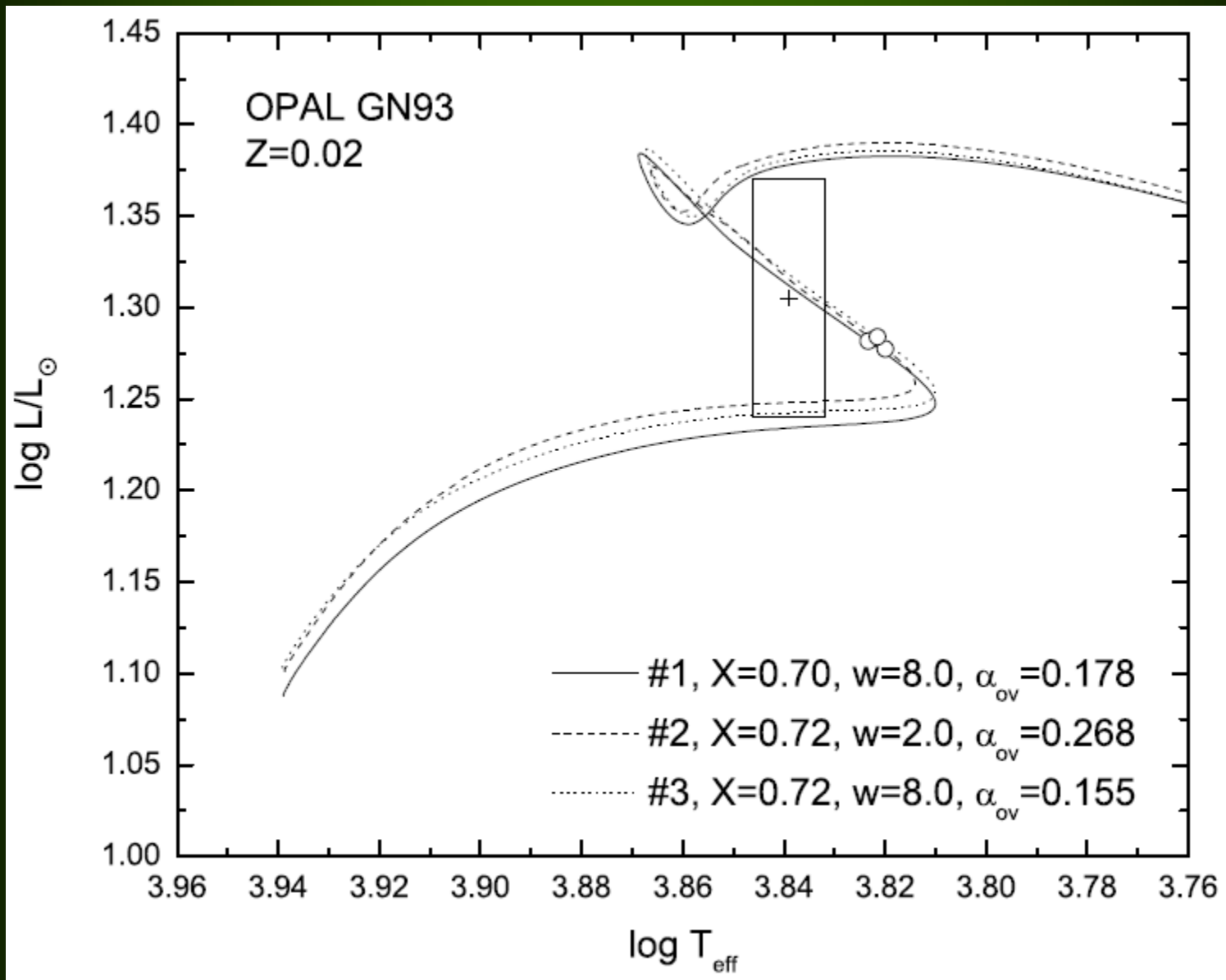
44 Tau, mode identification for 10 frequencies.



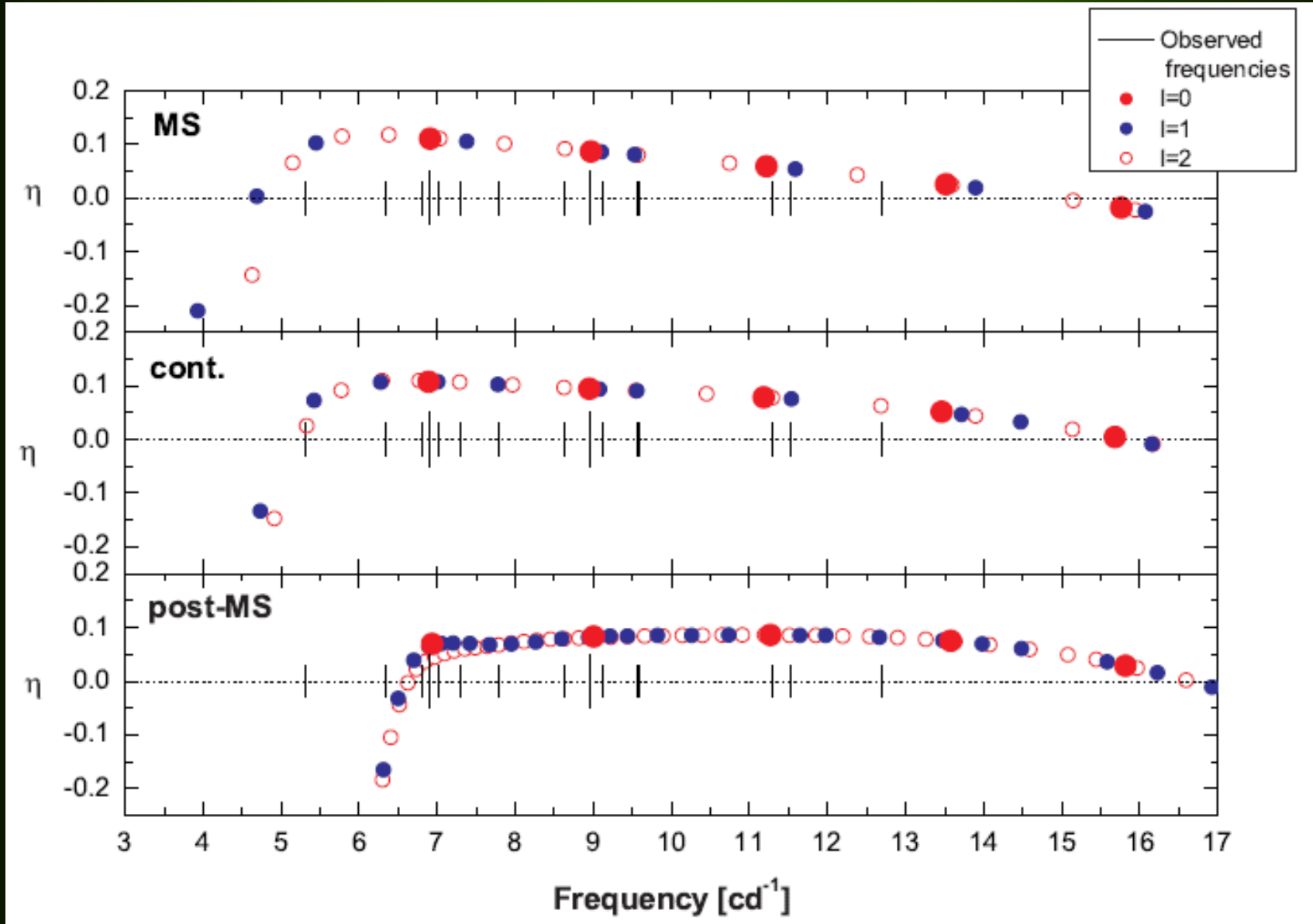
44 Tau, examples of the mode identification



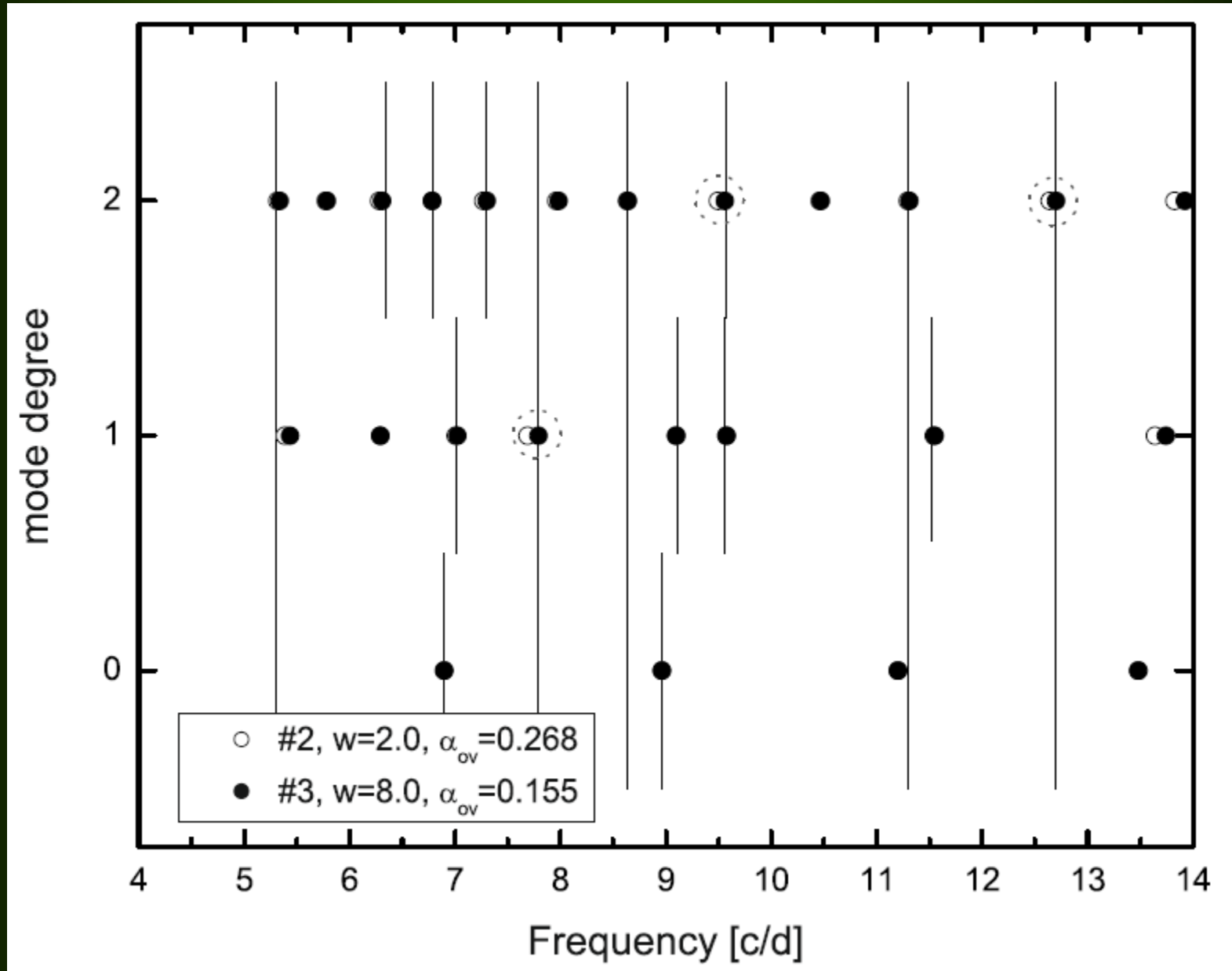
44 Tau. Evolutionary tracks for best models.



44 Tau, pulsational instability range



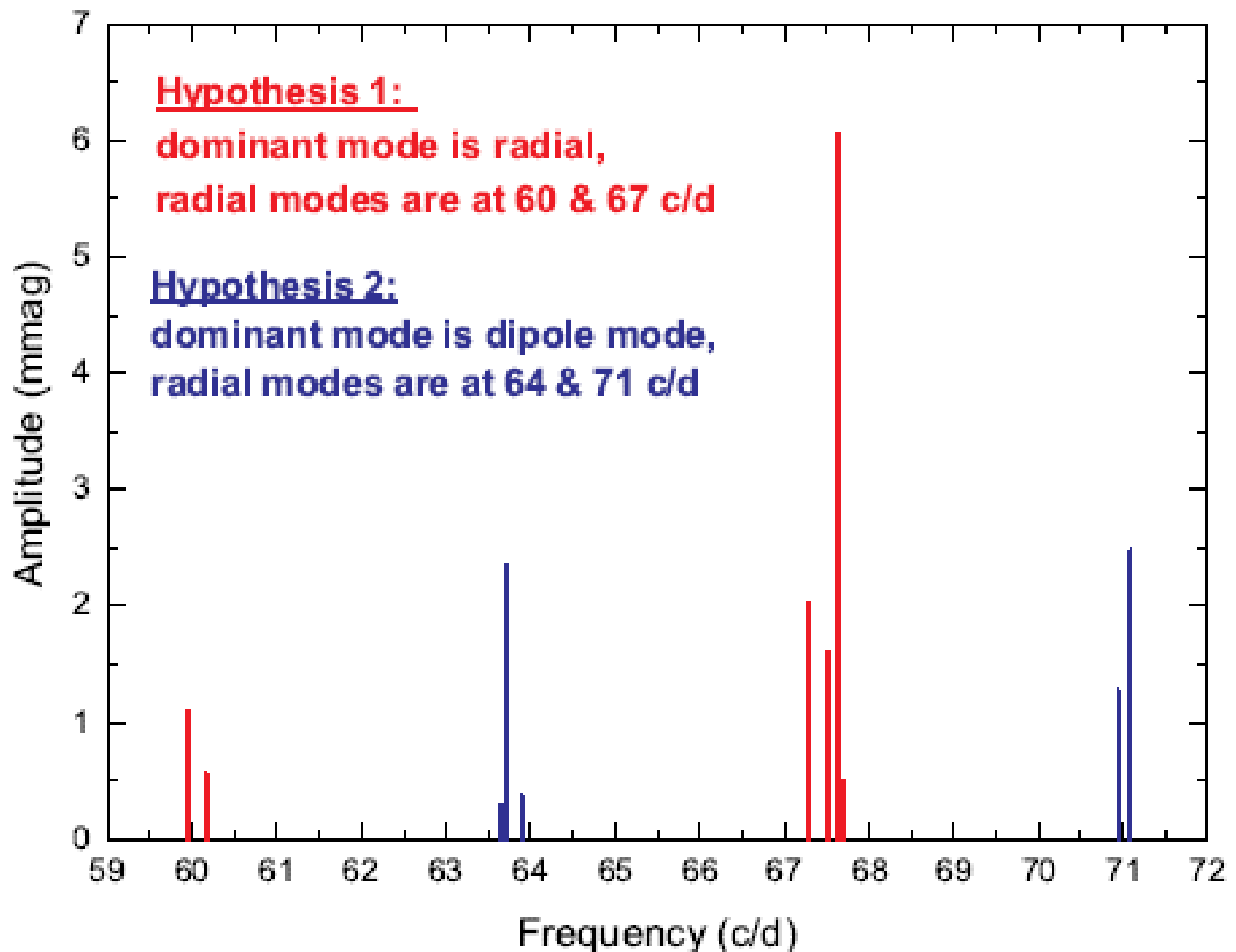
44 Tau. Frequency fitting for best models.



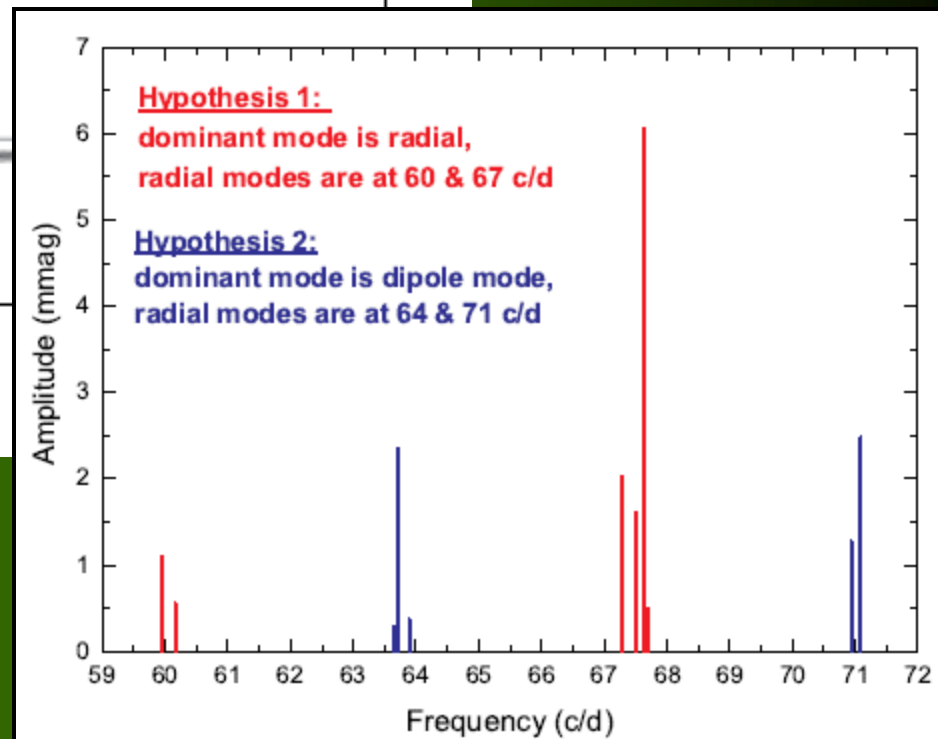
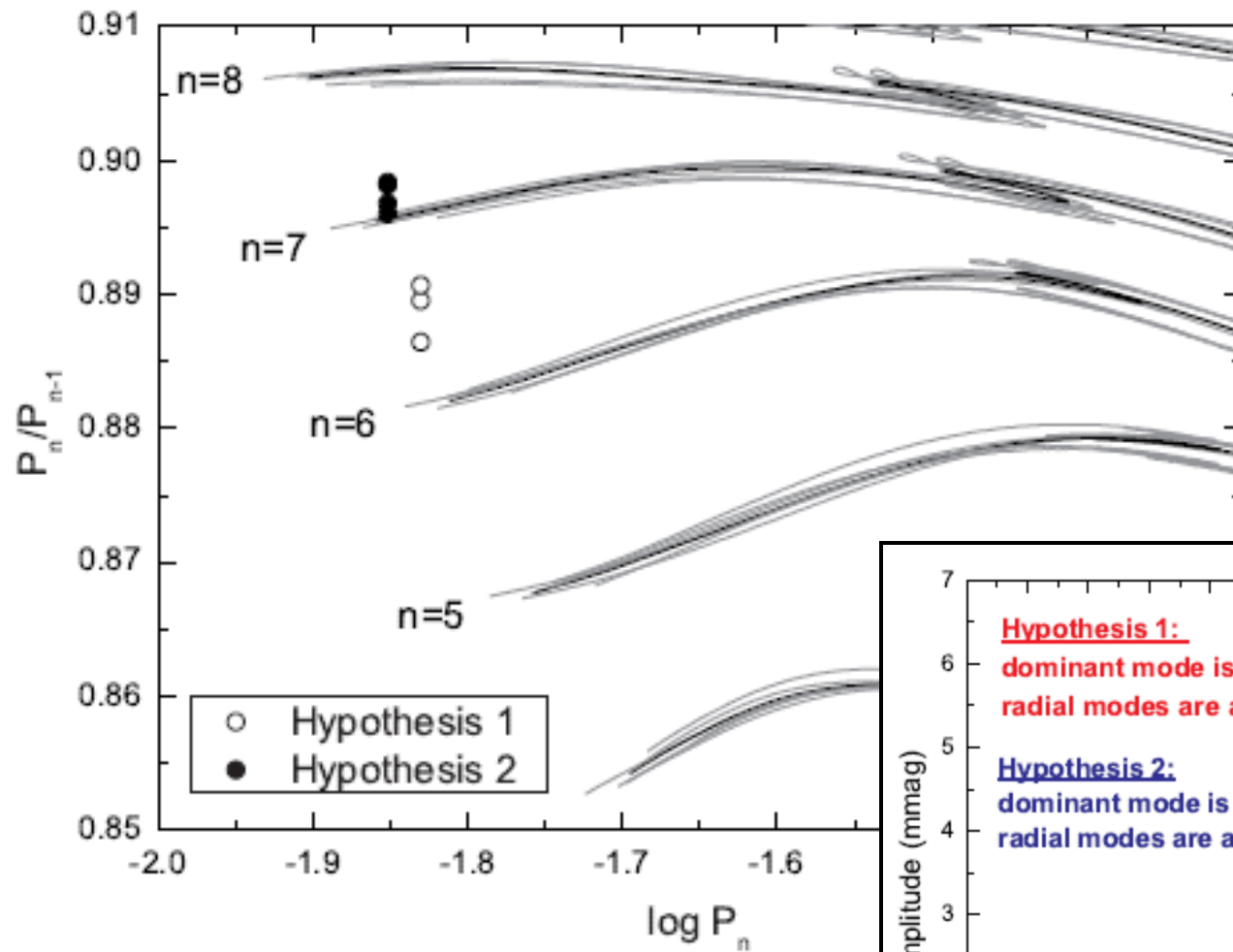
A δ SCUTI STAR HD 144277
(from the MOST observations)

Zwintz, Lenz, Breger, Pamyatnykh et al., 2011, A&A, 533, id. A133.

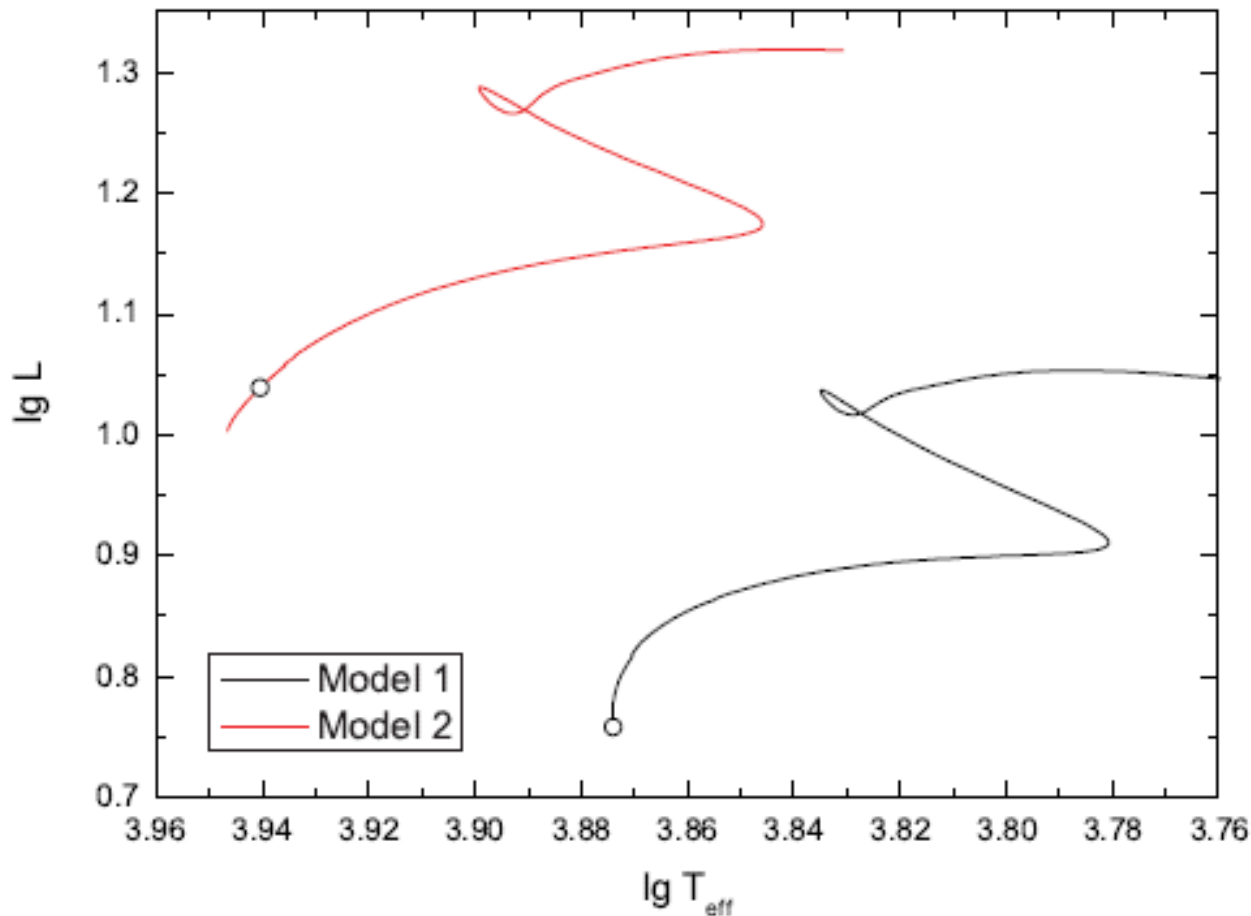
Pulsation frequency spectrum of HD 144277. Two hypotheses.



HD 144277. Period ratios of consecutive **radial** modes versus shorter periods.



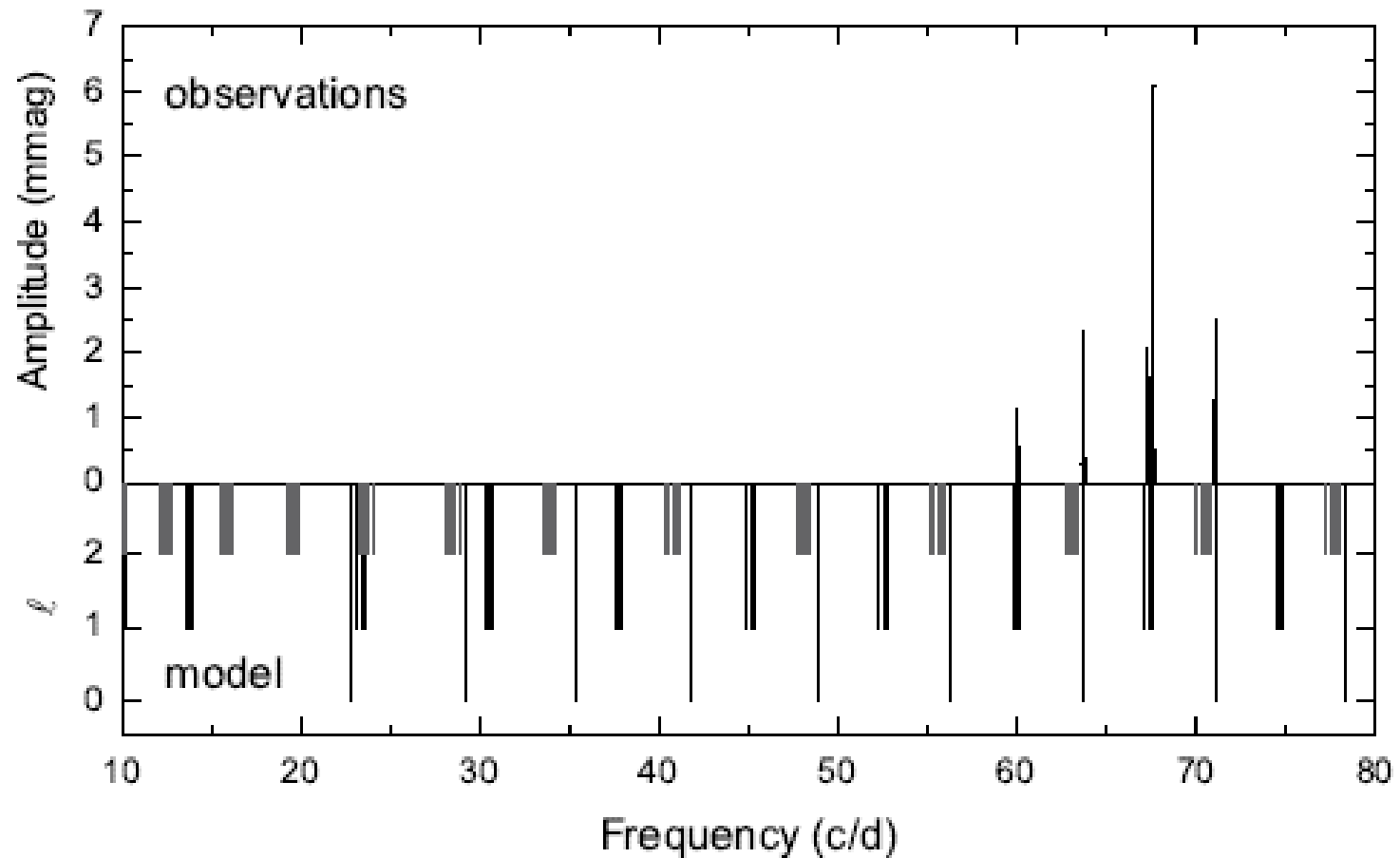
Evolutionary tracks of two representative models which fit two frequencies at 71 and 64 c/d as consecutive **radial** overtones (hypothesis 2). The fitted models are shown by open circles.



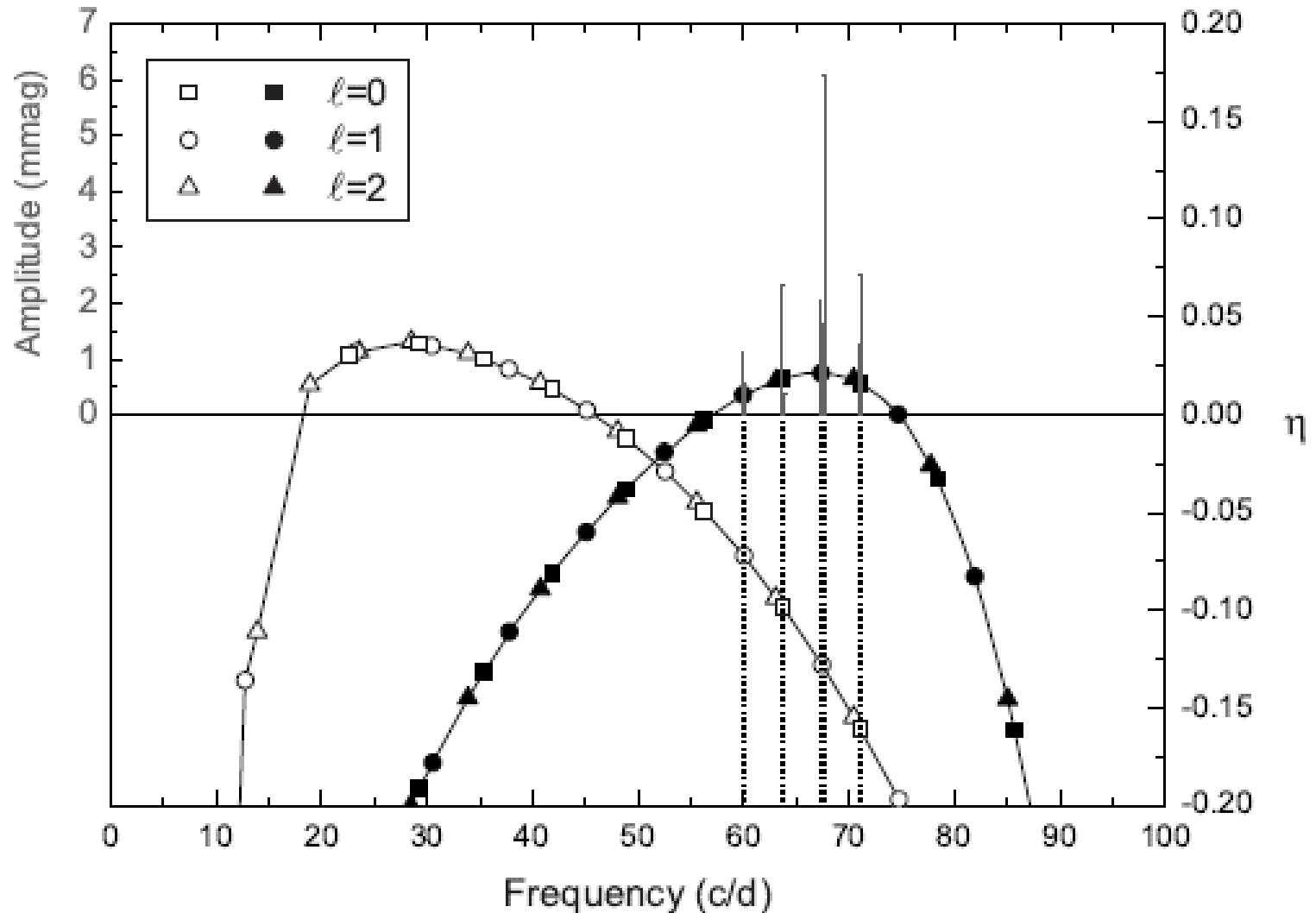
Model 1:
 $M=1.576$
 $X=0.74$
 $Z=0.0134$
 $\log T_{\text{eff}} = 3.874$
 $\log L = 0.757$

Model 2:
 $M=1.662$
 $X=0.70$
 $Z=0.01$
 $\log T_{\text{eff}} = 3.941$
 $\log L = 1.04$

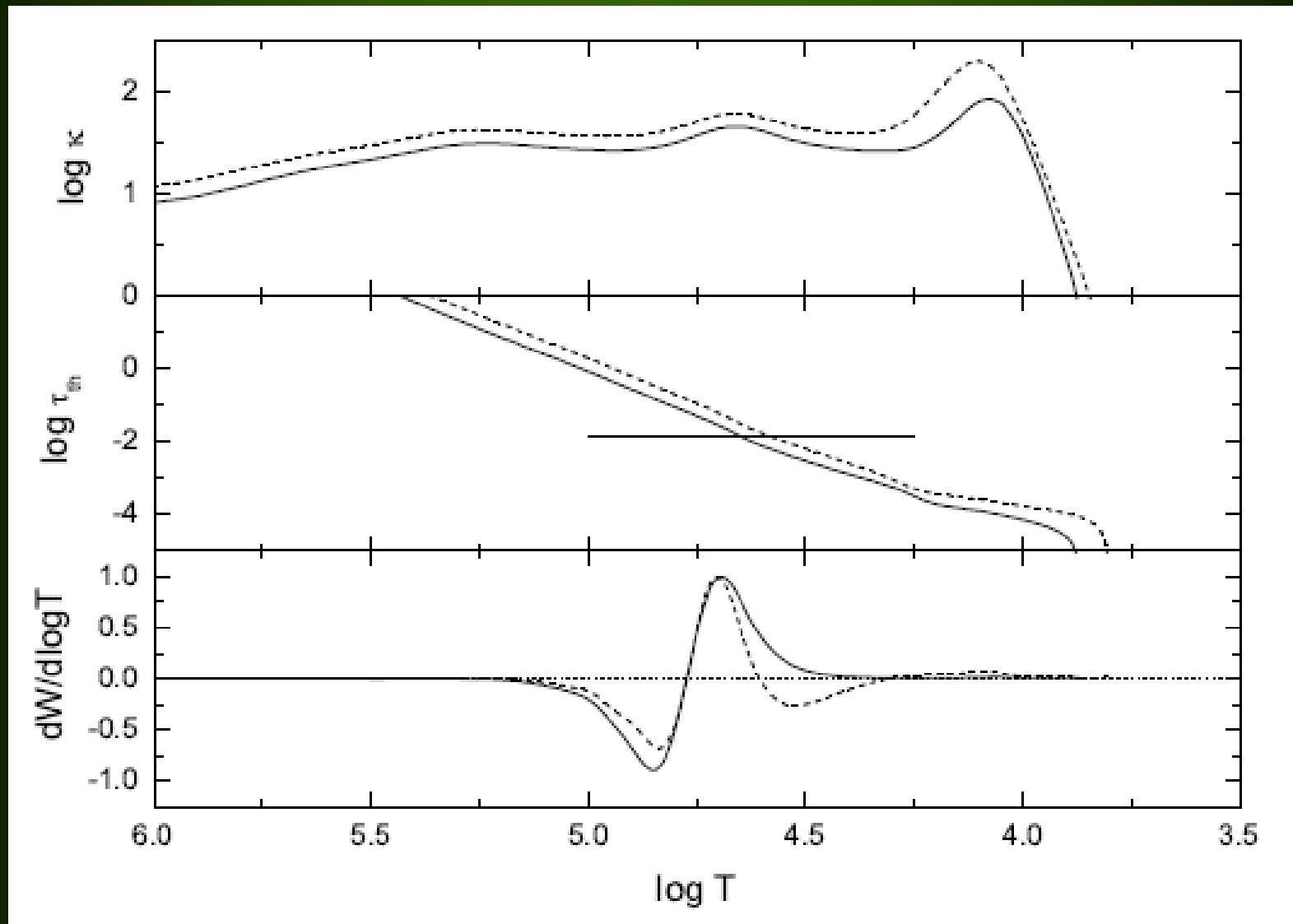
Comparison between observed frequencies and the theoretical Frequency spectrum according to the best model ($V_{\text{rot}} = 15 \text{ km/s}$)



Instability parameter, η , in a model with solar composition (open symbols)
 And in a model with modified metallicity and helium abundance (filled symbols)
 $\eta > 0$ for unstable modes. Both models fit two frequencies at 71 and 64 c/d as
 consecutive radial modes. Vertical lines mark observed frequencies.



Opacity, local thermal timescale and differential work integral for the dipole mode at 67 c/d (dominant frequency). Dashed line – model of solar composition (damped mode), solid line – modified model (excited mode)



Examples: β CEPHEI STARS

Daszyńska-Daszkiewicz, Dziembowski & Pamyatnykh, 2005, A&A 441, 641

See also posters 61 and 62:

W. Szewczuk, P. Walczak & J. Daszyńska-Daszkiewicz

ν Eridani

14 frequencies (degree l is identified for 8 of them),

Sp B2 III,

$m_V = 3.920$,

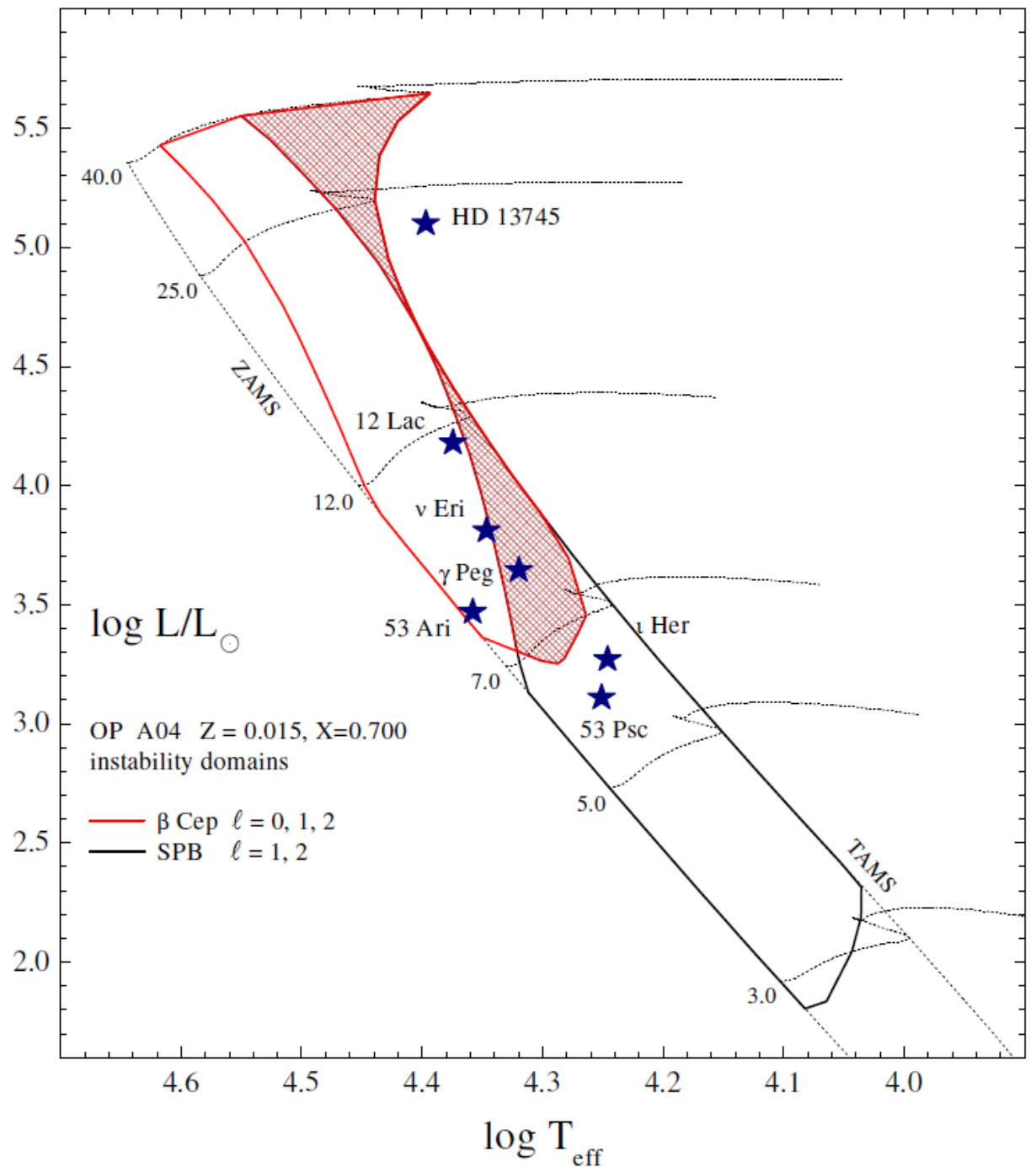
$\pi = 5.56 \pm 0.88$ mas,

$V_{\text{rot}} = 6$ km/s (SIMBAD: $V_{\text{sini}} = 7, 20, 25$ km/s),

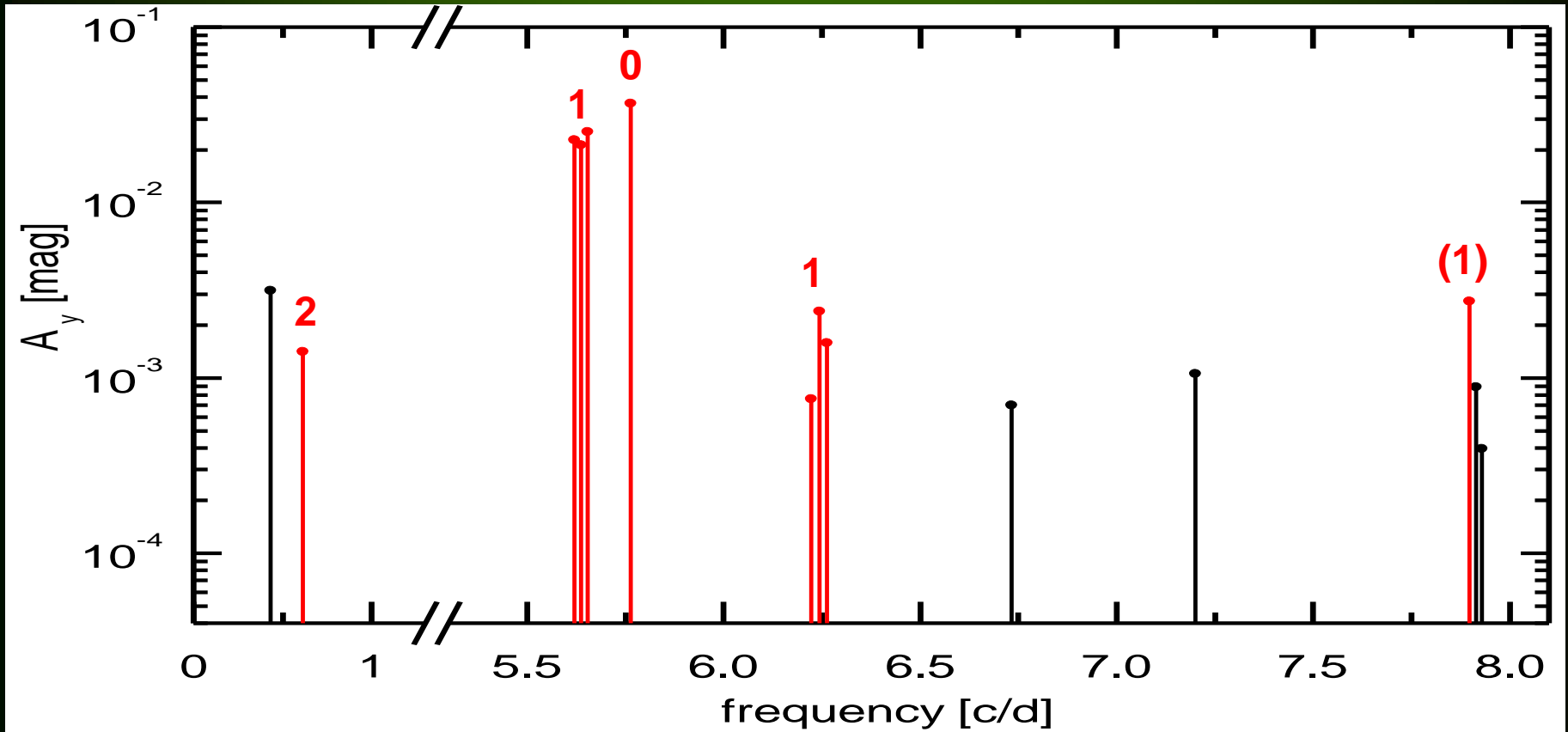
$[m/H] = 0.05 \pm 0.09$,

$T_{\text{eff}} = 22200 \pm 600$ K

ν Eridani –
 a hybrid
 β Cep / SPB
 star

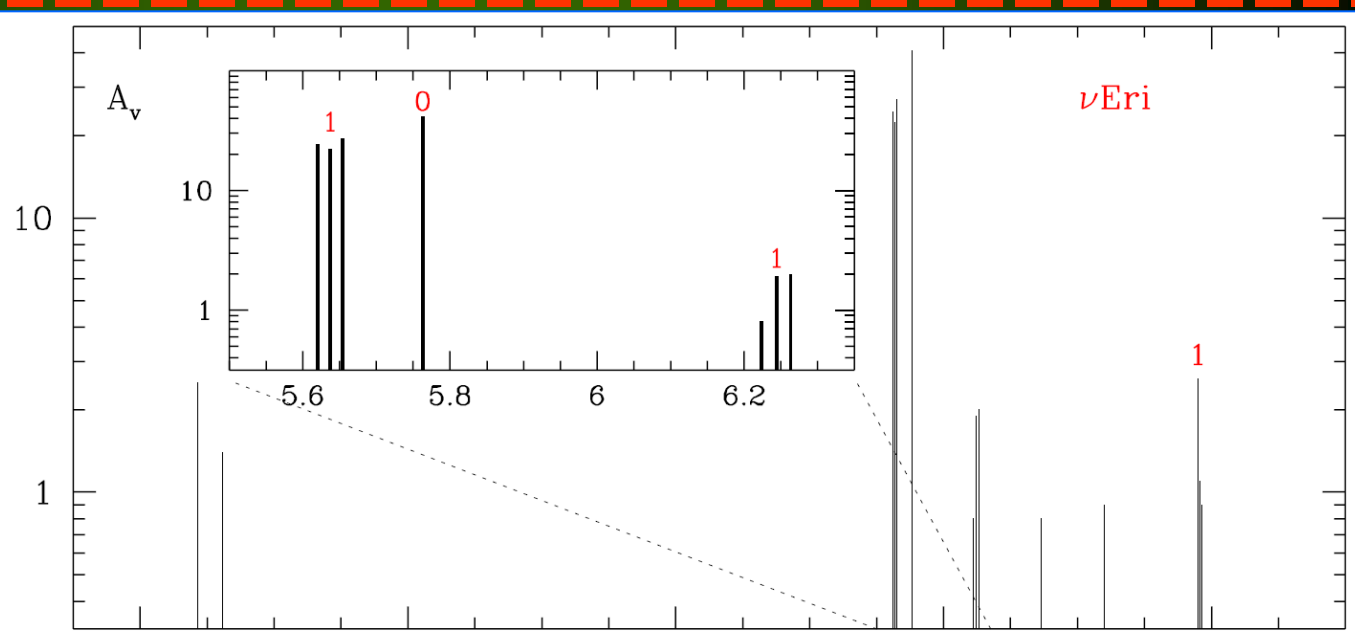


ν Eridani – the multiperiodic β Cephei star
14 oscillation frequencies (from ground-based observations)

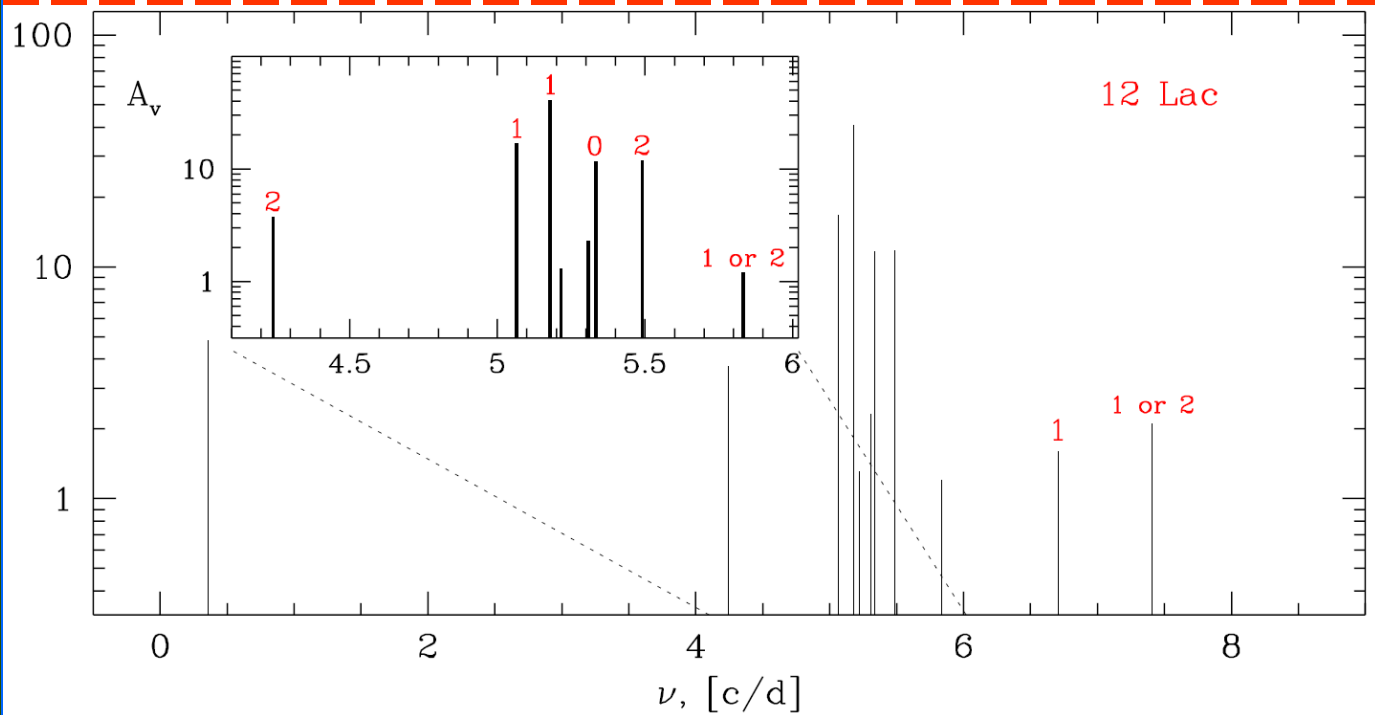


Oscillation spectra of ν Eri and 12 Lac

ν Eri:
Jerzykiewicz et al. 2005



12 Lac:
Handler et al. 2006

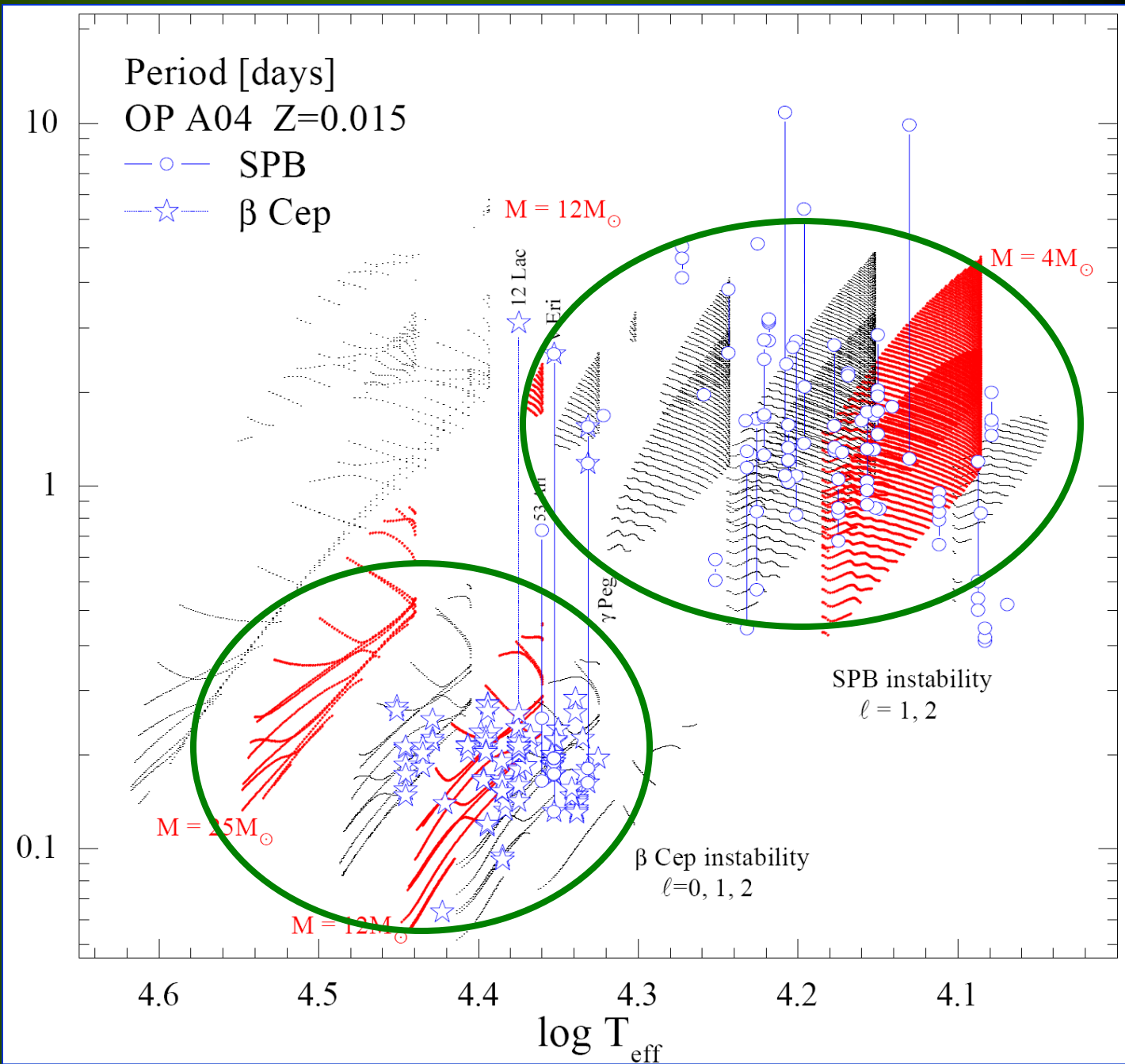


Dziembowski &
Pamyatnykh 2008

Periods of observed β Cep and SPB stars in domains of theoretical periods of unstable modes

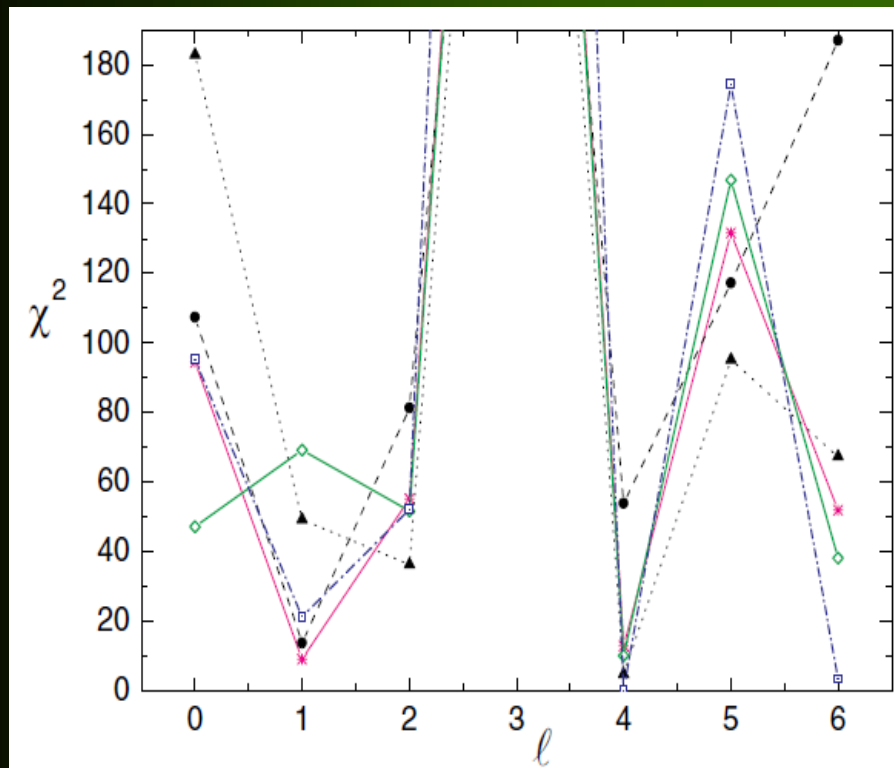
κ OP A04
 $Z=0.015$

Some hybrid stars (with both β Cep and SPB pulsations) are clearly seen

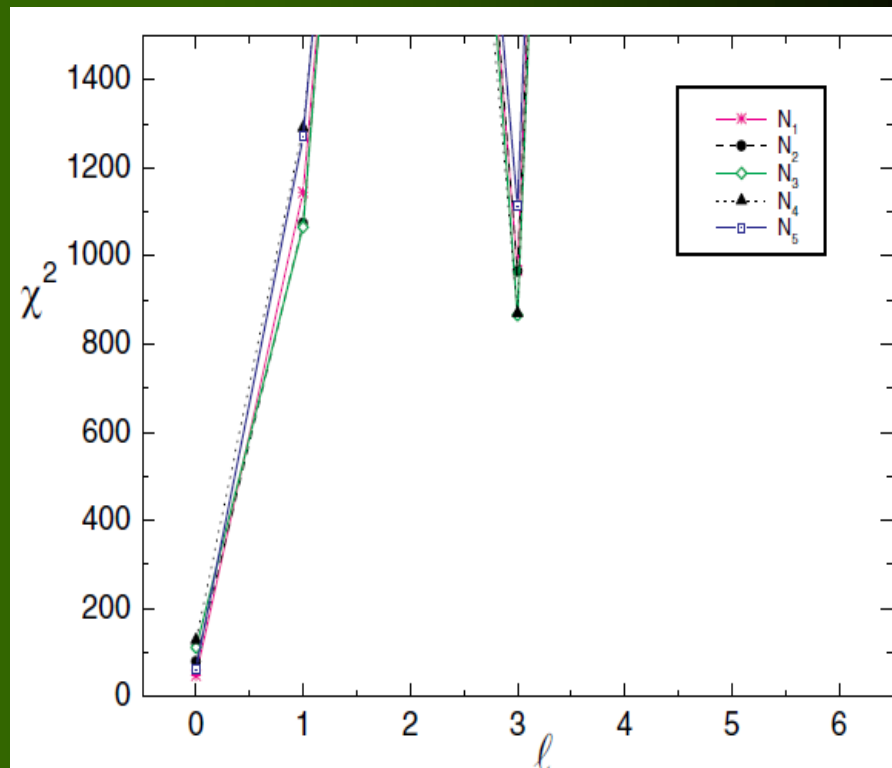


Identification of ℓ for ν_1 (5.763 c/d)

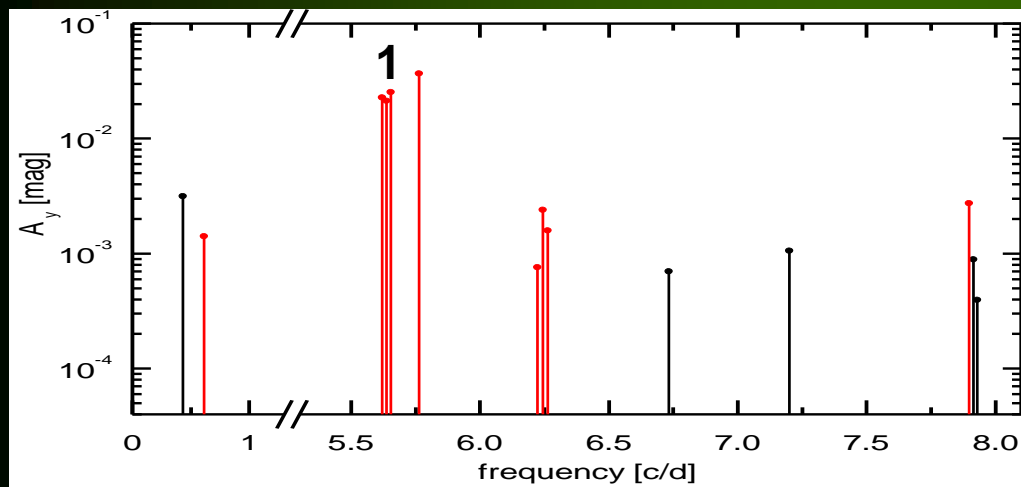
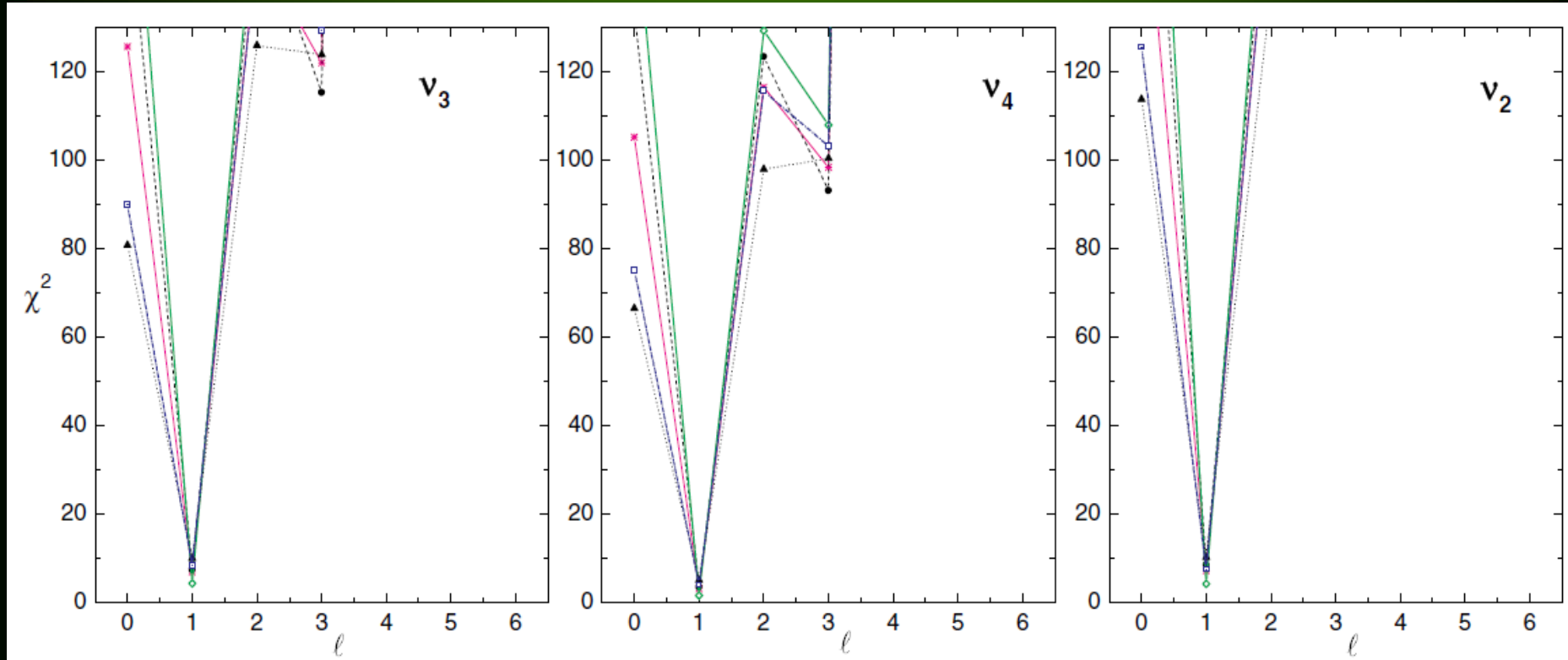
photometry



photometry + spectroscopy



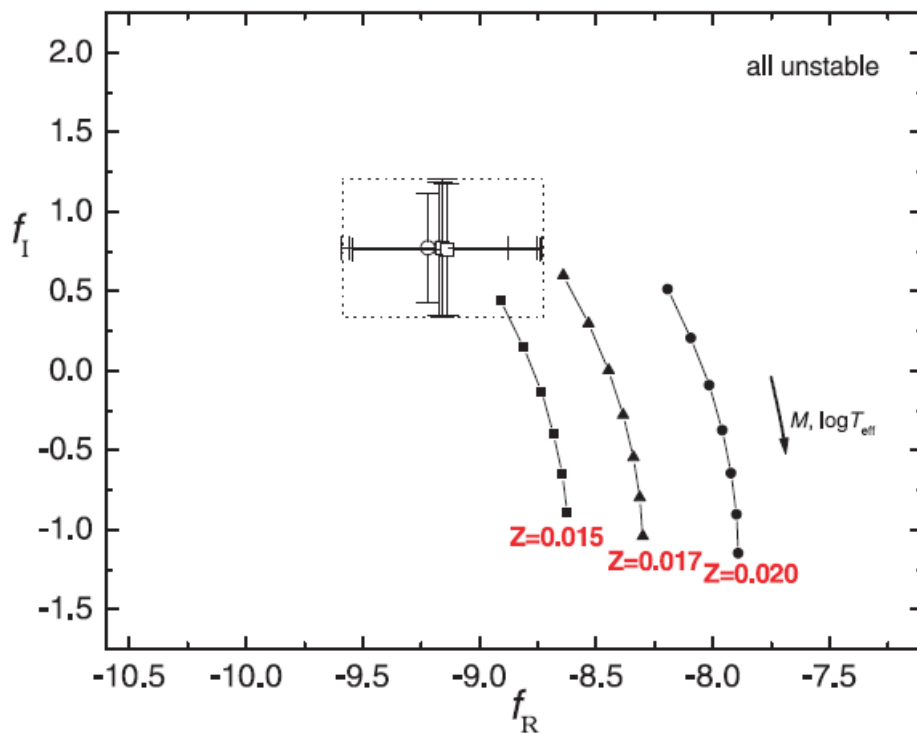
Identification of ℓ for the close frequency triplet ($\nu_3 \nu_4 \nu_2$)



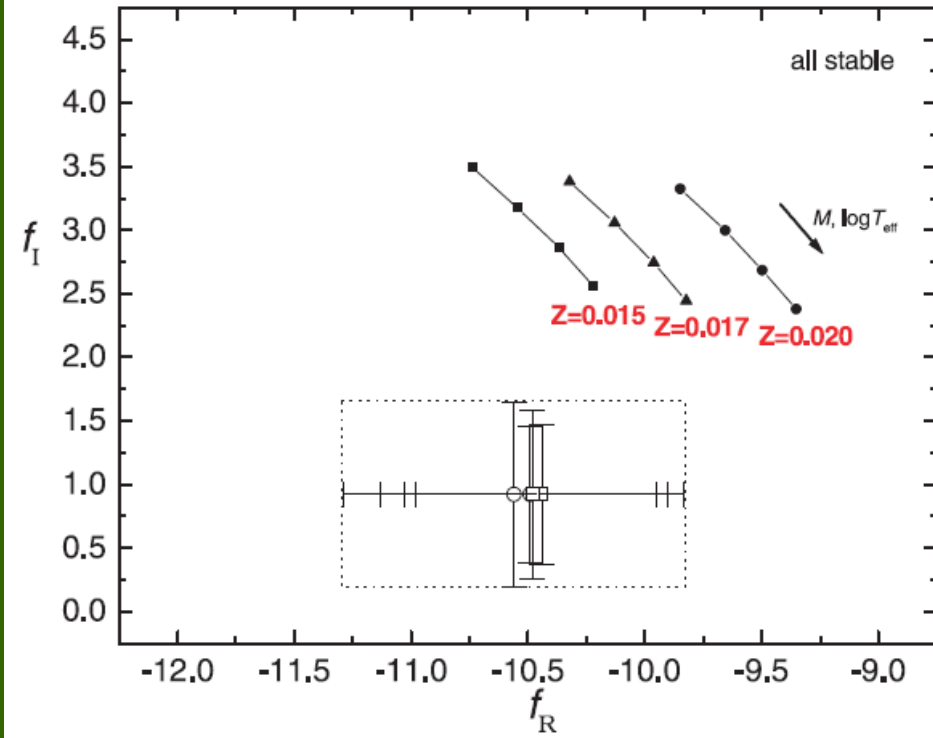
Triplet
5.620, 6.637, 5.654 c/d

Daszyńska-Daszkiewicz, Dziembowski
& Pamyatnykh, 2005

ν Eri. Theoretical and empirical f values for radial mode ν_1 assuming various stellar parameters within the error box.

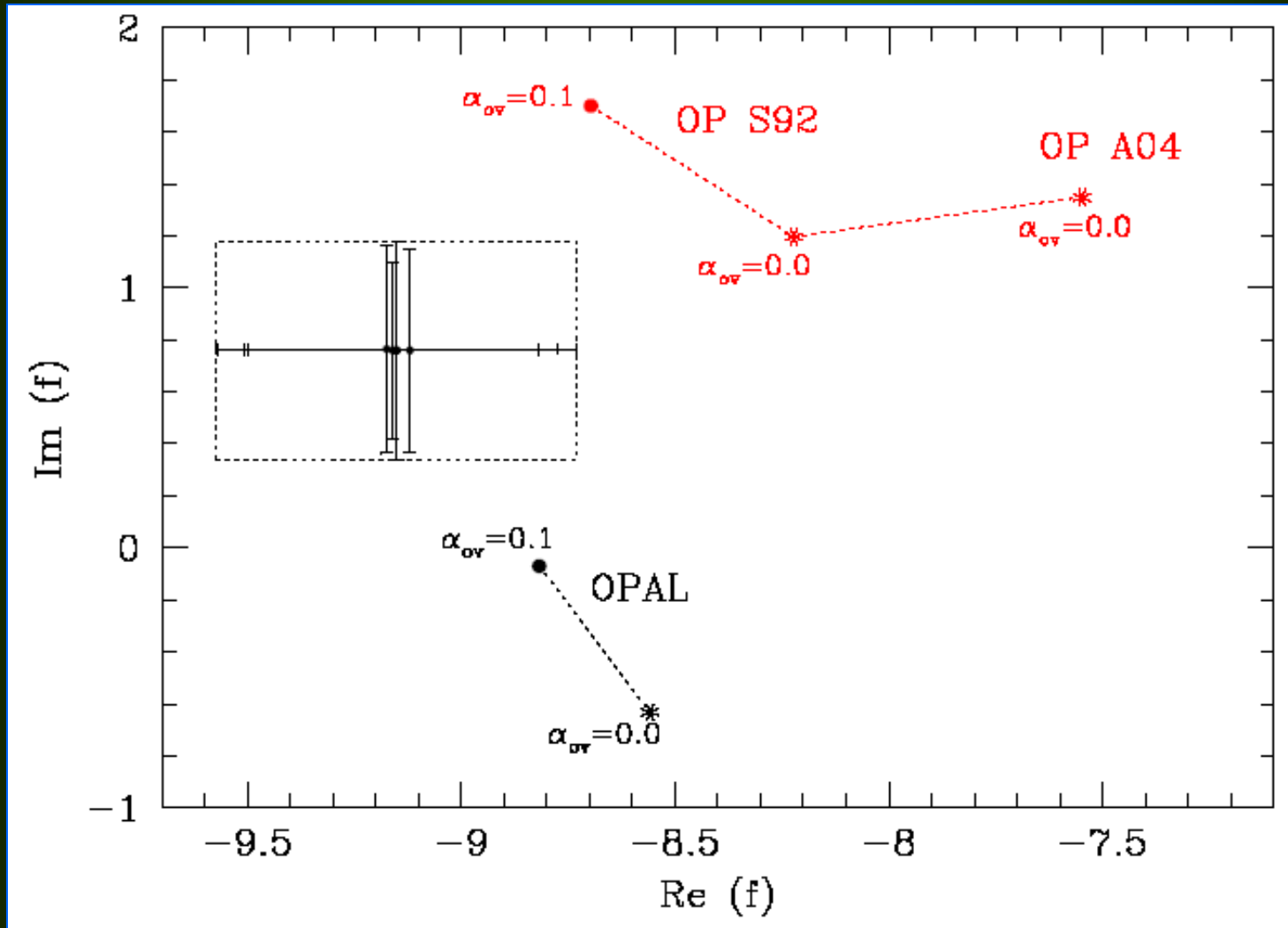


Fundamental mode hypothesis



First overtone hypothesis

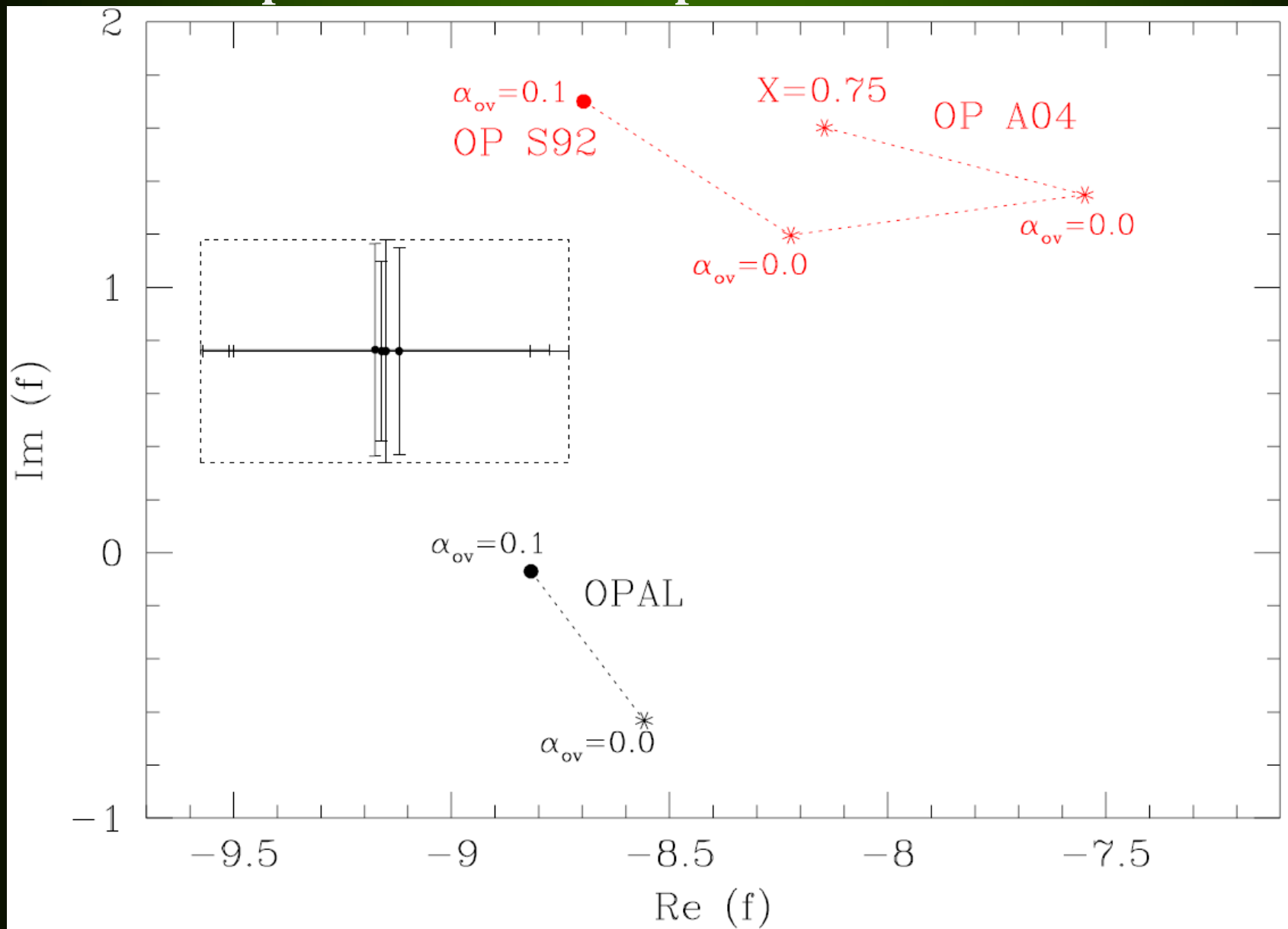
ν Eri: Relative luminosity variations for different seismic models in comparison with the empirical estimations



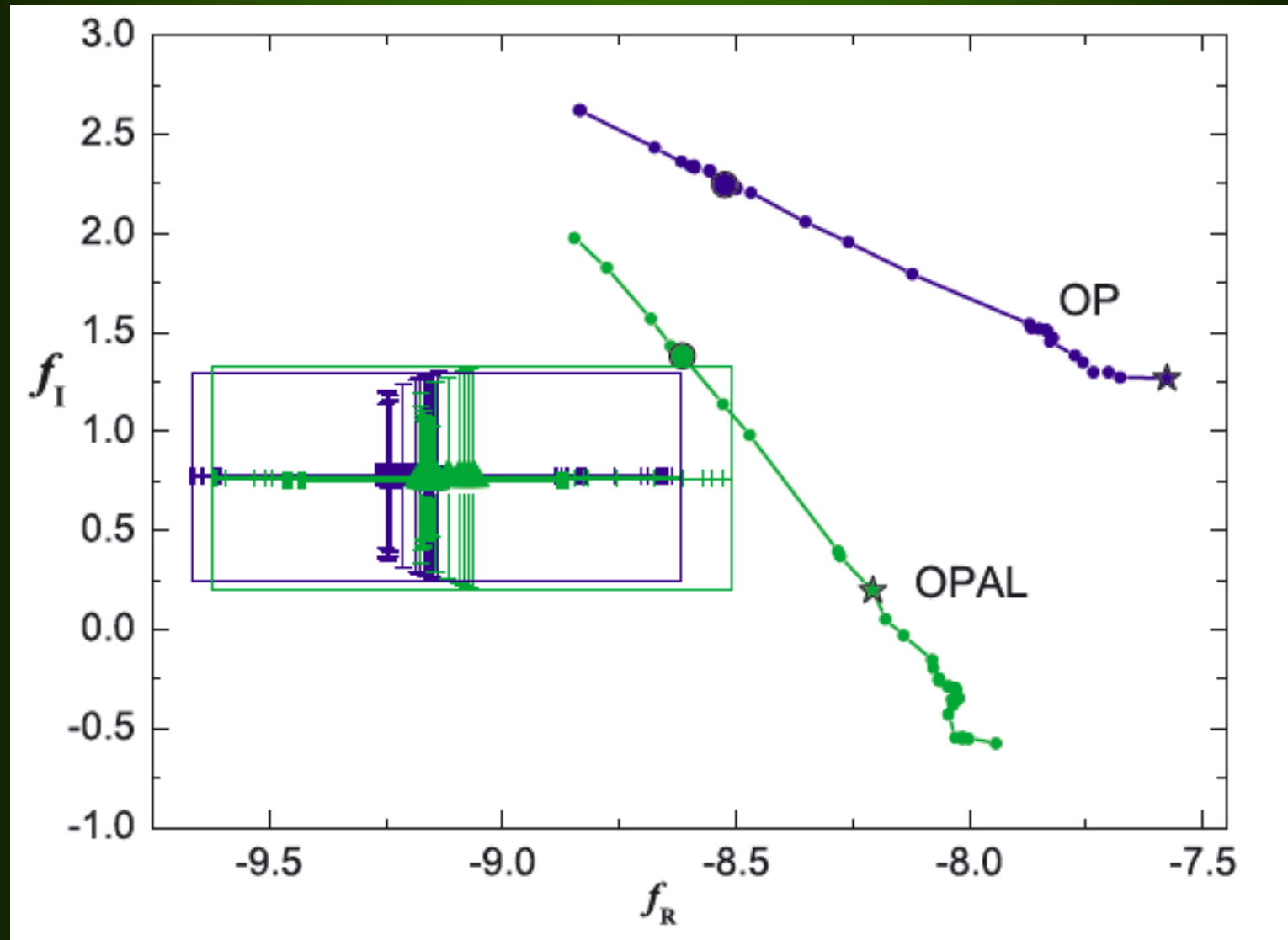
$$\delta r(R, \theta, \varphi) = R \operatorname{Re}\{\varepsilon Y_{\ell}^m e^{-i\omega t}\}$$

$$\frac{\delta \mathcal{F}_{\text{bol}}}{\mathcal{F}_{\text{bol}}} = \operatorname{Re}\{\varepsilon f Y_{\ell}^m e^{-i\omega t}\}$$

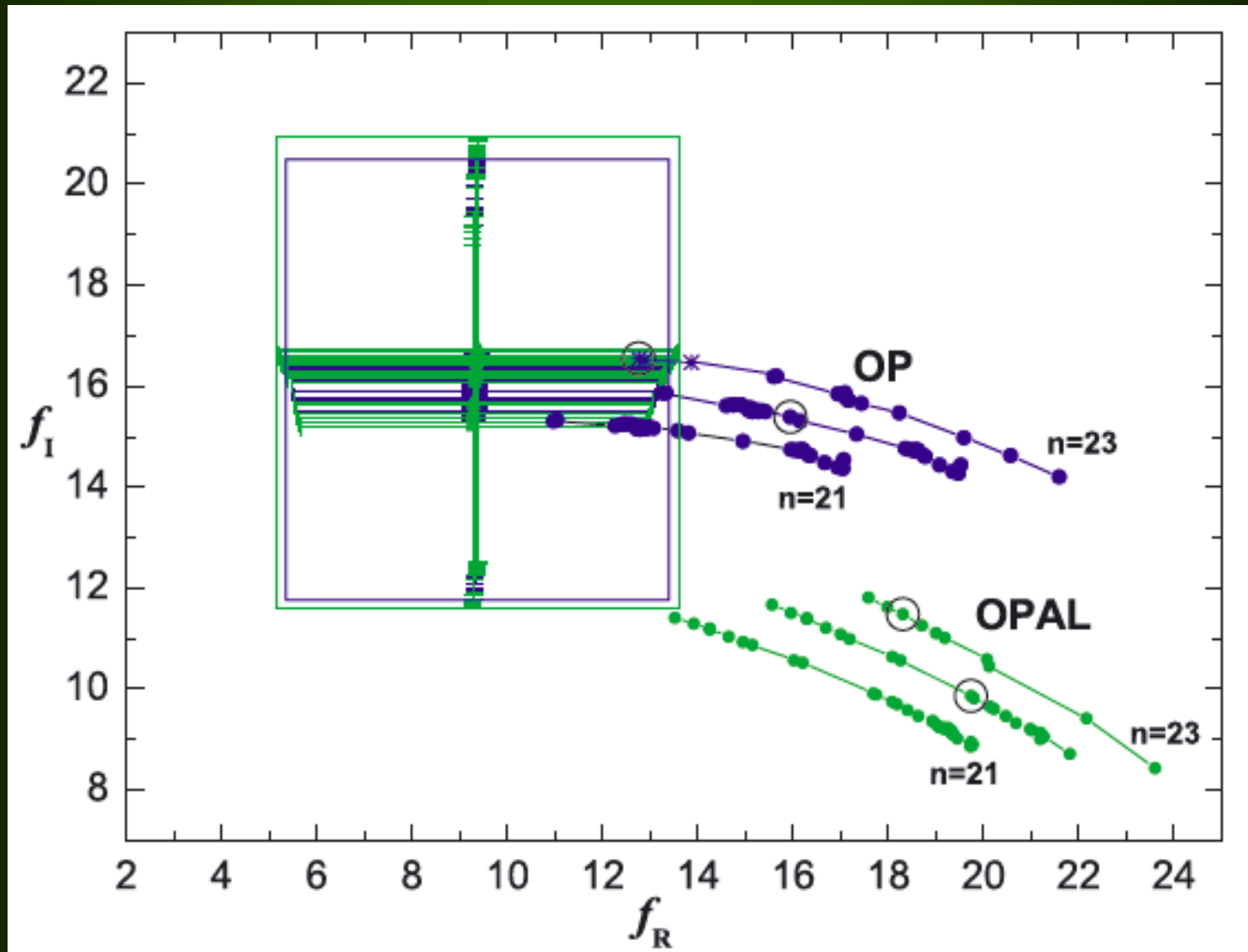
Relative luminosity variations for different seismic models in comparison with the empirical estimations



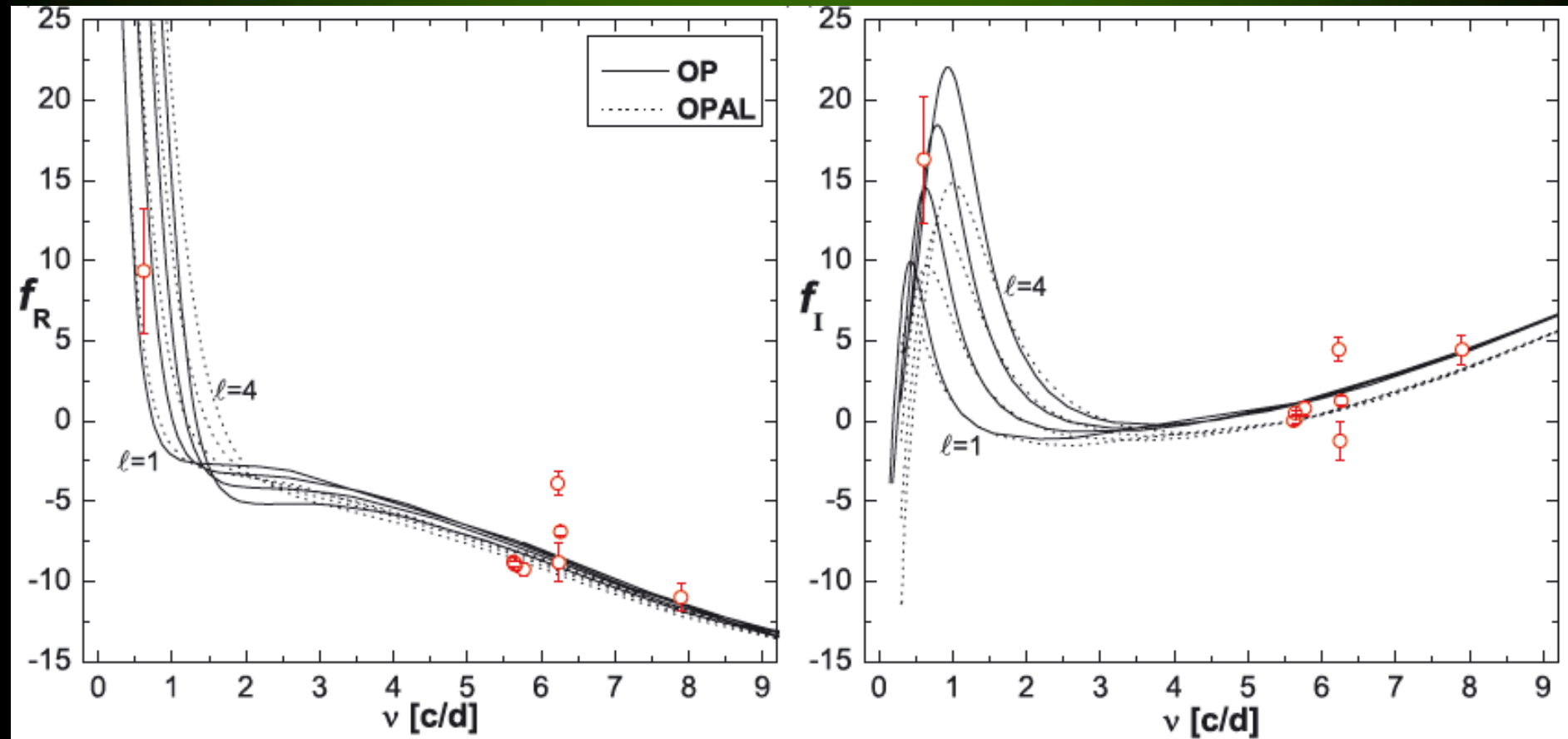
ν Eri. Empirical and theoretical f values for radial p1 mode, $\nu 1$



ν Eri. Empirical and theoretical f values for long-period g, $l=2$ mode, ν B



ν Eri. Empirical and theoretical f values



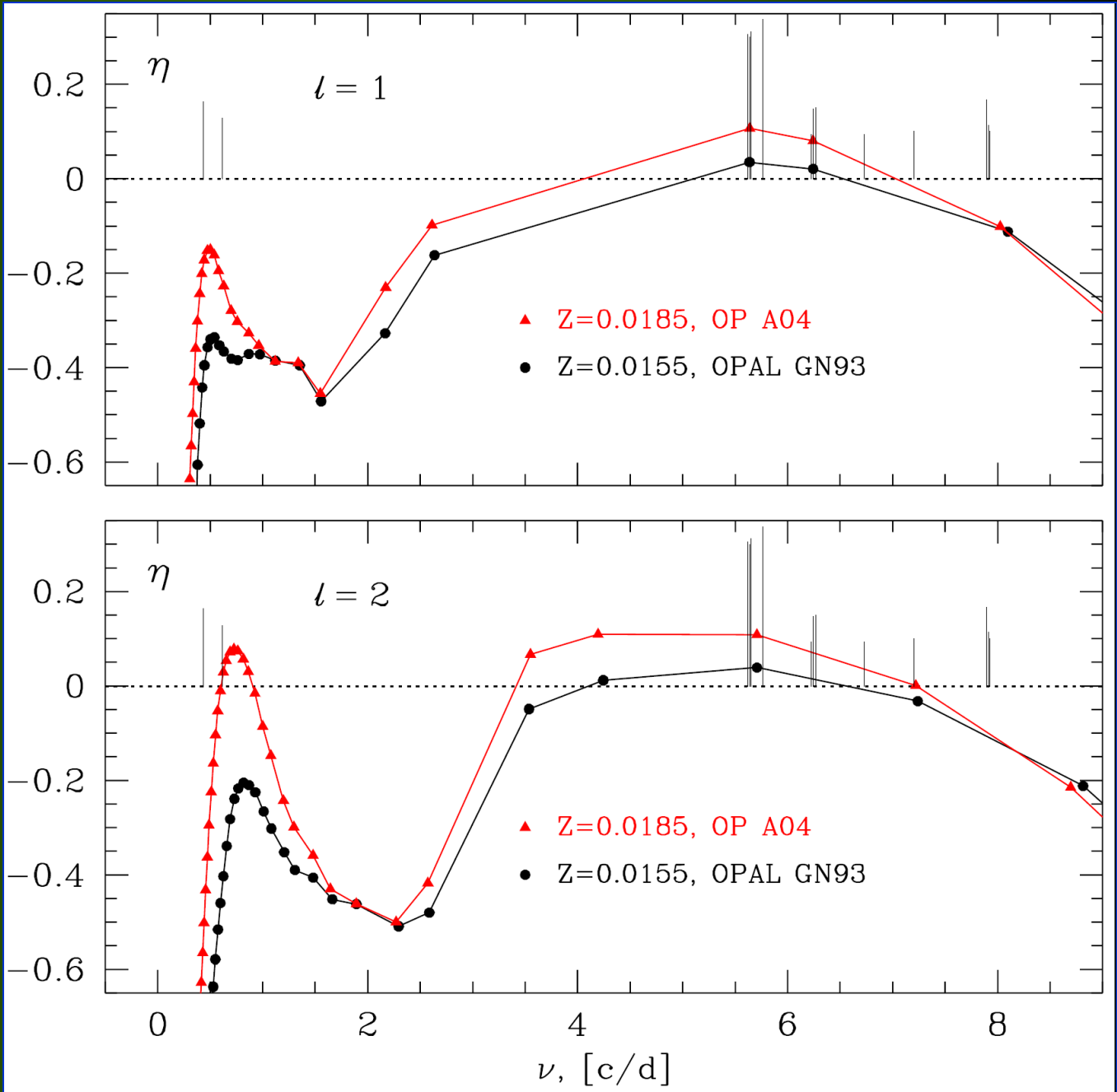
The most recent identification of ℓ

frequency [c/d]	photometry (theoretical f 's)	phot.+ V_{rad} (empirical f 's)
$\nu_1 = 5.7632828$	$\ell=0$	$\ell=0$
$\nu_2 = 5.6538767$	$\ell=1$	$\ell=1$
$\nu_3 = 5.6200186$	$\ell=1$	$\ell=1$
$\nu_4 = 5.6372470$	$\ell=1$	$\ell=1$
$\nu_5 = 7.898200$	$\ell=1$	$\ell=1$
$\nu_6 = 6.243847$	$\ell=1$	$\ell=1$
$\nu_7 = 6.262917$	$\ell=1,3$	$\ell=1,3$
$\nu_8 = 7.20090$	$\ell=?(2)$	-
$\nu_9 = 7.91383$	$\ell \leq 3$	-
$\nu_{10} = 7.92992$	$\ell=?$	-
$\nu_{11} = 6.73223$	$\ell=?(3)$	-
$\nu_{12} = 6.22360$	$\ell=1,2,3$	$\ell=1,2,3$
$\nu_A = 0.432786$	$\ell=1$	-
$\nu_B = 0.61440$	$\ell=2,4$	$\ell=2,5$

$$\eta = \frac{W}{\int_0^1 \left| \frac{dW}{dr} \right| dr}$$

Instability coefficient in models computed with OPAL and **OP** opacities

$\eta > 0$ for unstable modes

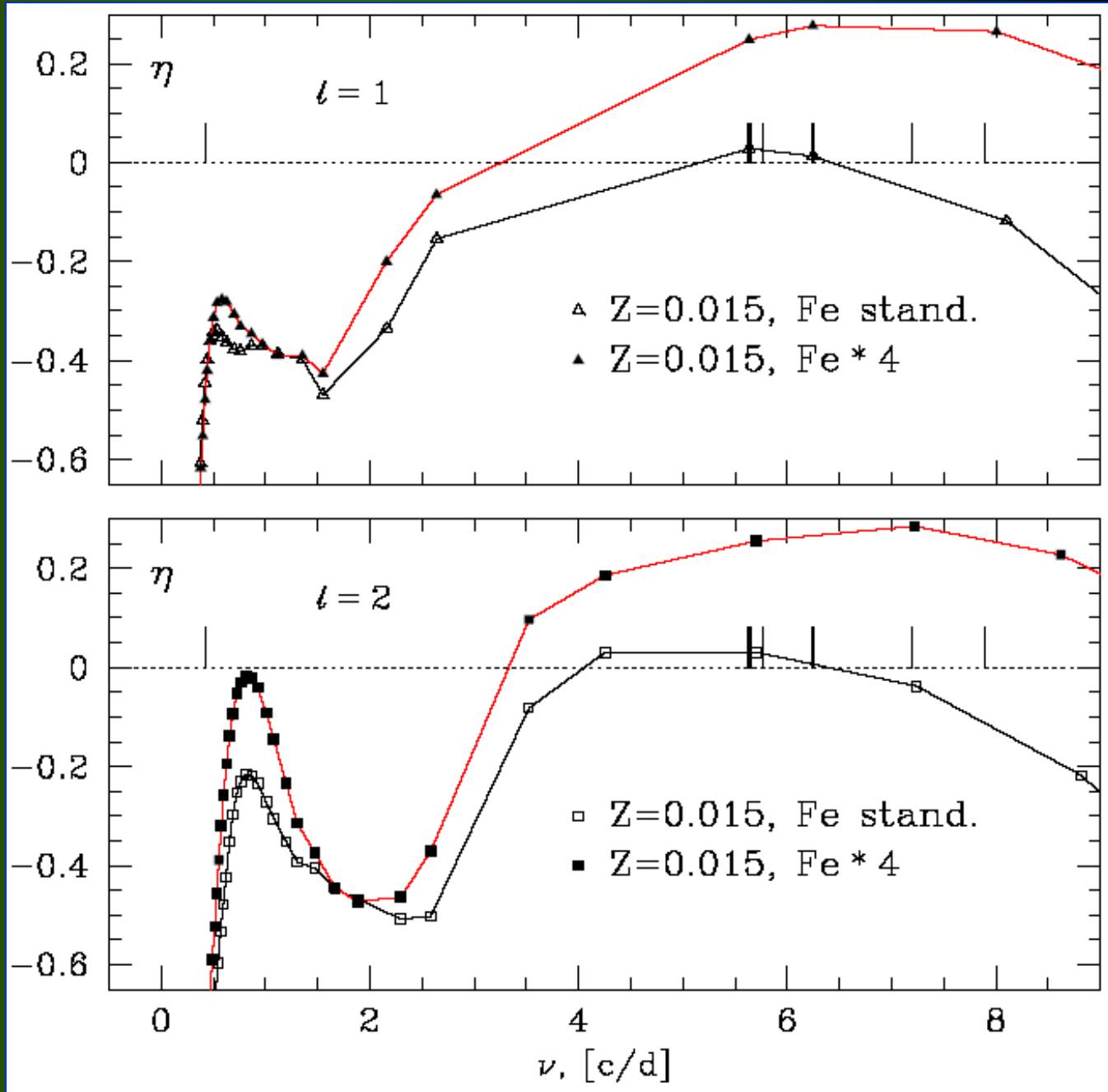


$$\eta = \frac{W}{\int_0^1 \left| \frac{dW}{dr} \right| dr}$$

Instability coefficient
in a standard model
and in the model with
the Fe accumulation
in the driving zone

OPAL opacity in both
cases

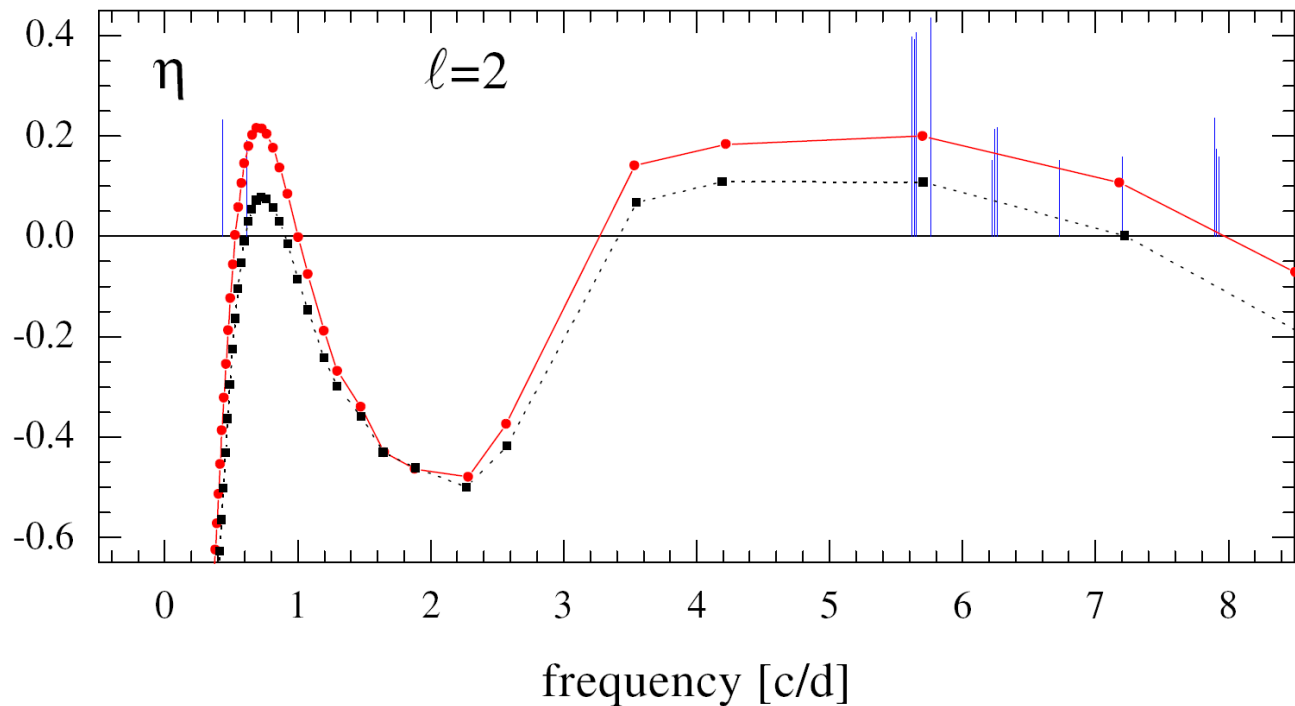
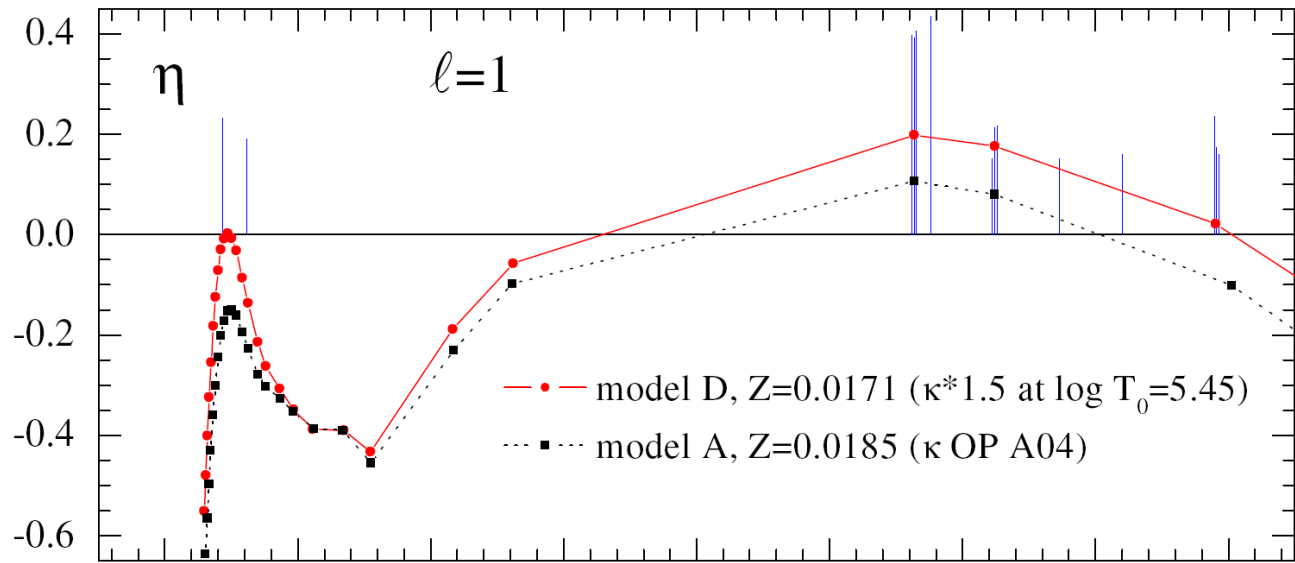
$\eta > 0$ for unstable
modes



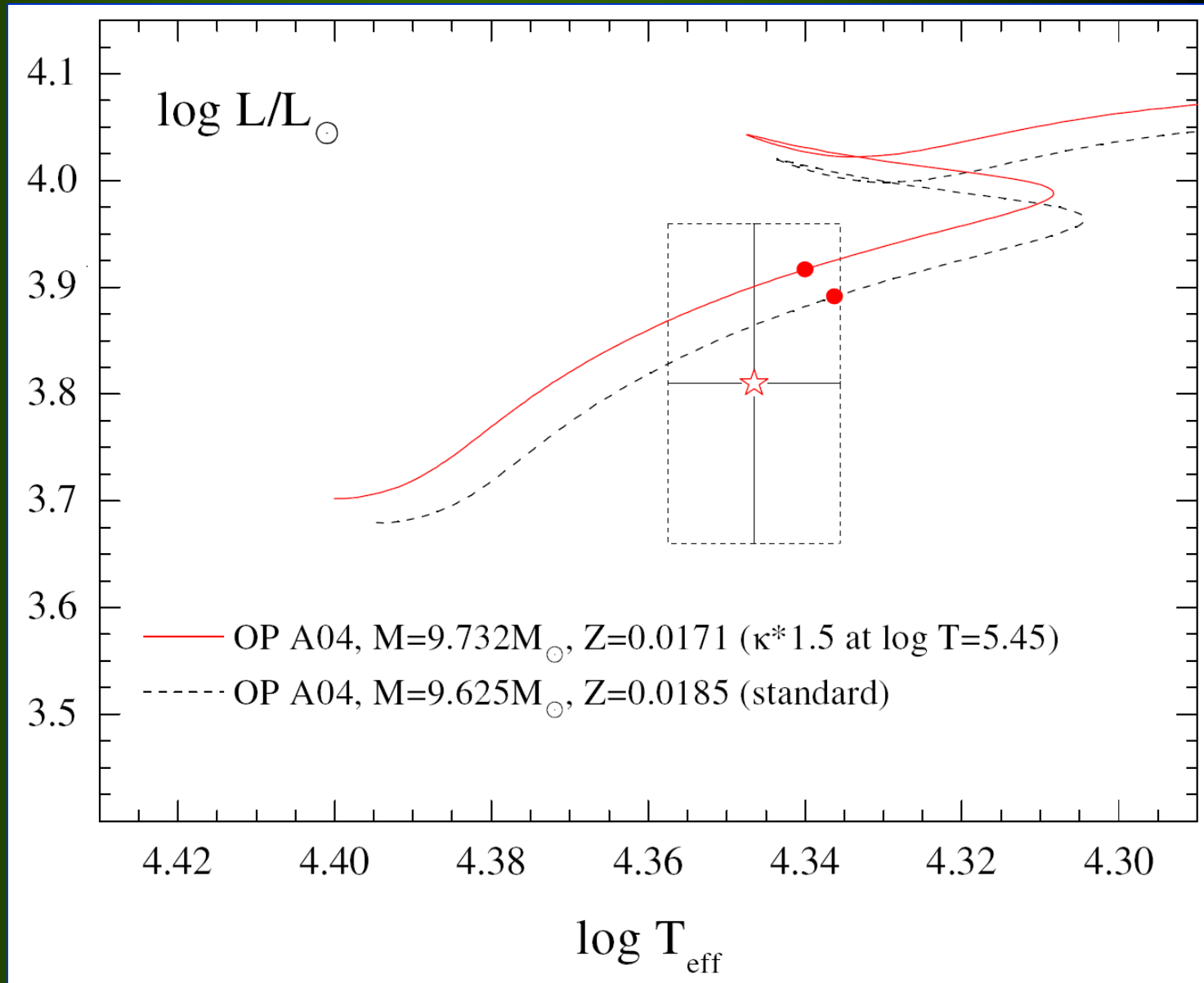
$$\eta = \frac{W}{\int_0^1 \left| \frac{dW}{dr} \right| dr}$$

Instability coefficient
in a standard model
and in the model with
enhanced opacity in
the Z bump region

$\eta > 0$ for unstable
modes

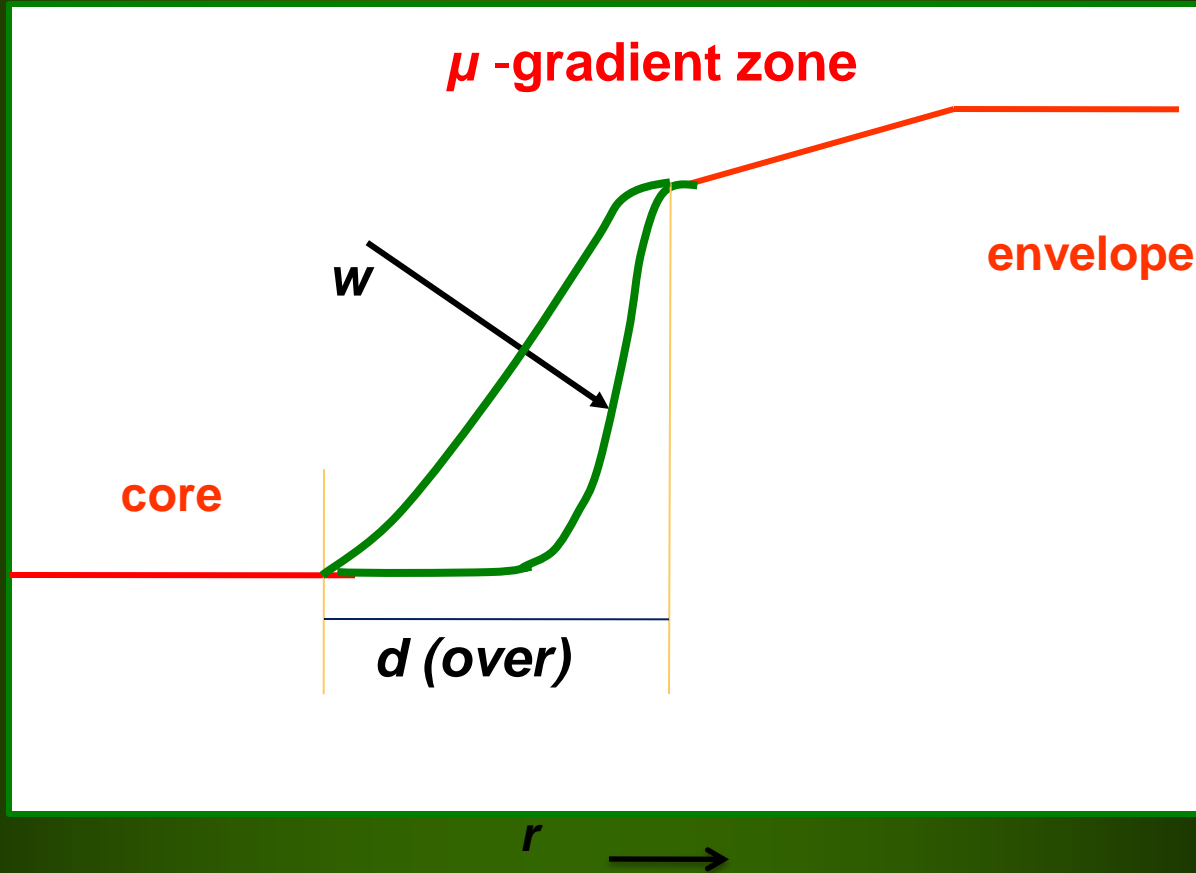


ν Eri : a standard model and the model with enhanced Z bump opacity

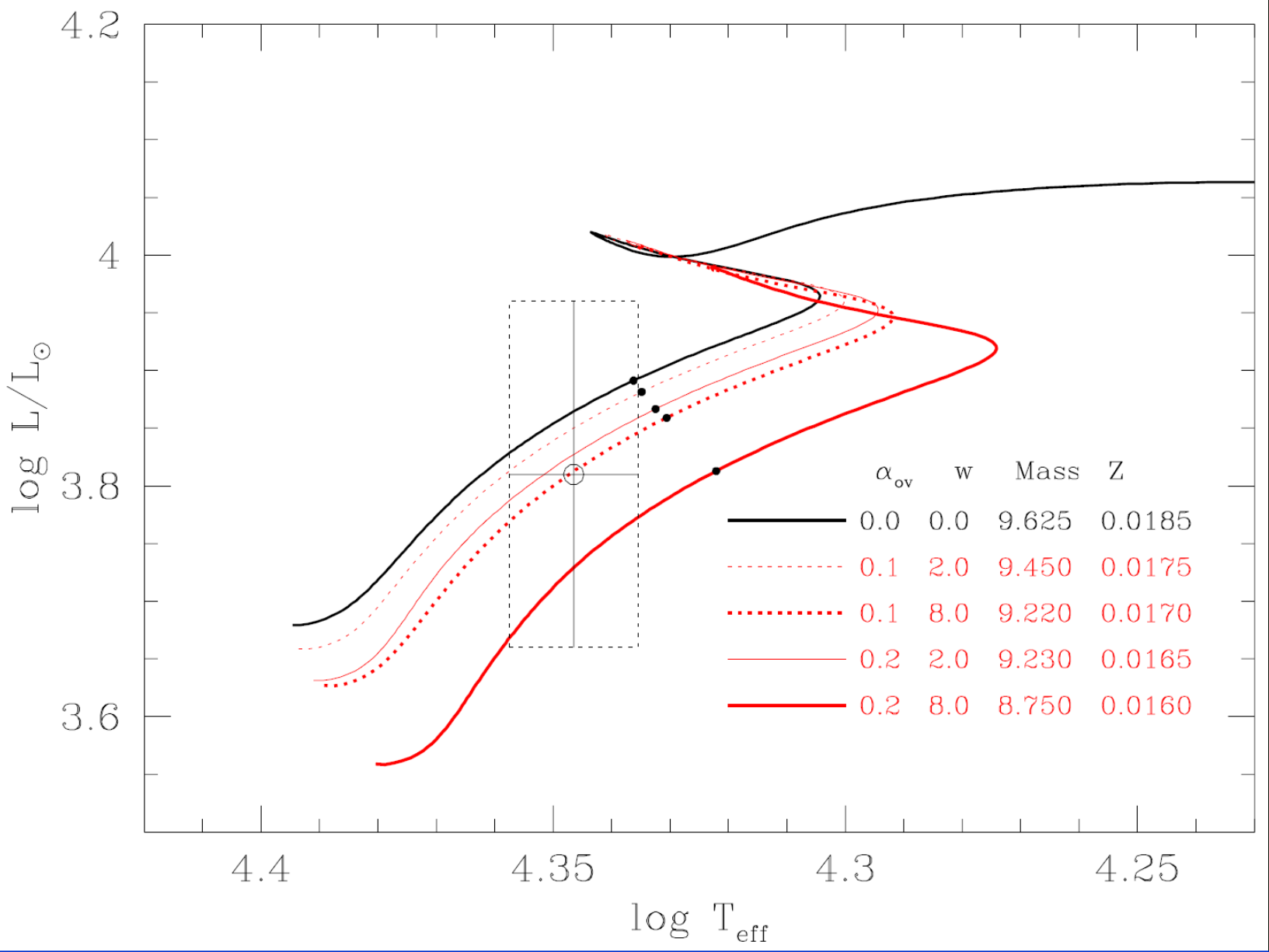


Testing overshooting

Two-parametric overshooting



Seismic models of ν Eri for different overshooting parameters in the H-R diagram



γ Pegasi

14 frequencies (8 - β Cep-type, 6 – SPB-type)

(degree l is identified for >2 of them),

Sp B2 IV,

$m_V = 2.83$,

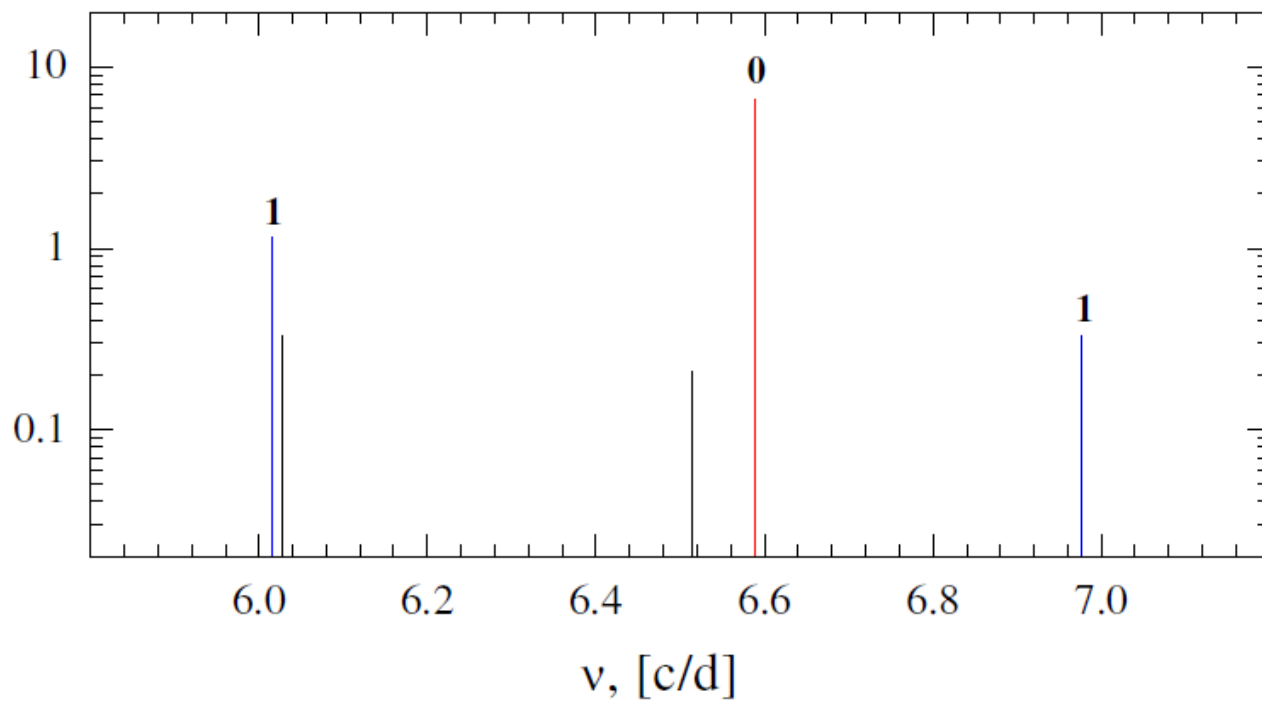
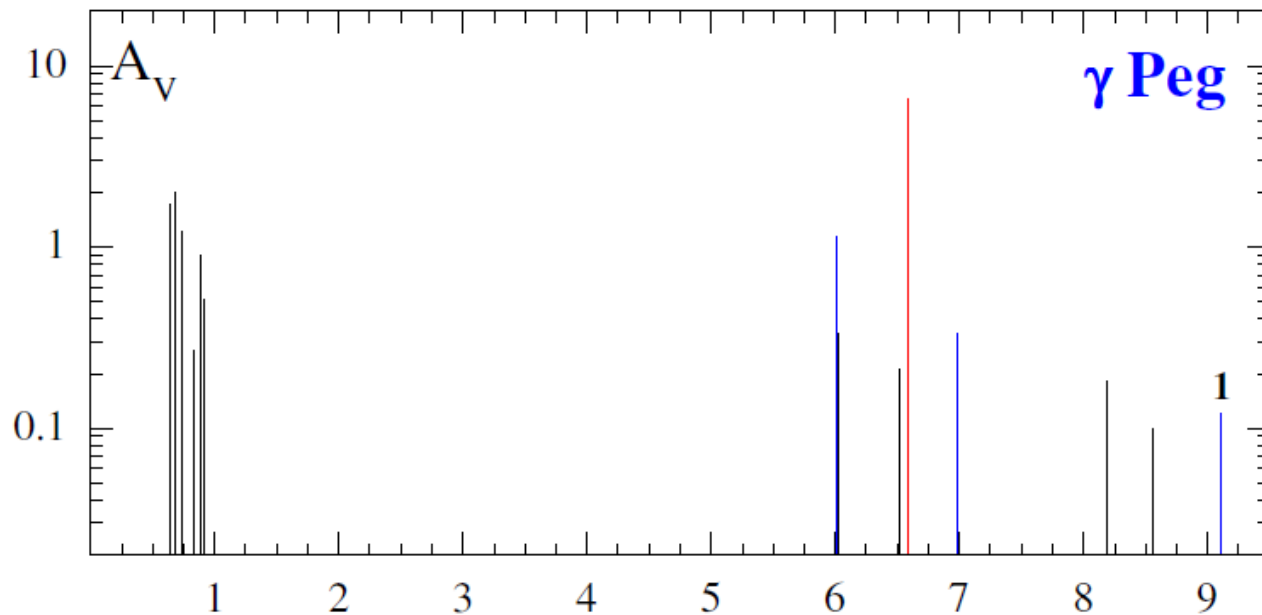
$\pi = 9.79 \pm 0.81$ mas,

$V_{\text{rot}} = 5.0$ km/s,

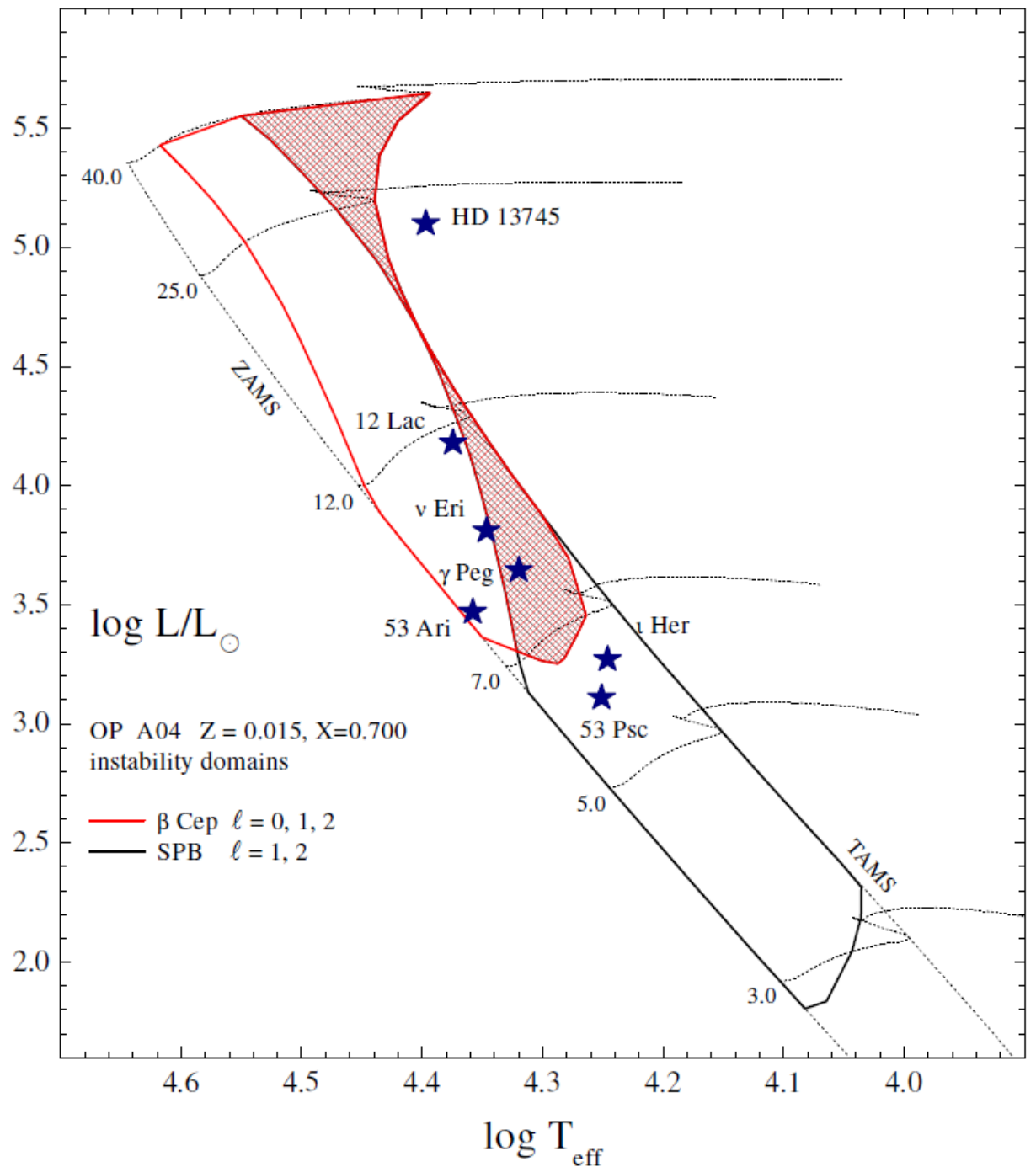
$[m/H] = \text{approx. } 0$,

$T_{\text{eff}} = 21450 \pm 800$ K

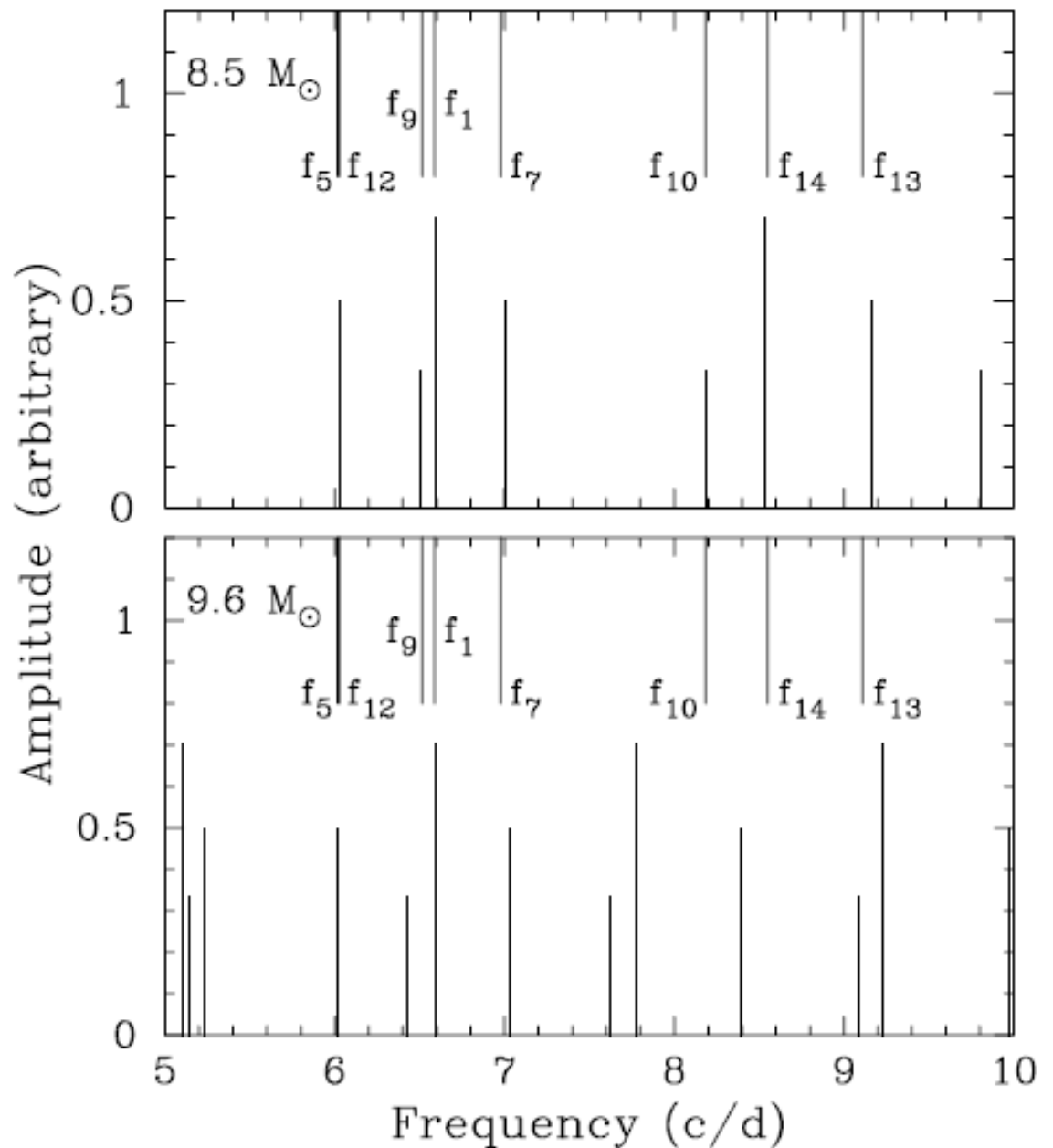
γ Pegasi –
a hybrid
 β Cep / SPB
star



ν Eridani –
 a hybrid
 β Cep / SPB
 star

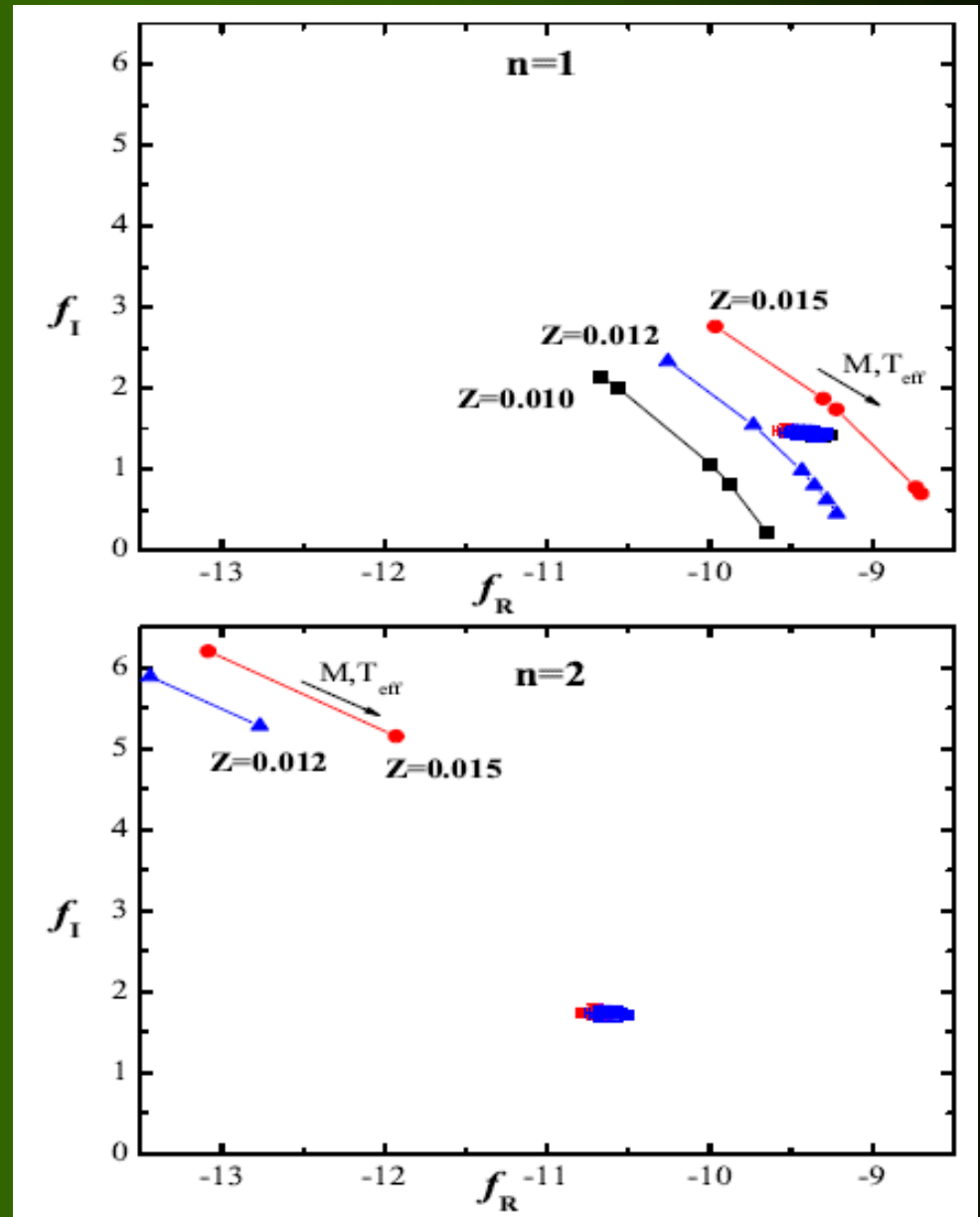


Comparison of theoretical and observed frequencies for two models fitting f_1 as radial mode and f_5 as dipole mode.



γ Peg,
empirical and
theoretical f values
for dominant frequency

Radial fundamental mode



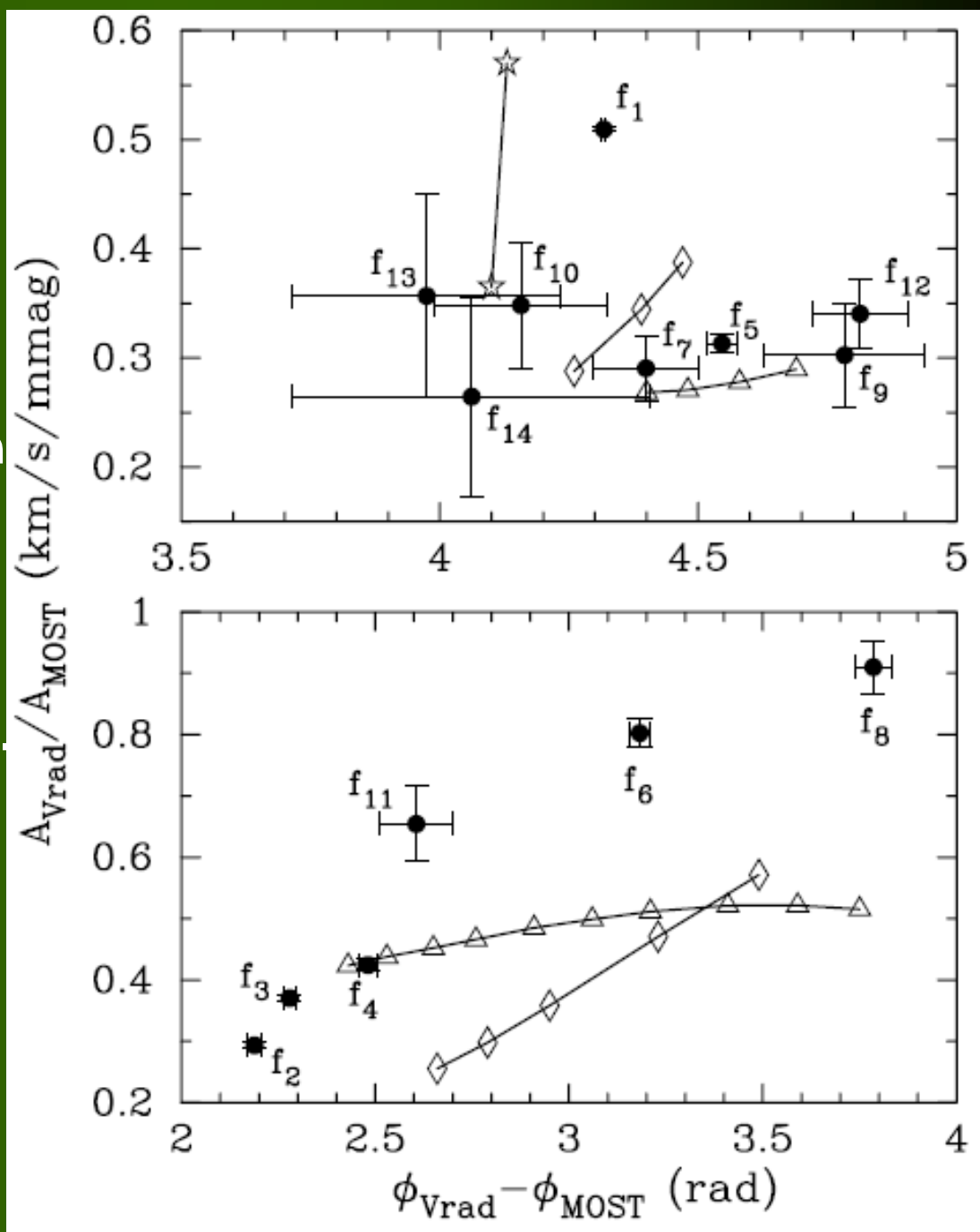
Radial first
overtone

γ Peg

Observed and theoretical
amplitude ratios and
phase differences.

Upper panel – β Cep pulsation
lower panel – SPB pulsations.

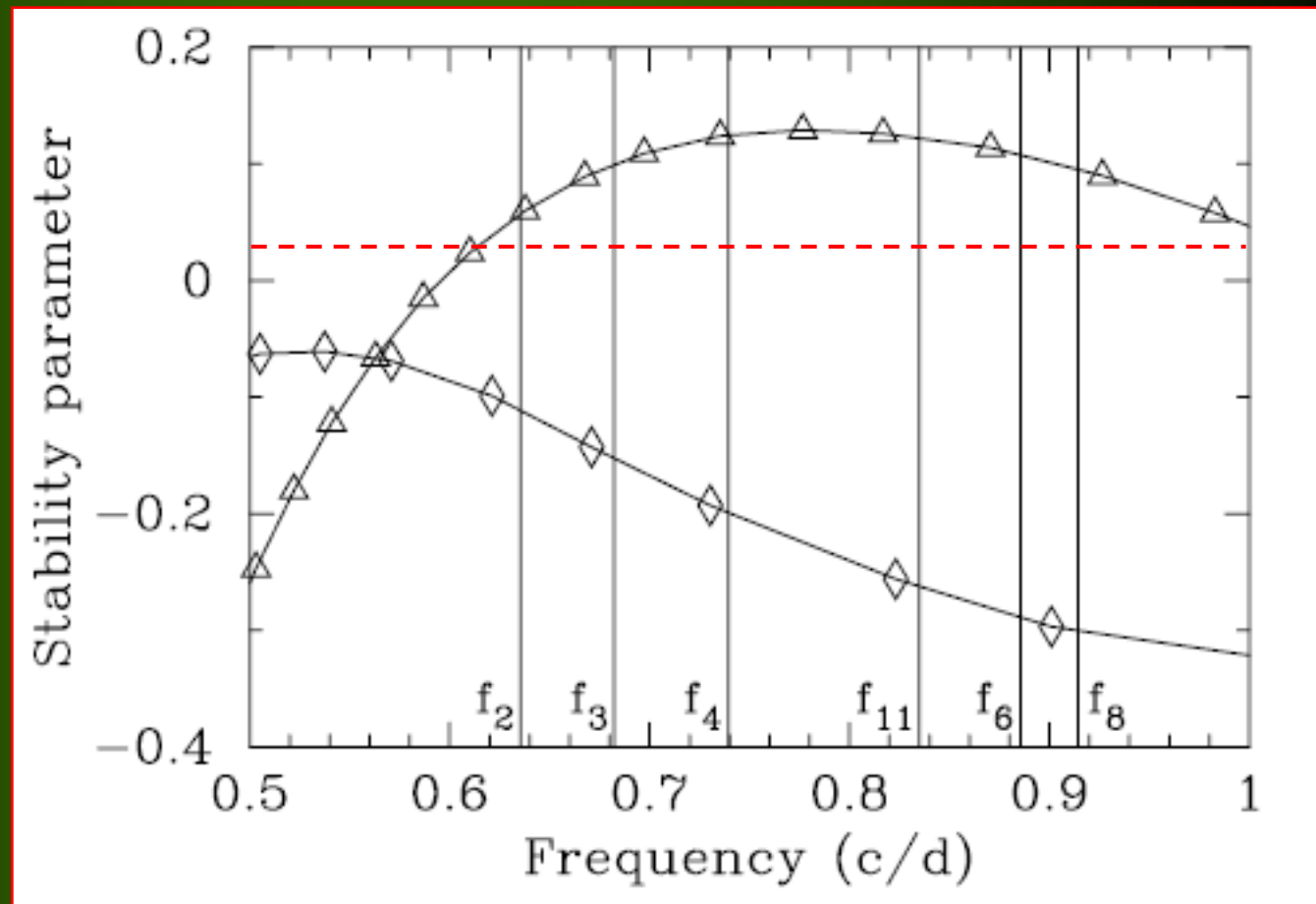
Star symbols – radial modes,
diamonds - dipole modes,
triangles – quadrupole modes.



γ Peg. Comparison of theoretical and observed g-mode pulsation frequencies.

The stability parameter is positive for excited modes

Diamonds - dipole modes,
triangles – quadrupole modes.



γ Peg, mode identification

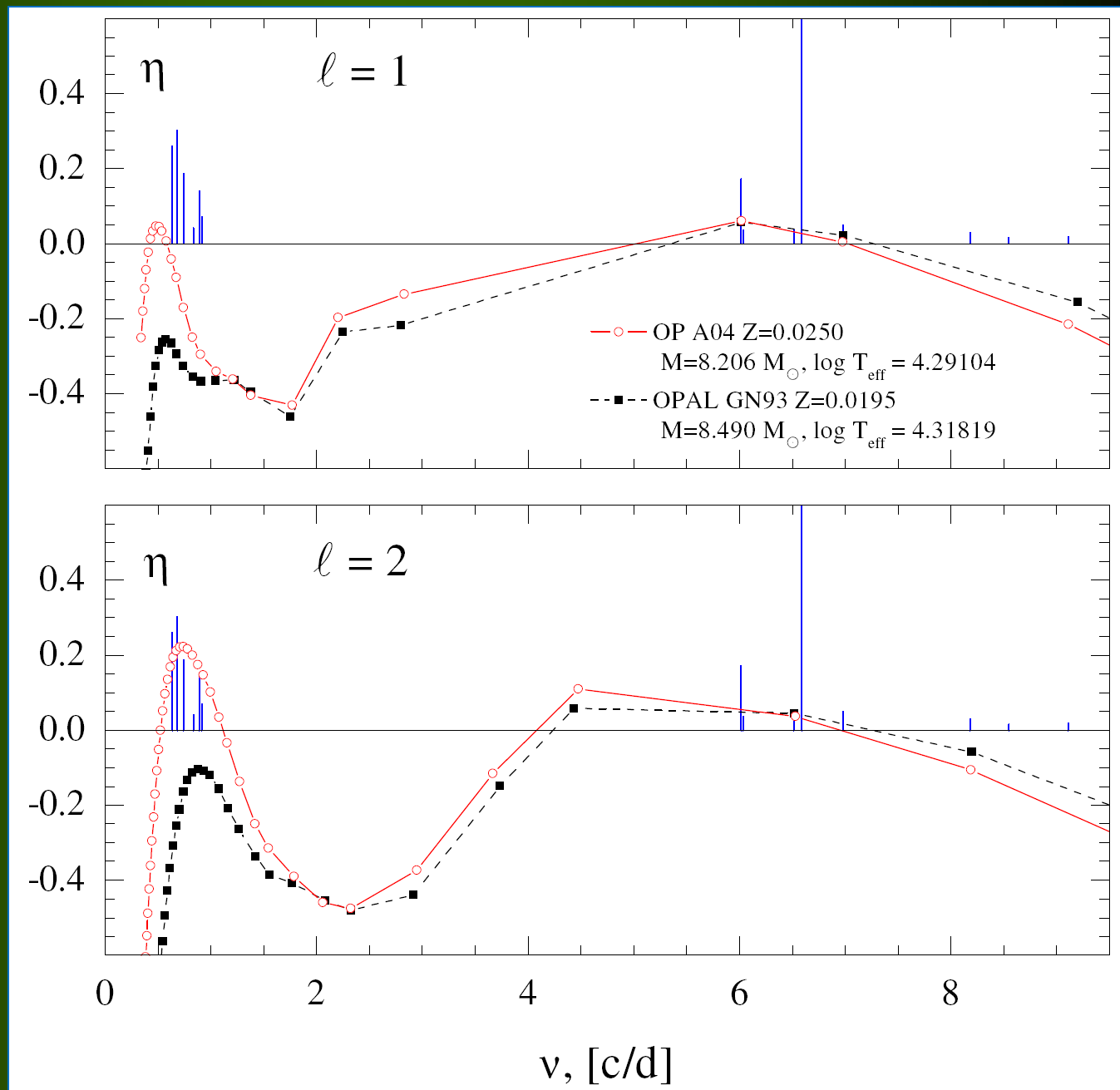
Table 1 The most probable identification of ℓ for the pulsational frequencies of γ Peg from three approaches.

frequency [c/d]	phot. theoretical f	phot.+ V_{rad} theoretical f	phot.+ V_{rad} empirical f
$\nu_1=6.58974$	$\ell=0$	$\ell=0$	$\ell=0$
$\nu_2=0.63551$	$\ell=2$	$\ell=2$	$\ell=2$
$\nu_3=0.68241$	$\ell=1$	$\ell=2$	$\ell=1,2$
$\nu_4=0.73940$	$\ell=2,1$	$\ell=2$	$\ell=1,2$
$\nu_5=6.01616$	$\ell=1,3$	$\ell=1,2$	$\ell=1,0,3$
$\nu_6=0.88550$	$\ell=2$	$\ell=2$	$\ell=2,5$
$\nu_7=6.9776$	$\ell=?$	$\ell=1,2,3,6$	$\ell=?$
$\nu_8=0.91442$	$\ell=2,3,4$	$\ell=1,2$	$\ell=2,3,5$
$\nu_9=6.5150$	$\ell \geq 1$	$\ell=1,2,3,6$	$\ell=?$
$\nu_{10}=8.1861$	$\ell=?$	$\ell=1,2,3,6$	$\ell=?$
$\nu_{11}=0.8352$	$\ell=1,2$	$\ell=1$	$\ell=1,2$
$\nu_{12}=6.0273$	$\ell=?$	$\ell=1,2$	$\ell=2,5$
$\nu_{13}=9.1092$	$\ell=?$	$\ell=1,2,6$	$\ell=?$
$\nu_{14}=8.552$	$\ell \geq 4$	$\ell=6$	$\ell=?$

γ Pegasi

Instability coefficient in a standard model and in the model with enhanced opacity in the Z bump region

$\eta > 0$ for unstable modes



EFFECTS OF ROTATION (Ω)

Rotational mode coupling

$$\omega_j - \omega_k \approx \Omega ; \ell_j = \ell_k \pm 2 ; m_j = m_k$$

Daszyńska-Daszkiewicz et al. 2002, A&A 392,151

Low-frequency modes, $\omega \approx \Omega$

perturbation approach fails

Daszyńska-Daszkiewicz et al. 2007, AcA 57,11

The photometric diagrams become dependent on:

- 1) the inclination angle, i ,
- 2) the azimuthal order, m ,
- 3) the rotational velocity, V_{rot}

THE PHOTOMETRIC COMPLEX AMPLITUDE OF THE COUPLED MODE

$$\mathcal{A}_\lambda(i) = \sum_k a_k A_{\lambda,k}(i)$$

Regularities in theoretical frequency spectra:

- high-order p-modes:

$$\nu_{nl} \approx \Delta\nu \cdot \left(n + \frac{l}{2} + d\right) - \frac{l(l+1)}{4\pi^2 n} \cdot f_c$$

$$\Delta\nu = \left(2 \int \frac{dr}{c}\right)^{-1}, \quad f_c = \int \frac{dc}{dr} \cdot \frac{dr}{r}$$

large separation:

$$\nu_{nl} - \nu_{n-1, l} \approx \Delta\nu$$

small separation:

$$\nu_{nl} - \nu_{n-1, l+2} = \delta\nu_{nl} \approx -\frac{4l+6}{4\pi^2 n} \cdot f_c$$

- high-order g-modes:

$$\Pi_{nl} \approx \frac{n}{l(l+1)} \cdot \Delta\Pi, \quad \Delta\Pi = 2\pi^2 \left(\int \frac{N}{r} dr\right)^{-1}$$

$$N = g \left(\frac{1}{\Gamma_1} \frac{d \ln P}{dr} - \frac{d \ln \rho}{dr} \right)$$

- Rotational splitting: (~ Goupil et al. 2000)

$$\underline{\nu_m = \nu_0 + m(1 - C_{ne}) \frac{\Omega}{2\pi} + \frac{\Omega^2}{2\pi \nu_0} (D_0 + m^2 D_1) + m \frac{\Omega^3}{\nu_0^2} T}$$

$$\Rightarrow \underline{\frac{\nu_m - \nu_{m=0}}{m} = \frac{\Omega}{2\pi} (1 - C_{ne} + m\mu D_1 + \mu^2 T)}$$

- rotation rate:

$$\frac{\nu_m - \nu_{-m}}{2m} = \Omega (1 - C_{ne} + \mu^2 T)$$

$$\mu = \frac{\Omega}{\nu_0}$$

- Effective gravity:

$$g_{\text{eff}} = g - \frac{2}{3} \Omega^2 r$$

- Ledoux constant:

$$C_{nl} = \frac{\int (2yz + z^2) \rho r^4 dr}{\int (y^2 + \Lambda z^2) \rho r^4 dr} \quad \Lambda = l(l+1)$$

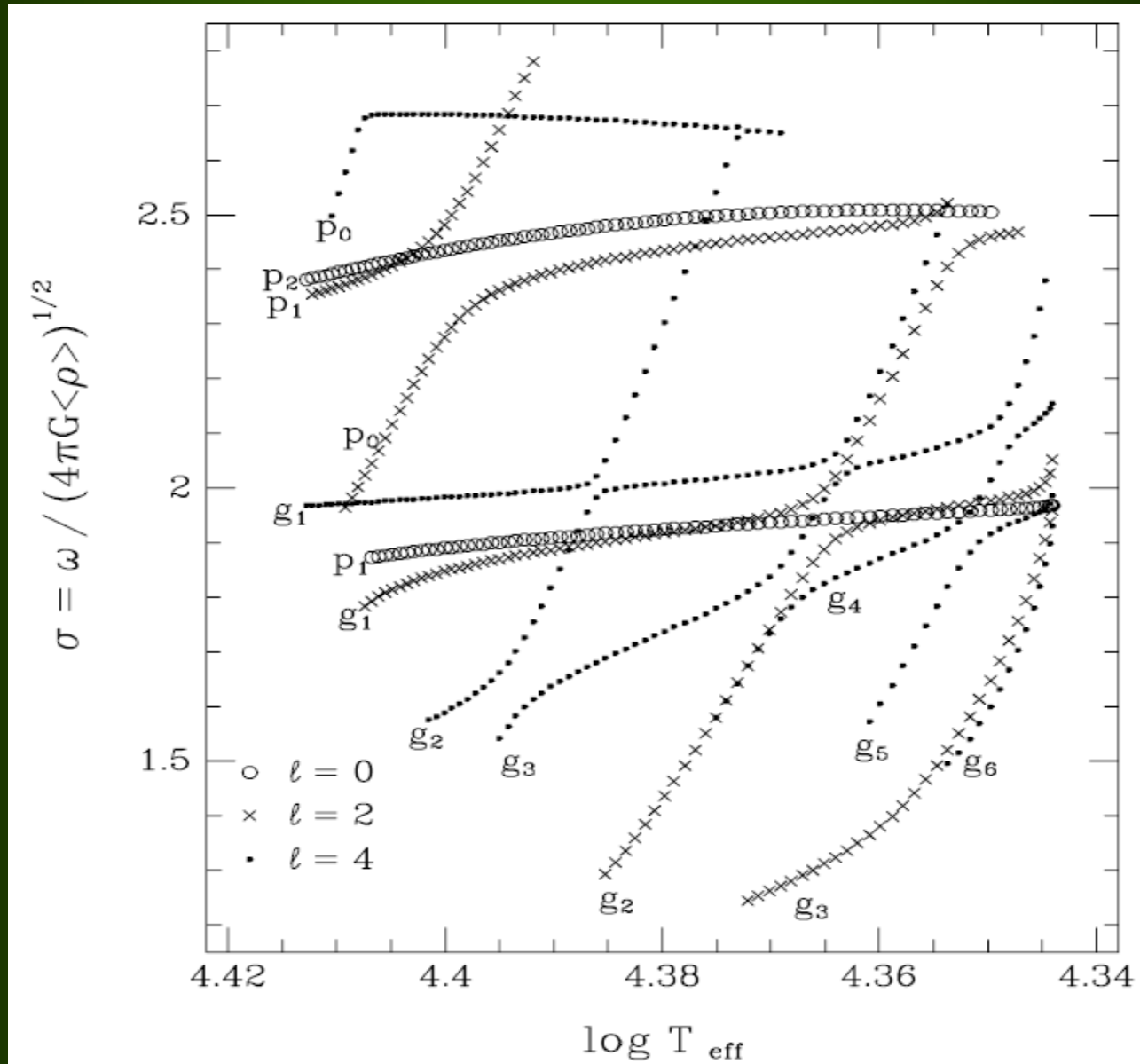
y, z - radial and horizontal components
of displacement

$C_{nl} \ll 1$ for high-order p -modes ($y \gg z$)

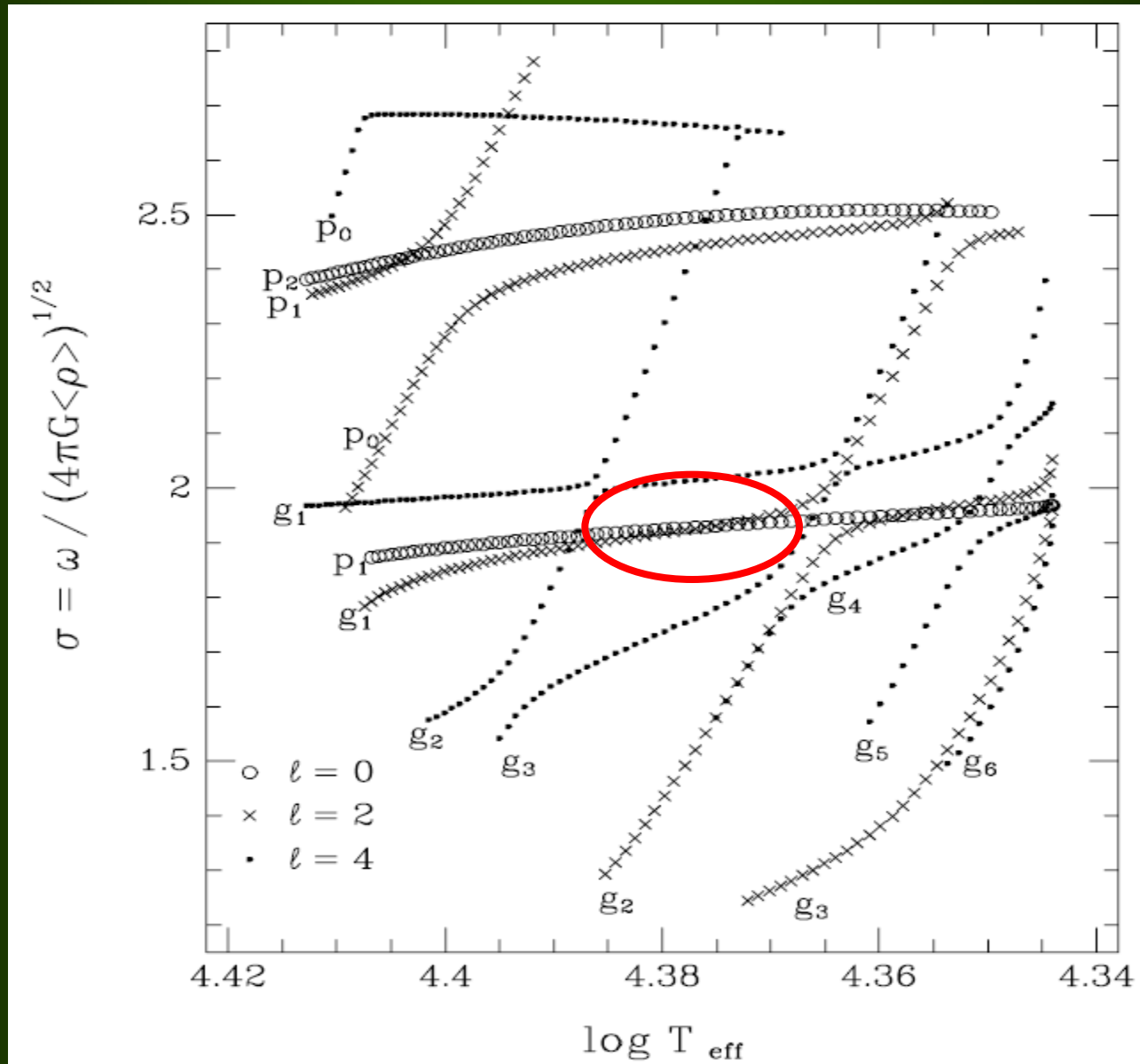
$C_{nl} \approx \frac{1}{l(l+1)}$ for g -modes ($z \gg y$)

$C \sim \frac{1}{2}$ for gravity modes of $l=1$

Unstable modes of $l = 0, 2, 4$ in β Cep star models



Unstable modes of $l = 0, 2, 4$ in a β Cep star model



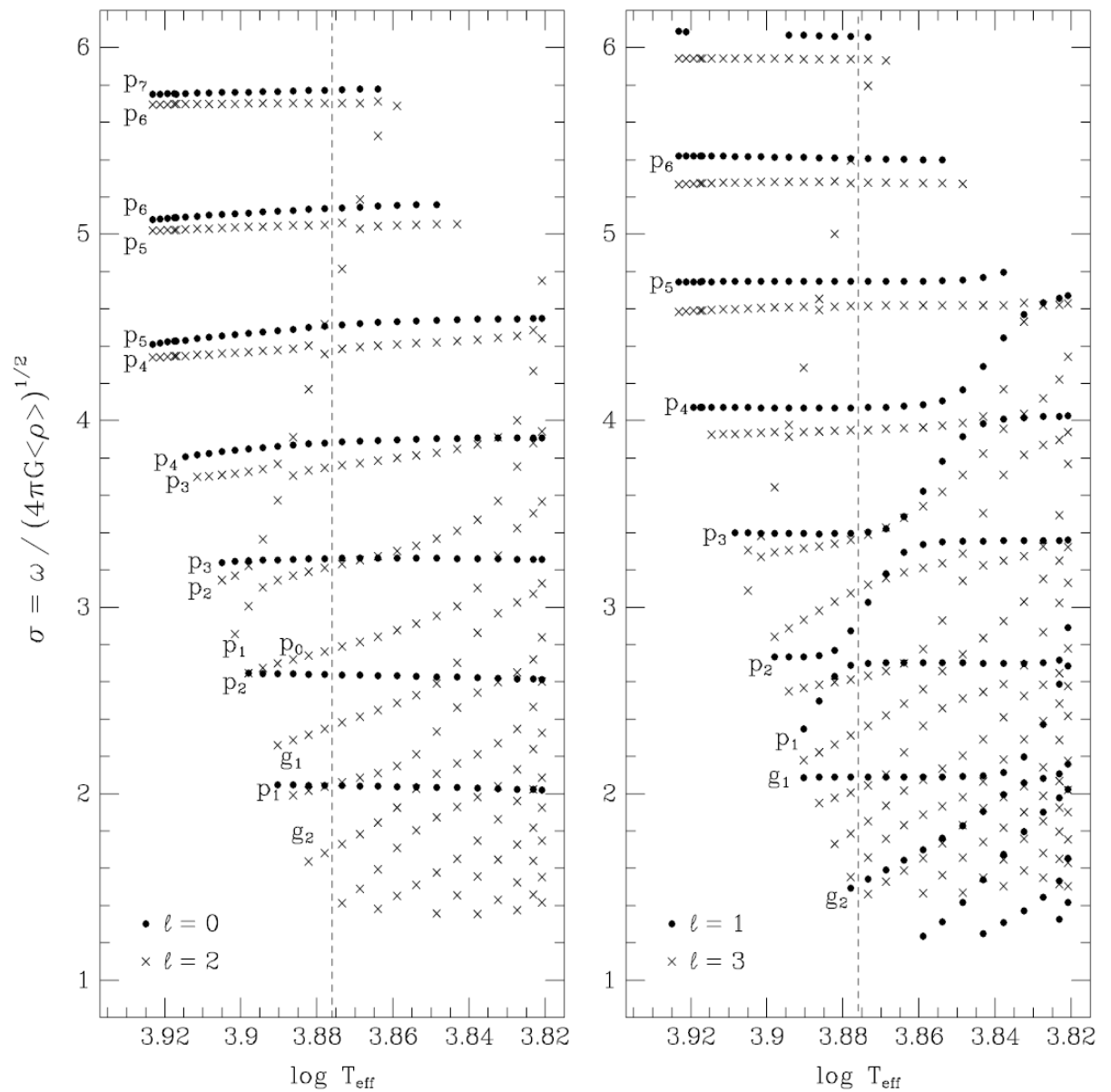
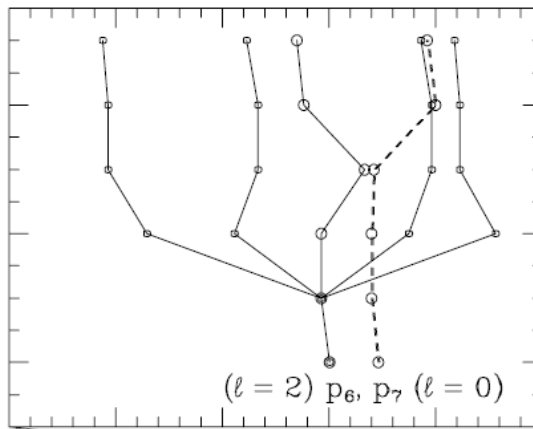
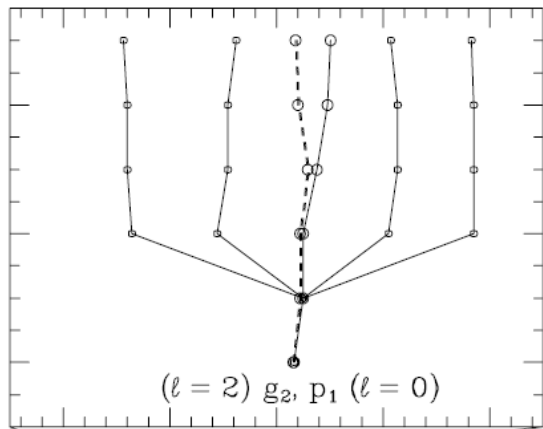
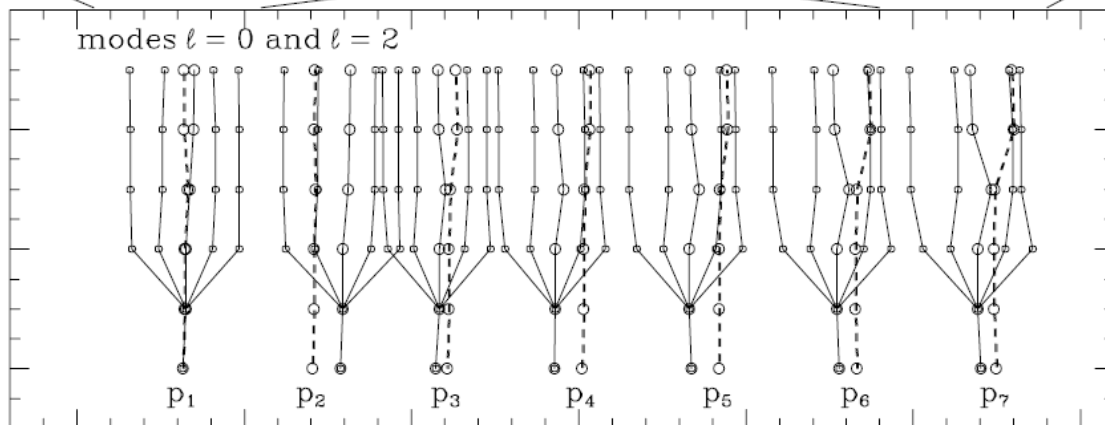


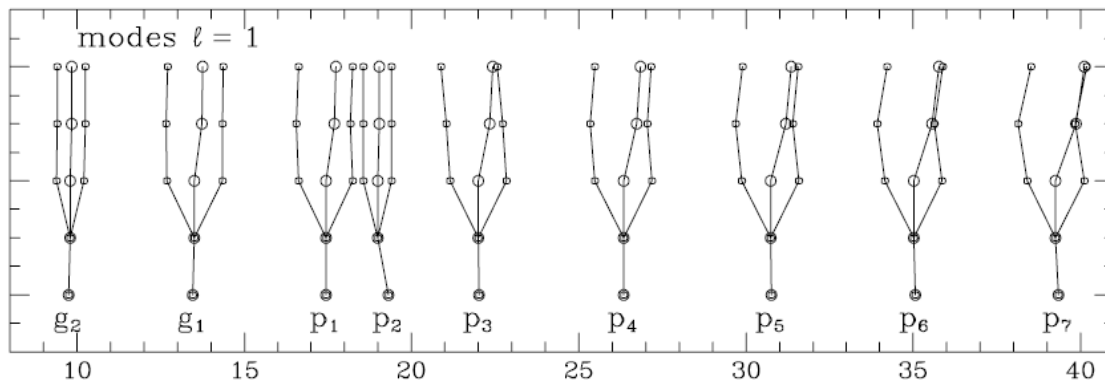
Figure 4. Evolution of frequency spectra of unstable modes with $\ell = 0, 2$ (left panel) and with $\ell = 1, 3$ (right panel) in a sequence of δ Sct models with mass of $1.8 M_{\odot}$. For simplicity, only modes of $\ell = 1$ are identified in the right panel. Dotted vertical line corresponds to the model of $T_{\text{eff}} = 7515$ K. Effects of rotation on frequency spectrum of this model are presented in Figure 5.



0, 2, 4 COUPLING
 0 & 2 COUPLING
 NON-SPH. DISTOR.
 LINEAR SPLITTING
 SPHER.-SYMM.
 $V_{\text{rot}} = 0$



0, 2, 4 COUPLING
 0 & 2 COUPLING
 NON-SPH. DISTOR.
 LINEAR SPLITTING
 SPHER.-SYMM.
 $V_{\text{rot}} = 0$

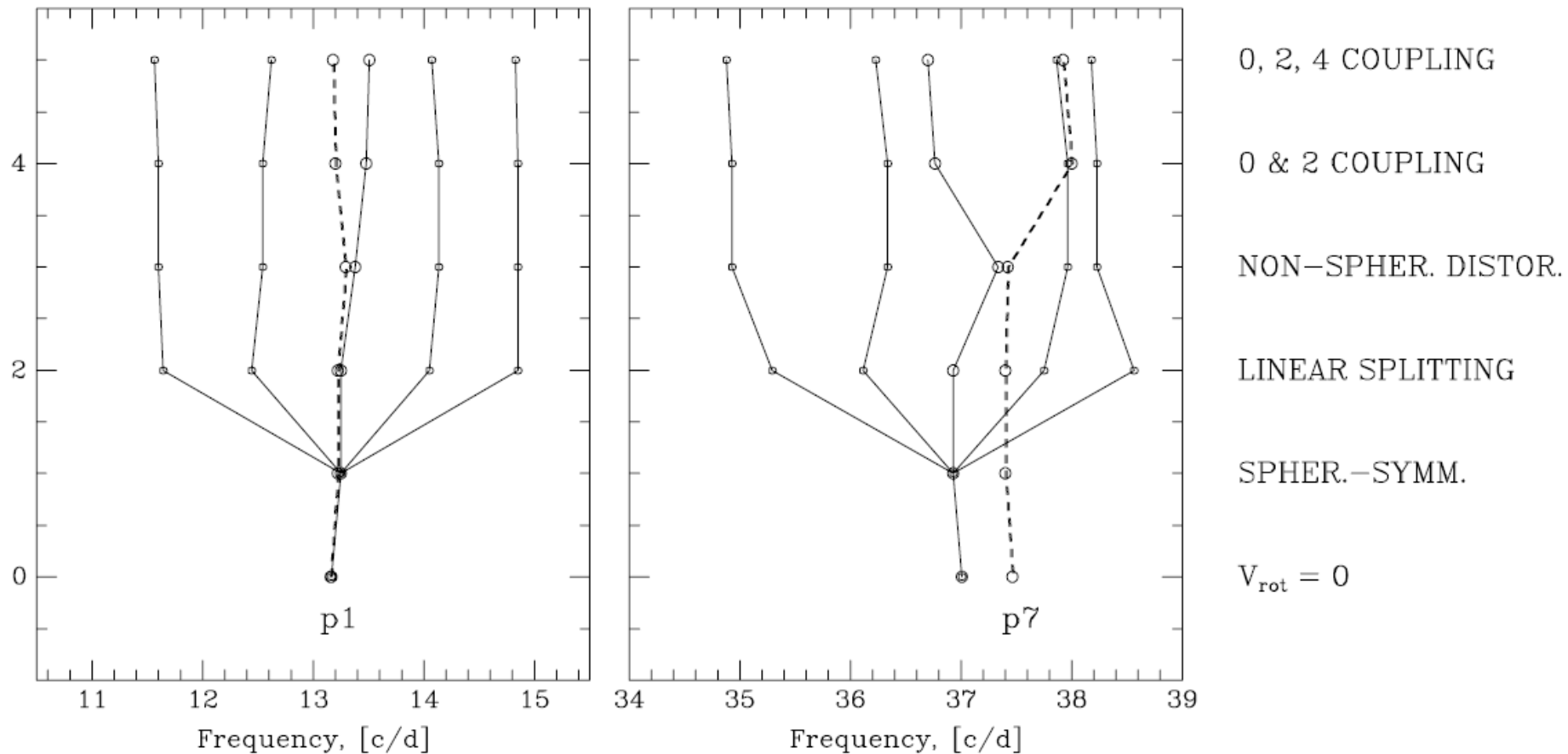


1 & 3 COUPLING
 NON-SPH. DISTOR.
 LINEAR SPLITTING
 SPHER.-SYMM.
 $V_{\text{rot}} = 0$

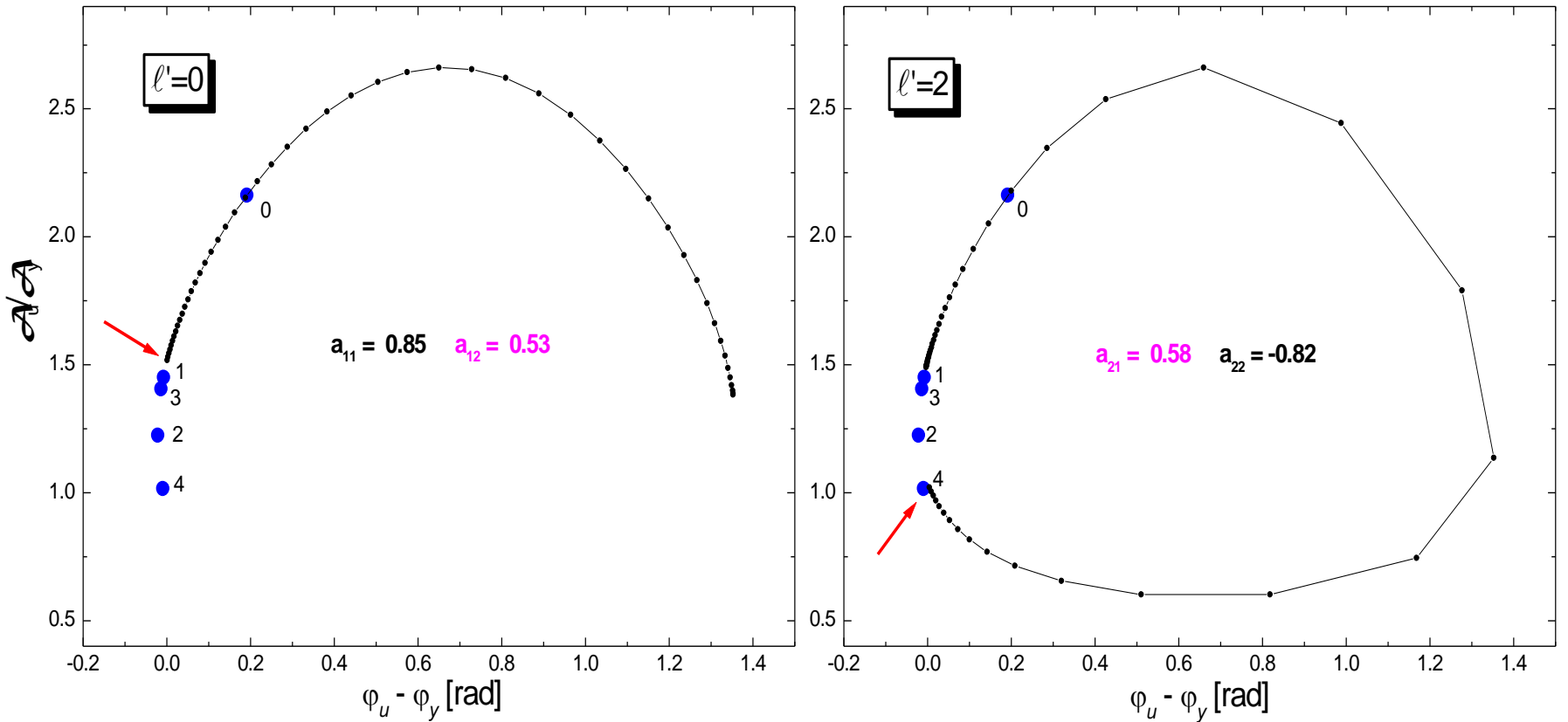
Frequency, [c/d]

Effects of rotational splitting of two $l=2$ modes (including rotational coupling with close radial modes)

$M = 1.8 M_{\odot}$, $T_{\text{eff}} = 7515 \text{ K}$, $R = 2.124 R_{\odot}$, $V_{\text{rot}} = 92 \text{ km/s}$



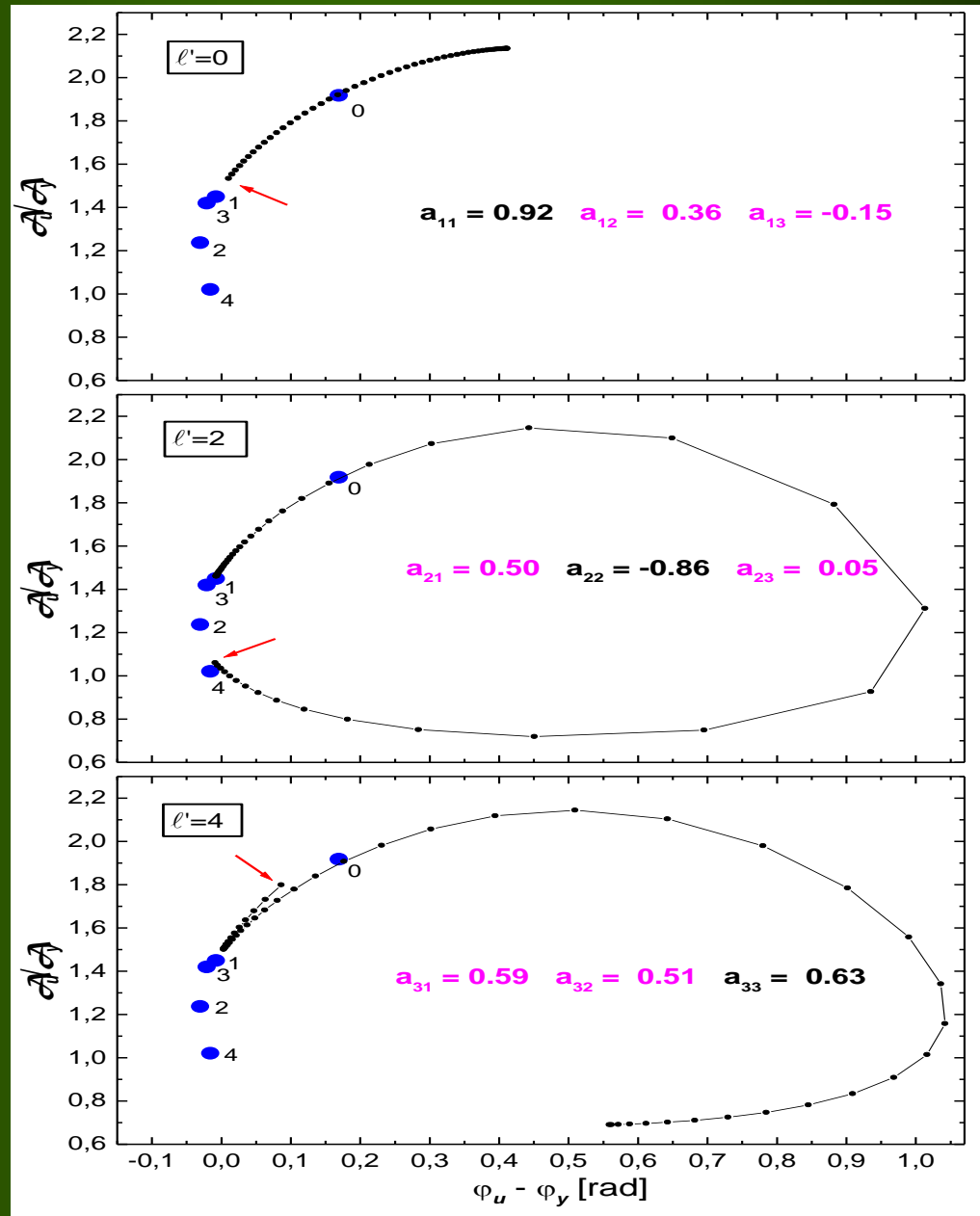
Effect of rotational mode coupling ($\ell = 0, p_1$ and $\ell = 2, g_1, m=0$), $\Delta\sigma_0=0.003$, for a model of $12 M_\odot$, $\log T_{\text{eff}}=4.374$, $V_{\text{rot}}=100$ km/s.

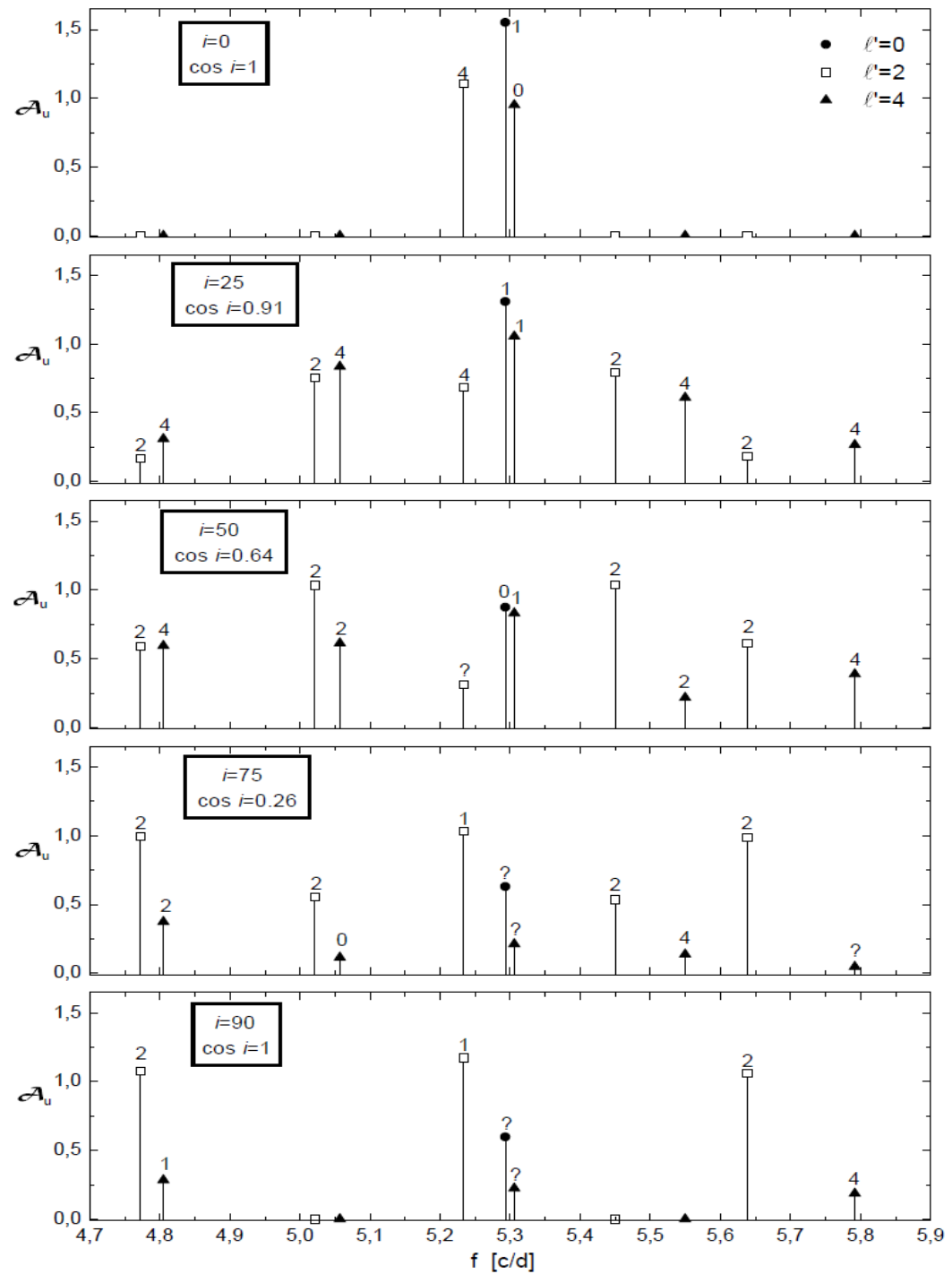


Spacing between consecutive dots is 0.02 in $\cos i$.

Arrows correspond to observations from the polar direction, $i=0^\circ$.

An example of the three mode coupling: $(\ell = 0, p_1)$, $(\ell = 2, g_1)$, $(\ell = 4, g_2)$





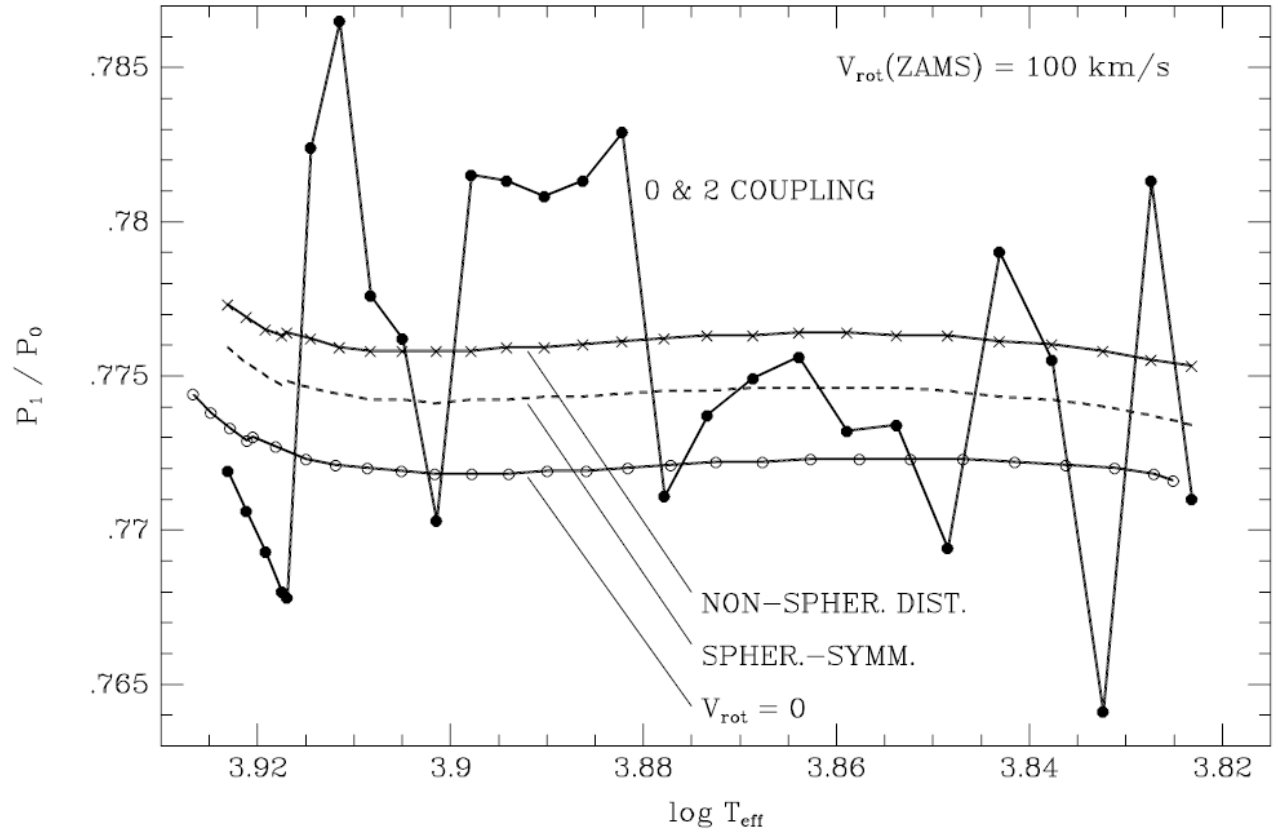
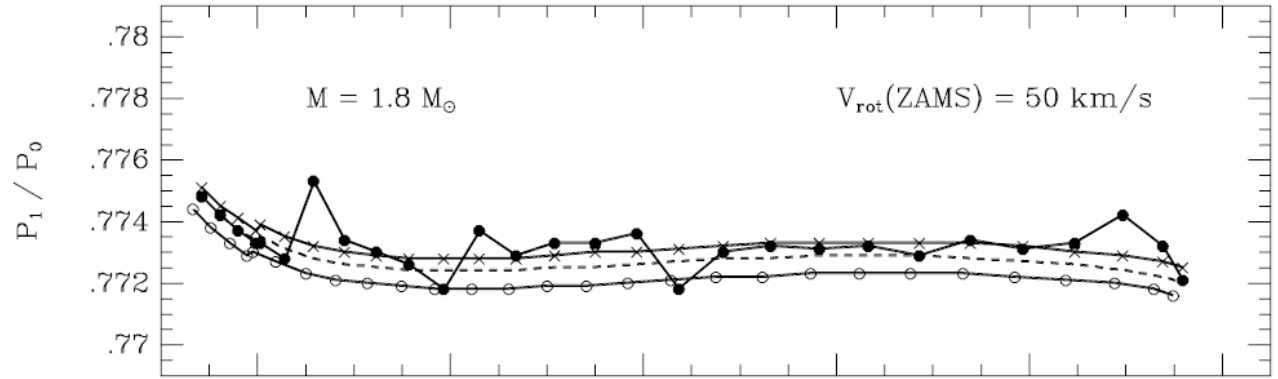
Daszyńska-
Daszkiewicz et al. 2002,
A&A 392, 151.

Due to rotational coupling, the higher degree modes, $\ell=4$ (5), can acquire significant contribution of $\ell=0$ (1).

This means that they can be detected in the ground-based observations.

The mode identification must be performed together with determination of the global stellar parameters, the rotation velocity and the inclination angle

Effect of rotational coupling on period ratio of radial modes.



SLOW (LOW-FREQUENCY) MODES

$$\omega \sim \Omega$$

Traditional approximation

e.g. Townsend 2003,
Daszyńska-Daszkiewicz, Dziembowski, Pamyatnykh 2007,
Shibahashi 2011, this Conference,
Aerts & Dupret, 2011, astro-ph, 31 August

An example:

$M = 6 M_{\odot}$, MS star

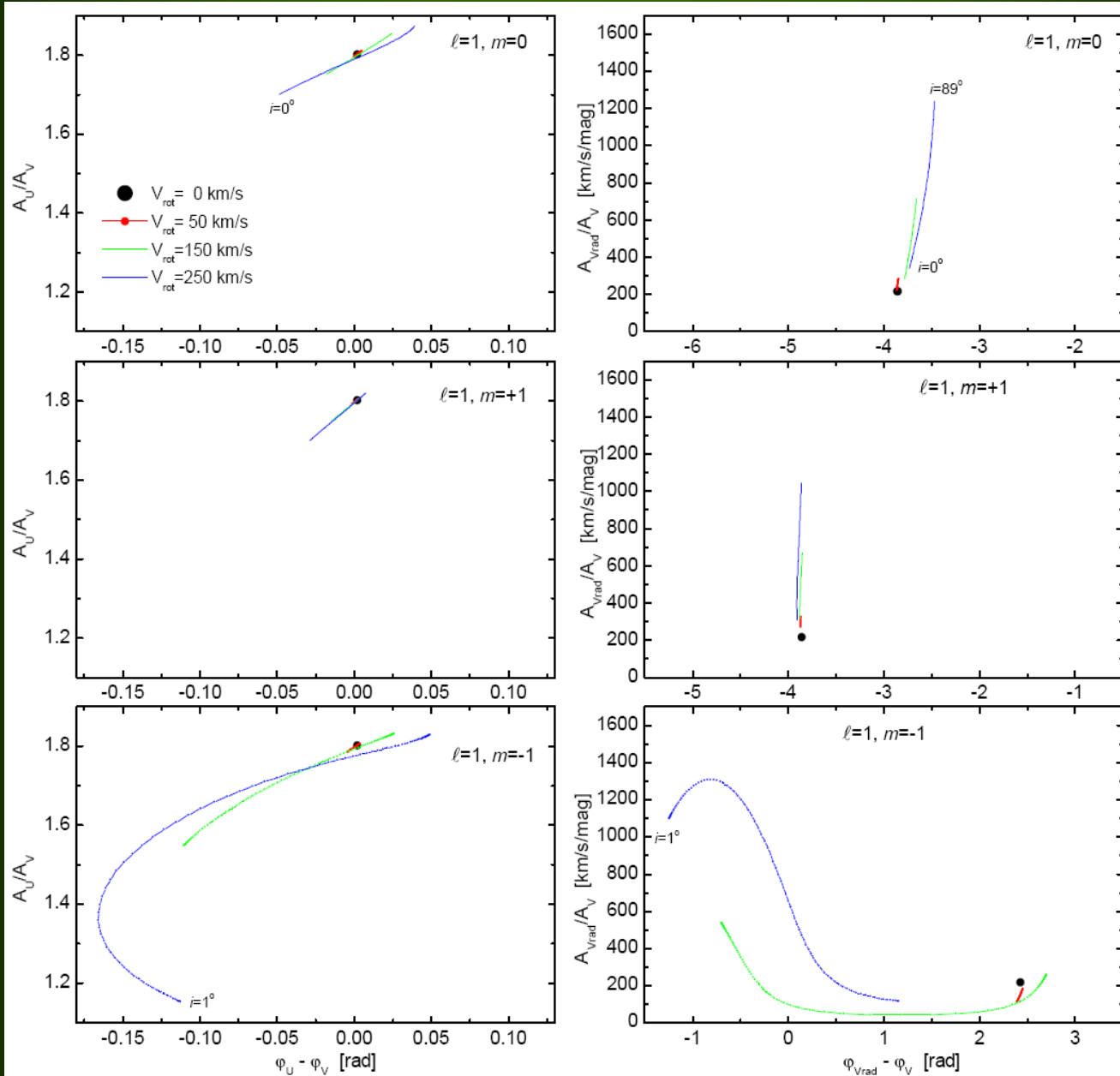
$\log T_{\text{eff}} = 4.205$ ($T_{\text{eff}} = 16\,000$ K)

$\log L/L_{\odot} = 3.204$

$V_{\text{rot}} = 0, 50, 150, 250$ km/s

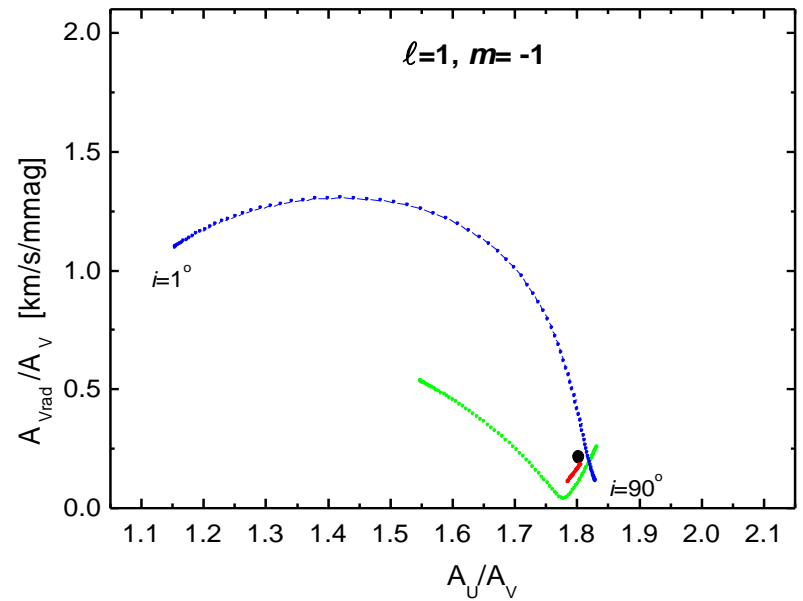
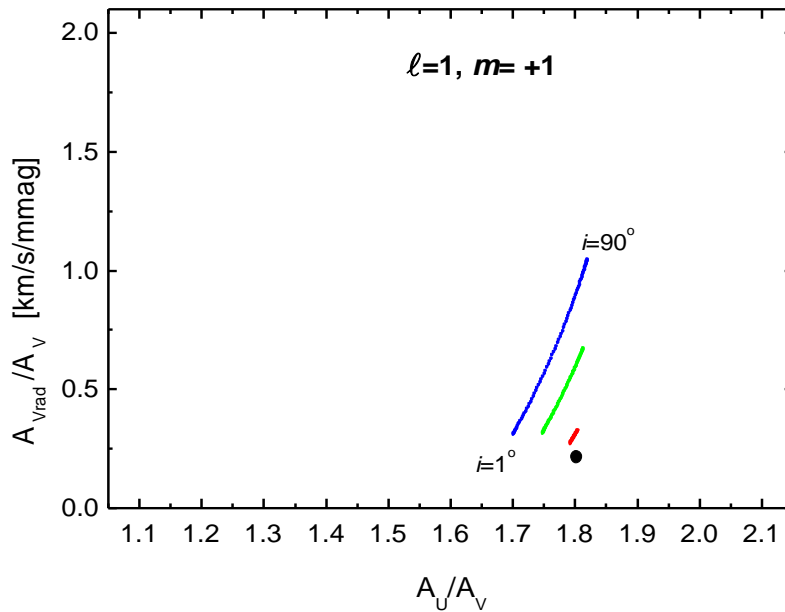
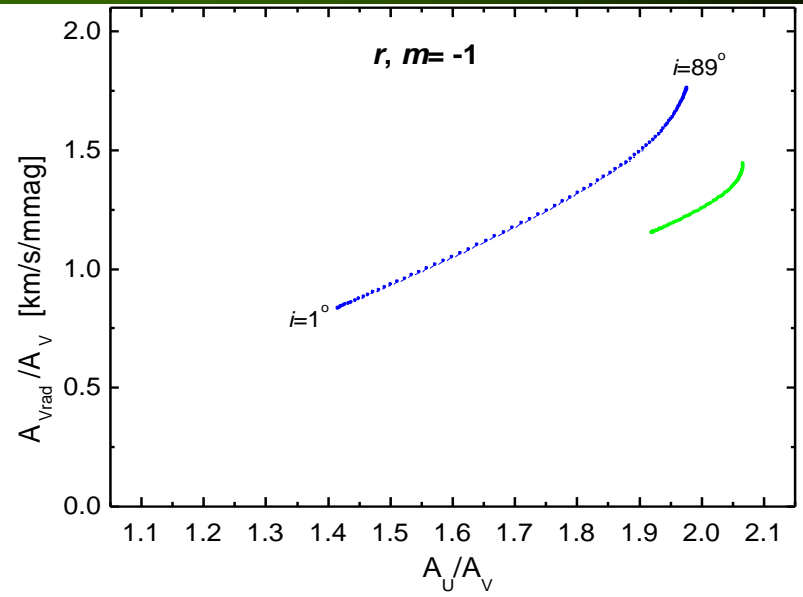
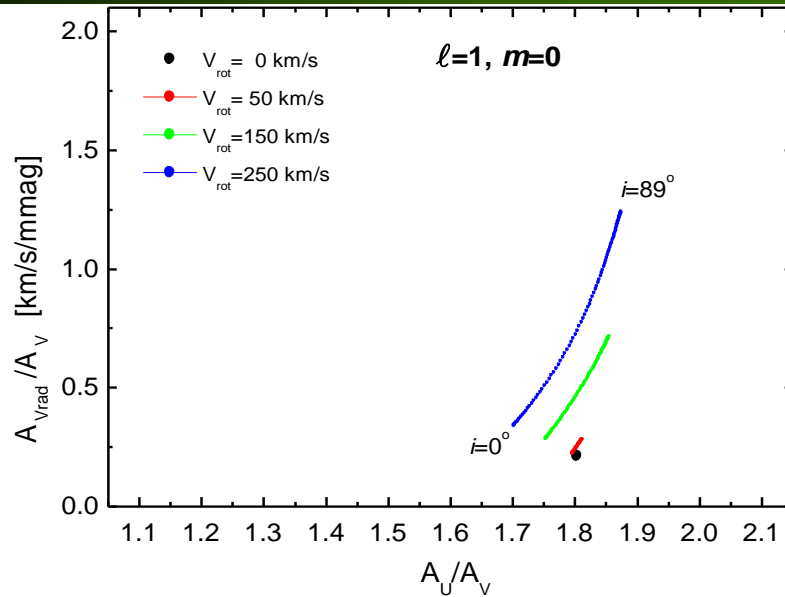
A_U/A_V versus $\phi_U - \phi_V$

A_{Vrad}/A_V versus $\phi_{Vrad} - \phi_V$



due to Daszyńska-Daszkiewicz, Dziembowski & Pamyatnykh 2007

$A_{\text{Vrad}}/A_{\text{V}}$ versus $A_{\text{U}}/A_{\text{V}}$



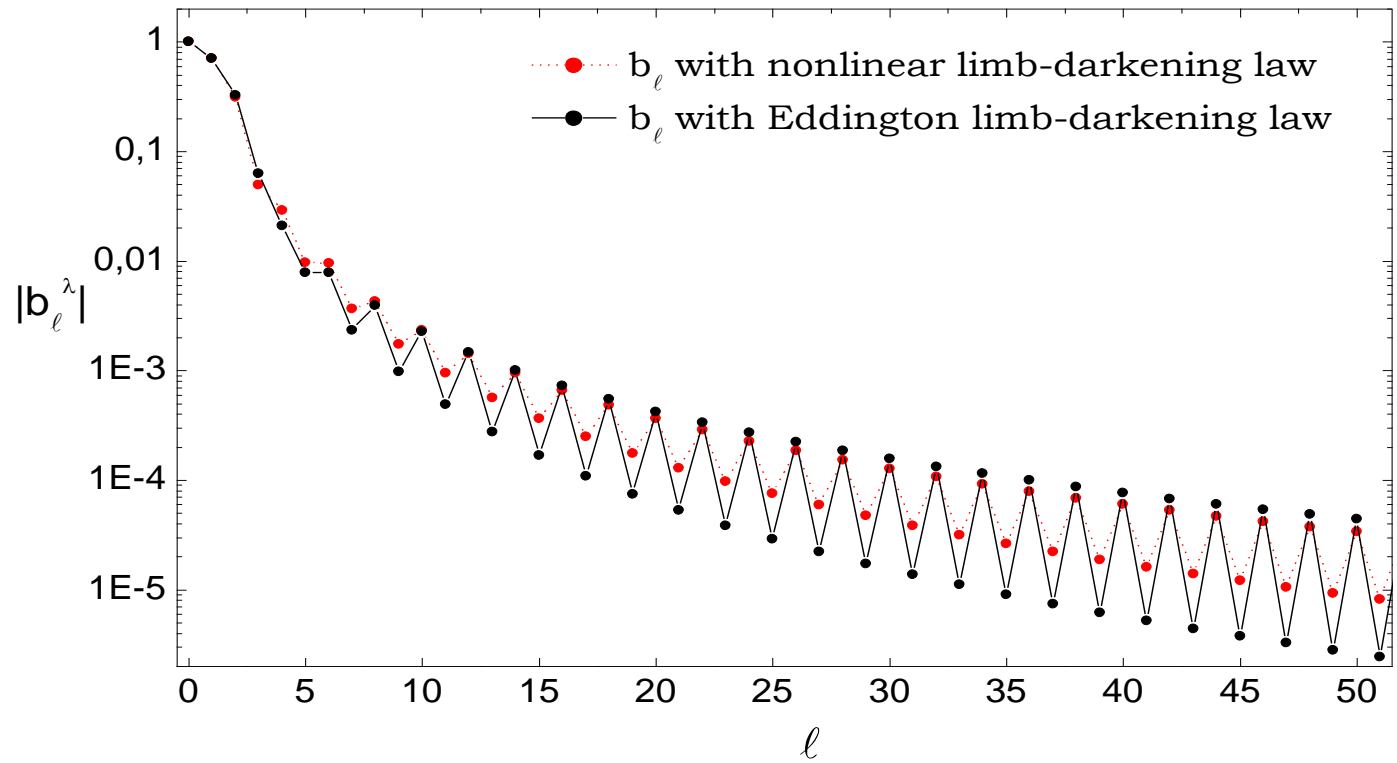
PHOTOMETRIC COMPLEX AMPLITUDES OF SLOW MODES ($\omega \sim \Omega$)

$$\mathcal{A}_x(i) = \varepsilon \sum_{j=1}^{\infty} \gamma_{\ell_j}^m(s) Y_{\ell_j}^m(i, \mathbf{0}) \left[\mathcal{D}_{\ell_j}^x f + \mathcal{E}_{\ell_j}^x \right]$$

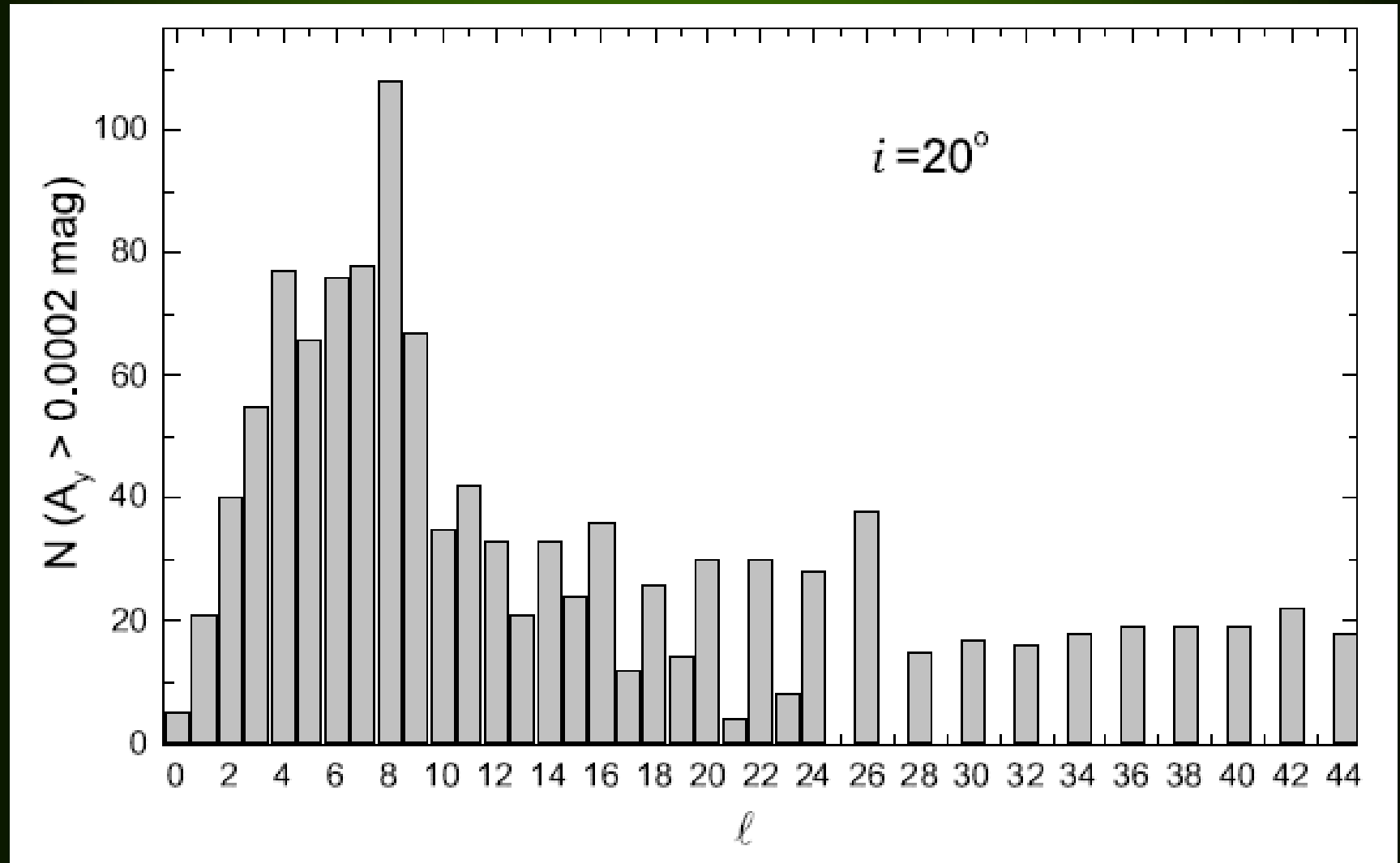
$$\ell_j = \begin{cases} |m| + 2(j-1) & \text{- even-parity modes} \\ |m| + 2(j-1) + 1 & \text{- odd-parity modes} \end{cases}$$

HIGH ℓ MODES

b_ℓ as a function of ℓ
 $\log T_{\text{eff}} = 3.86$, $\log g = 3.9$, $[m/H] = 0.0$



Number of modes with photometric $A_y > 0.2$ mag for different l .
Intrinsic amplitude of displacement is assumed to be $\varepsilon = 0.005$.



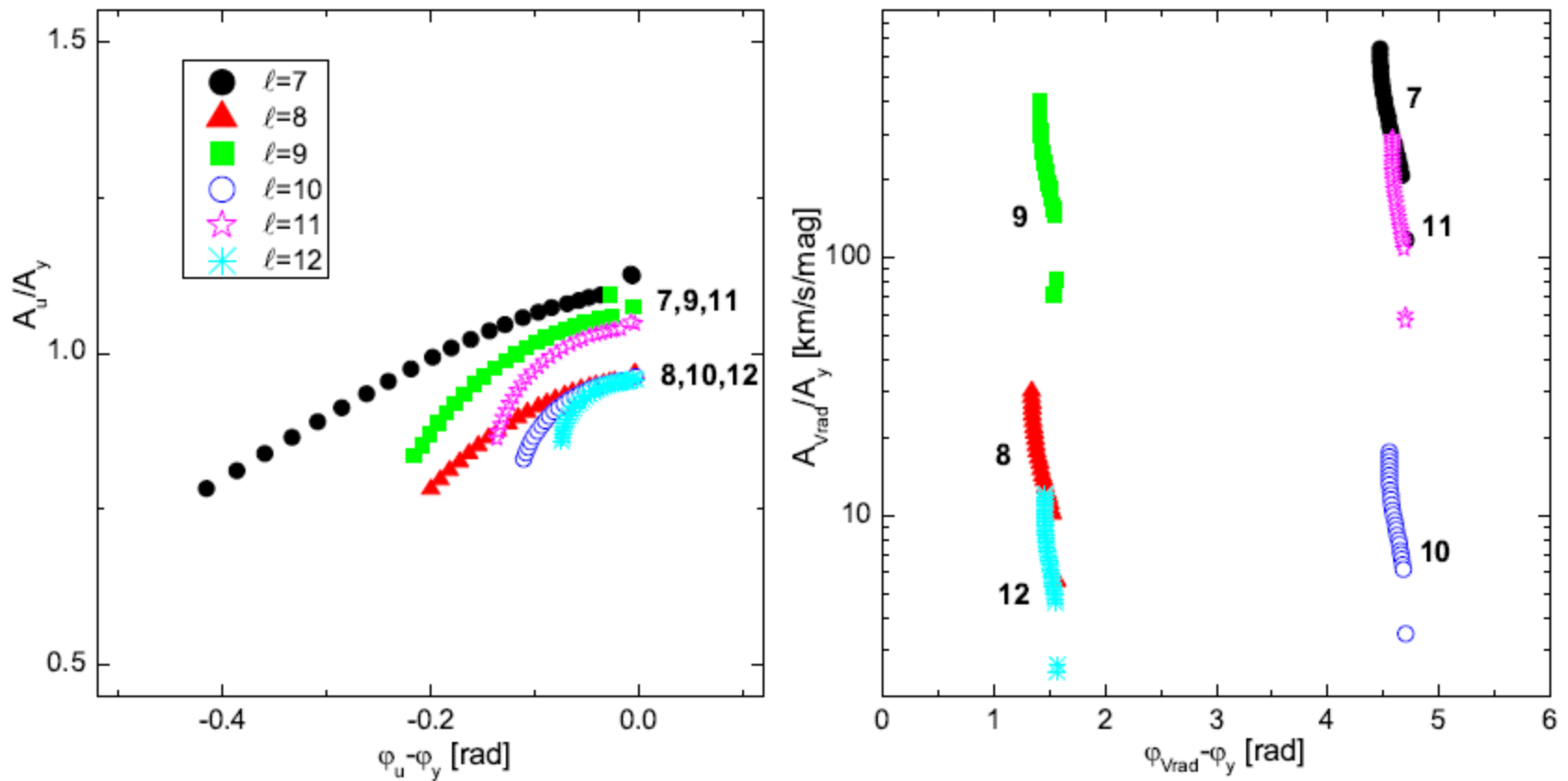


Fig. 4 Position of modes with ℓ from 7 up to 12 in the diagrams using the Strömgren uy passbands (left panel) and the radial velocity data and the y filter (right panel) for the β Cep model with $M = 8.5M_{\odot}$ and $\log T_{\text{eff}} = 4.322$. Only unstable modes are shown.

THE END

Additional plots

The parameters of the pulsation modes are derived only from the amplitude and phase across the line. The reduced χ_v^2 is calculated from complex amplitudes in order to combine amplitude and phase information in the following way

$$\chi_v^2 = \frac{1}{2n_\lambda - m} \sum_{i=1}^{n_\lambda} \left[\frac{(A_{R,i}^o - A_{R,i}^t)^2}{\sigma_{R,i}^2} + \frac{(A_{I,i}^o - A_{I,i}^t)^2}{\sigma_{I,i}^2} \right] \quad (1)$$

where n_λ is the number of pixels across the profile, m the number of free parameters, A^o and A^t denote observationally and theoretically determined values, respectively, $A_R = A_\lambda \cos \phi_\lambda$ and $A_I = A_\lambda \sin \phi_\lambda$ are the real and imaginary parts of the complex amplitude, and σ is the observational error. Equation (1) can be easily modified if the observed amplitude and phase from photometric passbands is included for the calculation of χ_v^2 .

Since the amplitude and phase of a given wavelength bin are treated as independent variables, the variances are calculated from

$$\sigma_{R,\lambda}^2 = \sigma(A_\lambda)^2 \cos^2 \phi_\lambda + \sigma(\phi_\lambda)^2 A_\lambda^2 \sin^2 \phi_\lambda \quad (2)$$

$$\sigma_{I,\lambda}^2 = \sigma(A_\lambda)^2 \sin^2 \phi_\lambda + \sigma(\phi_\lambda)^2 A_\lambda^2 \cos^2 \phi_\lambda. \quad (3)$$

ZMIANY PRĘDKOŚCI RADIALNEJ

Po scałkowaniu dostaniemy

$$V_{rad} = -i\varepsilon\omega RN_l^0 d_{lm0}(i)(u_\ell + \alpha_H v_\ell)e^{-i\omega t}$$

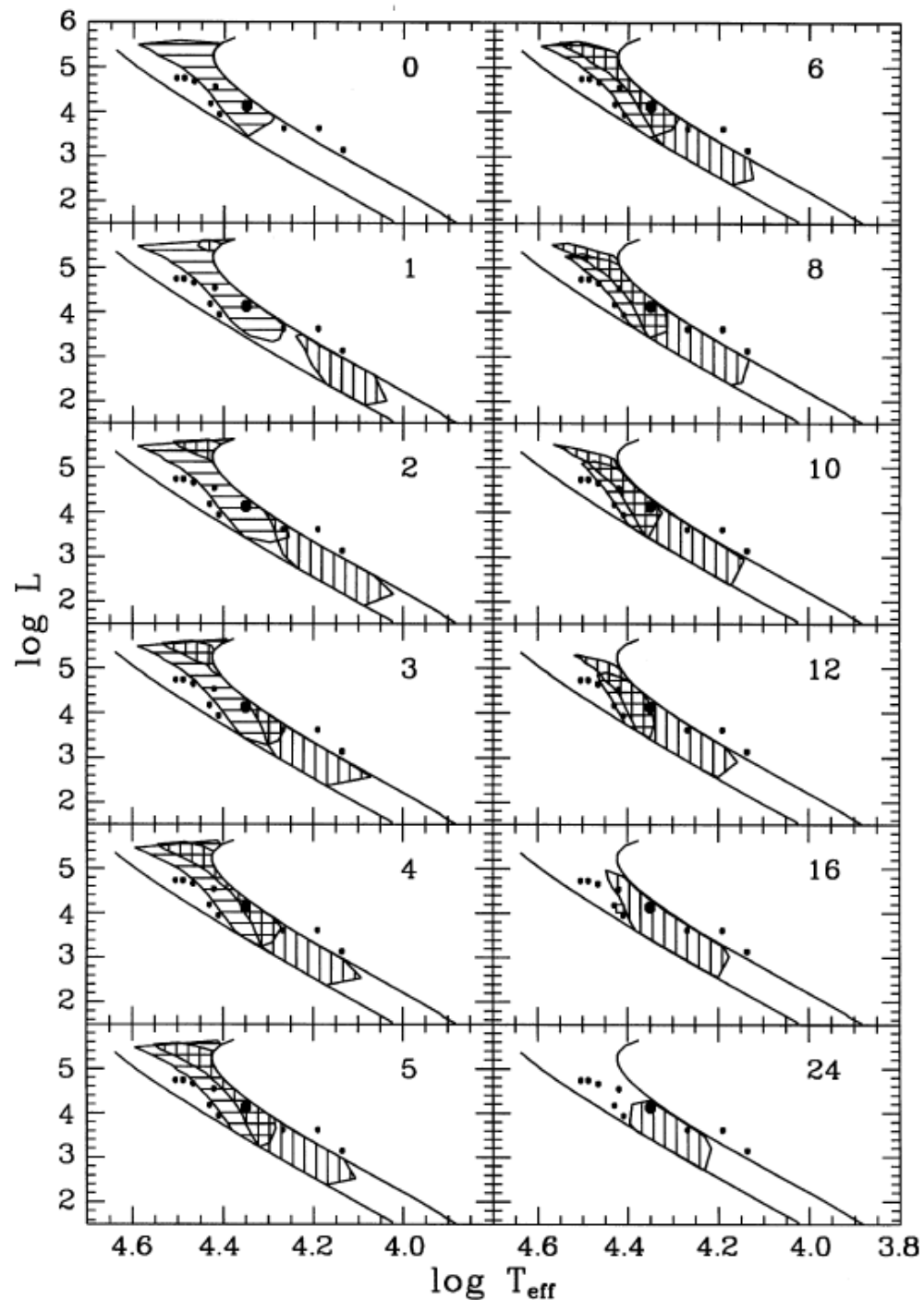
$$u_\ell = \int_0^1 h\mu^2 P_\ell(\mu) d\mu,$$

$$v_\ell = \ell \int_0^1 h(P_{\ell-1} - \mu P_\ell) \mu d\mu,$$

$$u_\ell^\lambda = \frac{1}{2\ell + 1} [(\ell + 1)b_{\ell+1}^\lambda + \ell b_{\ell-1}^\lambda]$$

$$v_\ell^\lambda = \frac{\ell(\ell + 1)}{2\ell + 1} [b_{\ell-1}^\lambda - b_{\ell+1}^\lambda]$$

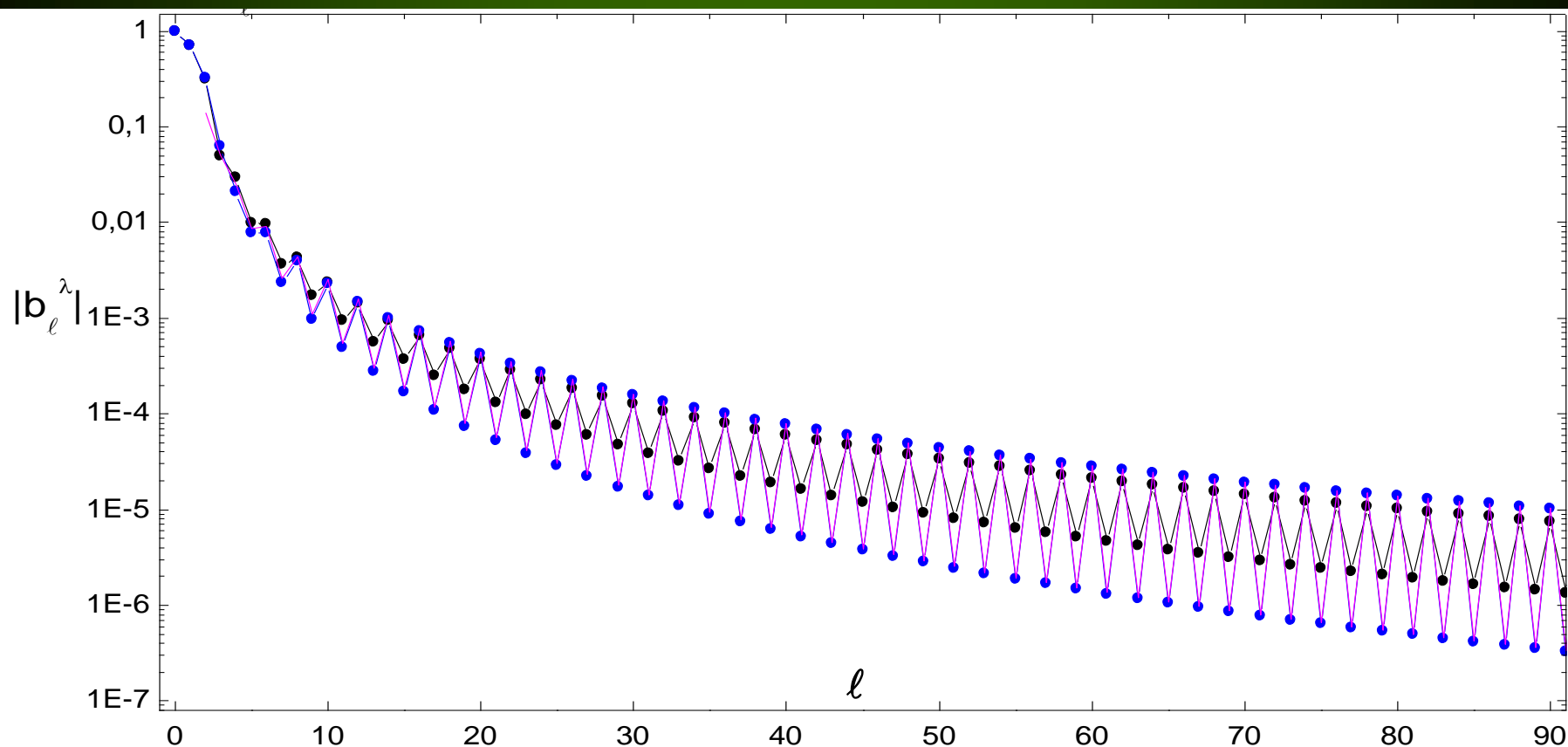
Short-period (β Cep) and long-period (SPB) instability strips for mode degree l from 0 to 24.



Balona & Dziembowski 1999

High degree modes

b_ℓ^λ in passband y , nonlinear $h_\lambda(\mu)$ (Claret)
 b_ℓ^λ - Eddington $h(\mu)$ ($h(\mu)=1.5\mu+1$)



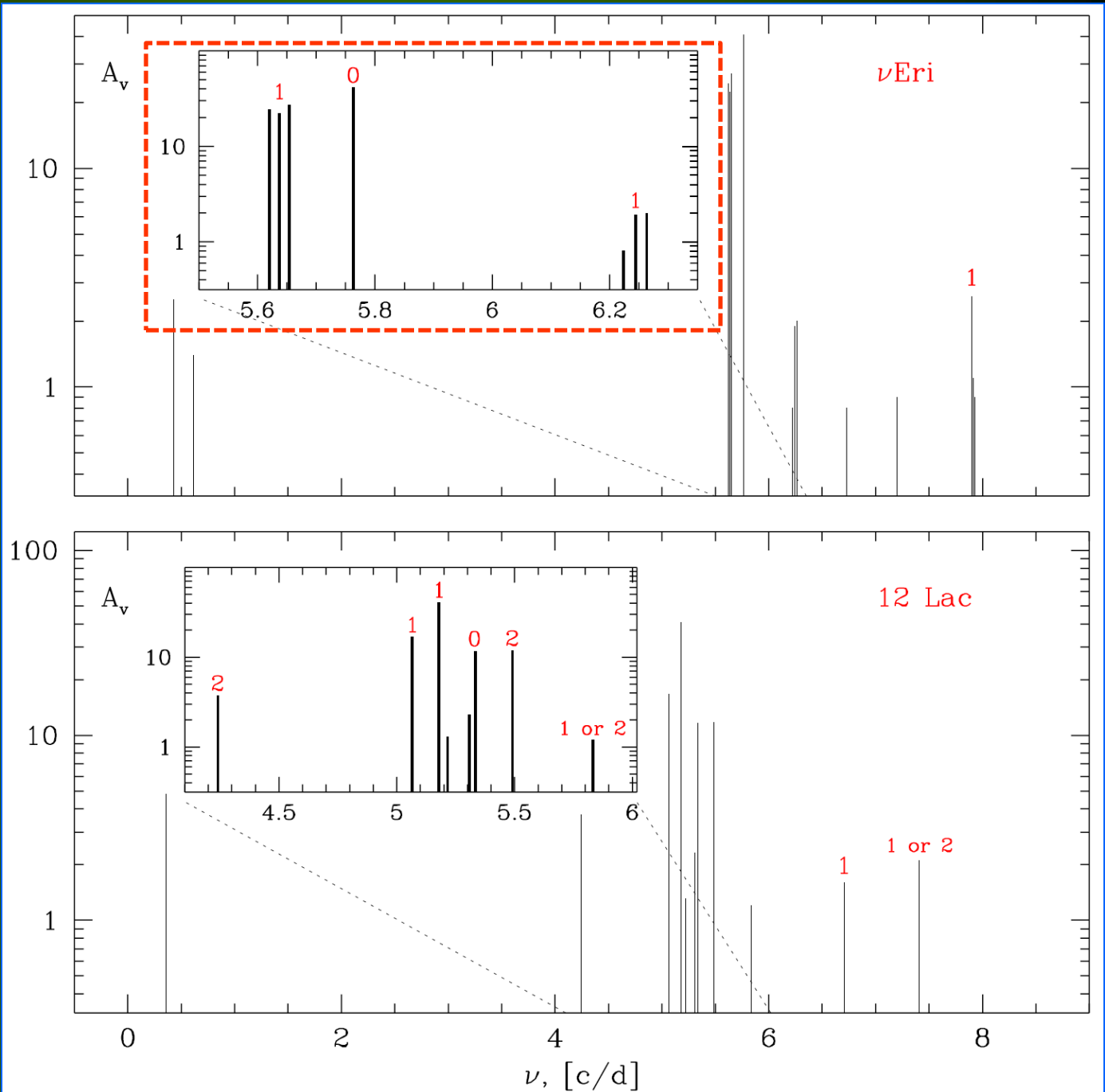
v Eridani

Testing rotation in interiors

(5 slides from lecture 01)

Oscillation spectra of ν Eri and 12 Lac

Two rotationally splitted triplets of $l=1$ modes (g1 and p1)

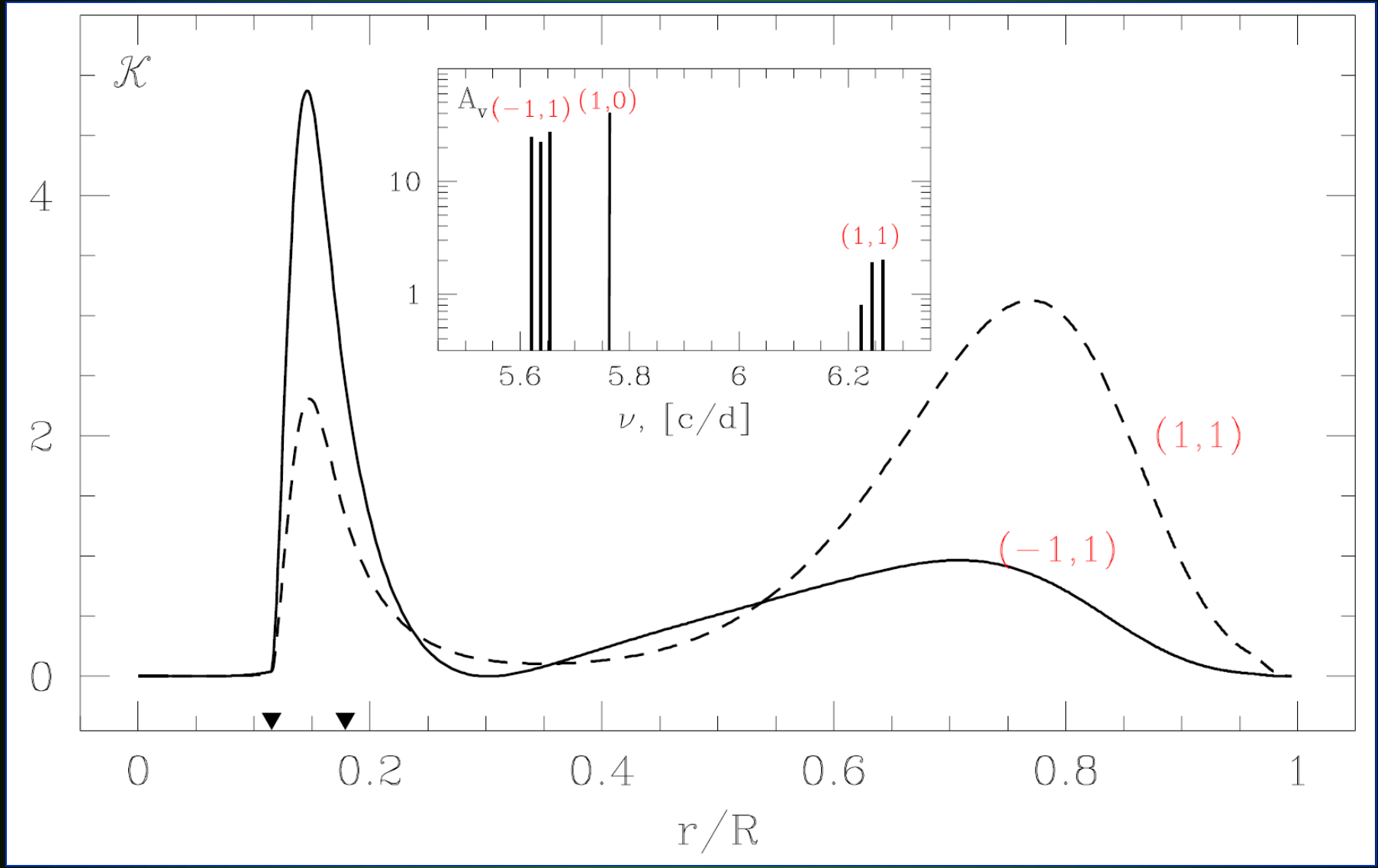


Dziembowski & Pamyatnykh 2008

Eri: the splitting kernels for two normal modes
 $l=1, g1$ (solid line), $l=1, p1$ (dashed line).
 Triangles mark boundaries of the μ -gradient zone.

$$S \equiv 0.5(\nu_+ - \nu_-) = \int_0^1 dx \mathcal{K}(x) \Omega / 2\pi$$

$S_g=0.017$, $S_p=0.020$ c/d



Simple rotation law

Results:

$$V_{\text{rot}} = 6 \text{ km / s}$$

$$\Omega_{\text{core}} = 5 * \Omega_{\text{envelope}}$$

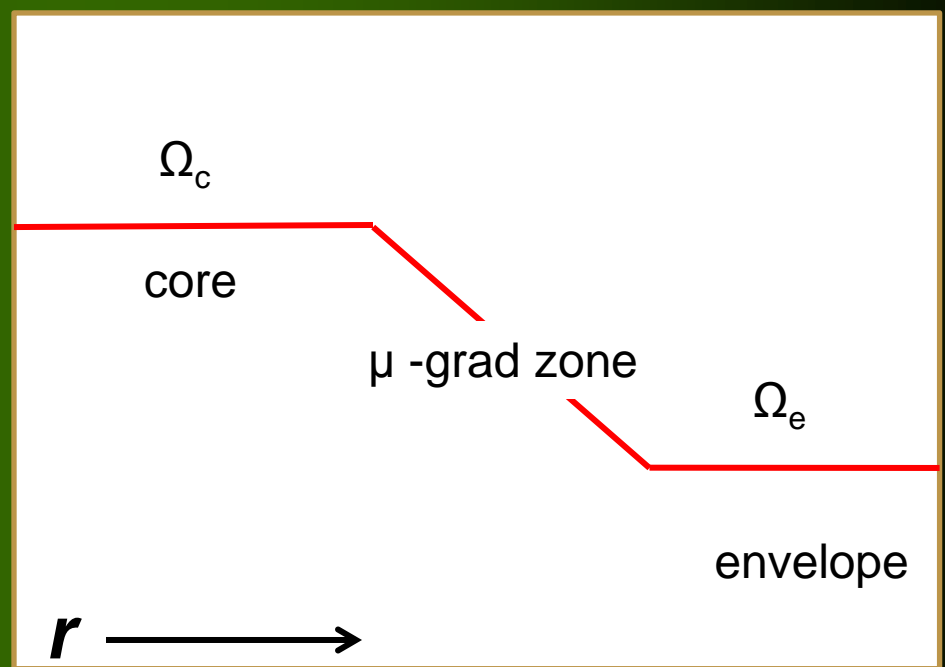


Table 1. The O-C (in cd^{-1}) for the $\ell = 1$, p_2 mode frequencies and the differences between observed effective temperature and that of the seismic model, $\Delta \log T_{\text{eff}} = \log T_{\text{eff,obs}} - \log T_{\text{eff,cal}}$. The observational uncertainty in effective temperature is $\Delta \log T_{\text{eff}} = 0.011$. Models with $\alpha_{\text{ov}} > 0$ were calculated with $w = 8$. V_{rot} is given in km s^{-1} .

κ	Mixture	α_{over}	OC	$\Delta \log T_{\text{eff}}$	Ω_c / Ω_e	V_{rot}
OP	A04	0.0	-0.127	-0.0103	5.55	5.93
OP	GN93	0.0	-0.151	-0.0075	5.36	5.95
OPAL	A04	0.0	-0.188	-0.0044	5.36	5.99
OP	A04	0.1	-0.085	-0.0159	5.82	5.91
OP	A04	0.2	-0.034	-0.0244	5.78	5.93

Summary of results for ν Eridani

- ν Eri has 14 independent modes, the strongest one is the radial fundamental mode, most of the others are $l = 1$ modes.
- Peaks at 0.432 and 0.614 c/d correspond to high-order g-modes (SPB-type pulsations). ν Eri – a hybrid star.
- Rotational splitting of two $l=1$ modes (g1 and p1) can be used to infer **information on internal rotation**. The core rotates approximately 5 times faster than the envelope.
- **Overshooting** from the convective core seems to be ineffective in ν Eri, but the estimate critically depends on the T_{eff} determination.
- For standard opacities **modes at lowest and highest observed frequencies are stable**. An additional **opacity enhancement** around Z bump region may solve the problem.
- A new way of **probing opacity**